CREEP IN PRESTRESSED LIGHTWEIGHT CONCRETE

By

Howard L. Furr

Research Engineer

and

Raouf Sinno

Assistant Research Engineer

Research Report Number 69-2

Creep in Prestressed Concrete

Research Project Number 2-5-63-69

Sponsored by

The Texas Highway Department
In Cooperation with the
U. S. Department of Transportation, Federal Highway Administration
Bureau of Public Roads

October 1967

TEXAS TRANSPORTATION INSTITUTE

Texas A&M University

College Station, Texas

ACKNOWLEDGMENT

The authors are deeply grateful to Mr. Larry G. Walker and Mr. H. D. Butler, both of the Texas Highway Department, and Dr. David Dar-wei Yang, Prairie View Agricultural and Mechanical College, for valuable assistance in planning and executing the work reported here; and to Mr. Leonard L. Ingram, of the Texas Transportation Institute, in carrying out the work of the program.

The opinions, findings, and conclusions expressed in this publication are those of the authors and not necessarily those of the Bureau of Public Roads.

ABSTRACT

A procedure, using the rate-of-creep method, is developed for predicting creep strains, camber, and prestress loss in pretensioned prestressed concrete highway bridge beams. The procedure uses shrinkage data and creep per psi data, both expressed as functions of time, developed from small concrete specimens.

Non-loaded pretensioned prestressed lightweight concrete beams 5 x 8 in. in section, 8 ft. long, were used to test the procedure. Creep and prestress losses taken from the beams were compared with values predicted by using the procedure developed in the paper.

The method was extended to accommodate precast prestressed beams with cast-in-place reinforced concrete slabs, and laboratory beams were tested to verify the procedures.

A full size highway beam and slab were instrumented in field installation to check out techniques proposed for use in a full size highway bridge installation.

A full size highway bridge using precast prestressed beams and cast-in-place slabs was instrumented for purposes of testing the prediction method. Data from beams has been collected for approximately one year; the slab was being readied for placing at the time of writing. Creep, shrinkage, camber, and prestress losses were taken by measurements of strain and elevations from the bridge beams. Predicted creep, camber, and prestress loss based on data from small specimens are compared with data developed from measurements with the 10 in. mechanical strain gage and an engineers level.

Reasonable agreement is reached between predictions and measurements. Prestress losses in lightweight full size bridge beams are approximately 23% and for normal weight, approximately 14% at 300 day age.

TABLE OF CONTENTS

LIST OF FIGURES

LIST OF TABLES

APPENDICES

Notation

α	Rotation of a cross section (radians)
ε_c	Creep strain (in./in.)
ε_s	Shrinkage strain (in./in.)
ε_{cs}	Creep strain at level of steel
ε_c^u	(Creep strain/unit stress); unit creep strain (in./in./psi)
ε^∞	Strain at infinite time (in./in.)
Δ	Denotes a change
t	Time (days) -- subscript denotes a specific time
f	Unit stress (force/unit area)
F	Force
A	Cross sectional area
I	Moment of inertia of a cross section with respect to its centroidal axis
d	Overall depth at a beam section
c_{top}, $c_{bot.}$	Distance from centroid of beam section to top and bottom surfaces, respectively; (in.)
y	Distance from centroid of beam section to beam fiber (in.)
cgs	Centroid of prestressing steel area
x	Distance along longitudinal axis of a beam
$\alpha(t)$, $\beta(t)$, $f(t)$, $g(t)$	Functions of time
G	Strain gage reading taken from specimens (in.)
S	Strain gage reading taken from standard bar (in.)
E	Modulus of elasticity (psi)

Ln	Natural logarithm
L	Length measured along geometrical axis
n	Age of specimen at the time when that specimen has strained 1/2 ε^{∞}
f'_c	Breaking strength of a standard size concrete cylinder in compression at age of test, (psi)

CHAPTER I

THE RESEARCH PROGRAM

1.1 Introduction

Structural engineers are concerned with creep in prestressed concrete because of stress losses and changes in camber of prestressed beams. The research reported in this paper was initiated in an effort to supply information on these two actions in structural lightweight prestressed concrete.

Considerable study has been made on creep in concrete, and both the theoretical and applied aspects have been treated (1). The work in lightweight concrete is relatively new and is generally covered in references (2) through (8) and (25).

Most of the creep tests have used specimens under concentric load applied by hydraulic cylinders (3), or by compressed springs (4). In most of the tests, it was required that the stresses in the test specimens be constant, and the loading systems were designed to meet that requirement.

Prestressed concrete carries the sustained load of prestressing steel, but that load changes considerably after the time of loading. The change is brought about by shortening of the member due to shrinkage and creep. The loss of prestress is of vital concern in providing a safe structure, and creep of the concrete is an important factor in camber that develops in prestressed beams. The change of initial camber of a prestressed beam after it has been installed in a structure can cause cracking and structural misalignment which could affect its serviceability.

In bridges, grade changes due to camber growth affects the riding qualities of the deck slab. These, and possibly other reasons, require a knowledge of methods for predicting camber with confidence.

It is known that the magnitudes of creep and shrinkage are influenced by concrete materials and mix design, and that creep magnitude is closely associated with the level of stress. Because of these factors, creep and shrinkage vary with different concretes and with different loading conditions.

This research was undertaken to develop and prove a method for predicting creep camber and prestress loss in a concrete for which fundamental properties of the material were known or would be developed. Once that method was proved to be valid, the creep camber and prestress loss of any prestressed beam could theoretically be determined provided that basic properties of the material were known. Such a capability would be valuable in the design of prestressed beam highway bridges as well as in other structures.

1.2 Objectives

The specific objectives of the program were to develop a numerical method for predicting creep in pretensioned lightweight concrete specimens, to develop theoretical predictions for creep camber of full size prestressed bridge beams and check them against field measurements, and to determine prestress loss in prestressed lightweight bridge beams.

The numerical method for predicting creep and the tests

enumerated below were developed and carried out for purposes of meeting the objectives stated above.

1.3 Numerical Creep Prediction Method

Creep of a given concrete depends primarily on time under load, magnitude of sustained stress, constituents of the mix, and conditions of curing and service. All of those factors should come into play in a method designed to predict creep in a concrete member or structure.

A rate-of-creep method treated by Ross (9) is rational and it involves most of the factors having major influence on creep. Others (10) expanded on the method for its application to prestressed concrete, and Yang (7) made detailed computations for creep in prestressed beams by using the general method. It is a numerical method which converts unit creep and shrinkage into step functions having constant values over relatively short time increments. The use of short time increments entails a great number of mathematical operations and, for that reason, it is handled best by computer.

The rate-of-creep method was applied in this research to predict creep of prestressed beams at any age. Deflections of the beams were then computed from that predicted creep by a numerical integration technique. Detailed steps in the prediction technique were developed, and laboratory tests were made to collect data needed for carrying out the prediction computations.

Other tests were designed for testing the validity of the predictions, and later, field tests were made on a full size bridge.

The basic steps of the method are listed below in the order of their application in this program. The shrinkage and creep functions were developed from data collected in the tests mentioned above.

The basic steps of the computational method that were worked out for this program are listed below, and an IBM 7094 computer was used in its application. Mathematical functions of creep-and-time and of shrinkage-and-time, necessary for application of the method , were developed from tests on small specimens. Those test results bring into account a number of the factors that influence creep.

Steps in carrying out the method of predicting creep and deflection in a prestressed beam are:

1. Develop shrinkage versus time and creep per unit of stress versus time functions from results of laboratory tests.

$$\varepsilon_s = f(t) \qquad \text{Eqn. 1-1}$$

$$\varepsilon_c^u = g(t) \qquad \text{Eqn. 1-2}$$

2. Divide the beam into a number of small incremental lengths, and perform each operation listed below on each increment. If the beam is symmetrical the calculations may be reduced.
3. Divide time to be covered by the prediction into a number of periods of fairly short duration - a few days - depending on the time rate of change of the functions.

4. Compute stresses at any level of the cross section. The points of interest in this program are top, bottom, and middle gage levels and centroid of prestressing steel.

5. Compute the creep strain increment occurring over time increment t_1 to t_2 at any level in the cross section as the product of stress at that level and the incremental unit creep over that time interval.

$$\varepsilon_{c_{1-2}} = f_{c_1} \times \varepsilon^u_{c_{1-2}} \qquad \text{Eqn. 1-3}$$

6. Read shrinkage strains at times t_1 and t_2 from shrinkage curve. Compute incremental shrinkage strain, $\varepsilon_{s_{1-2}}$, over that time increment.

$$\varepsilon_{s_{1-2}} = \varepsilon_{s_2} - \varepsilon_{s_1} \qquad \text{Eqn. 1-4}$$

7. Compute total change in strain at steel level over time increment t_1 to t_2.

$$\varepsilon_{st1_{1-2}} = (\varepsilon_c + \varepsilon_s)_{1-2} \qquad \text{Eqn. 1-5}$$

8. Compute steel stress loss over the time interval.

$$\Delta f_{s_{1-2}} = \varepsilon_{st1} \times E_{st1} \qquad \text{Eqn. 1-6}$$

$$\Delta F_{s_{1-2}} = \Delta f_{s_{1-2}} \times A_s \qquad \text{Eqn. 1-7}$$

9. Compute stress in steel at time t_2.

$$f_{s_2} = f_{s_1} - \Delta f_{s_{1-2}} \qquad \text{Eqn. 1-8}$$

10. Compute concrete stress change due to the loss of prestress over the time interval by reversing ΔF_s and applying it at

cgs. That stress change is due to the axial stress component and the bending component.

$$f_{c_{1-2}} = \left(\frac{\Delta F_s}{A} \pm \frac{\Delta F_s ey}{I} \right)_{1-2} \qquad \text{Eqn. 1-9}$$

11. Compute the concrete stresses at time t_2, the end of the particular time interval being treated and the beginning of the next time interval.

$$f_{c_2} = f_{c_1} + \Delta f_{c_1} \qquad \text{Eqn. 1-10}$$

12. Compute the corresponding concrete strain at the end of the time interval. That strain consists of an elastic rebound component due to the stress relaxation over the time interval, and the creep and shrinkage components.

$$\Delta\varepsilon_{\text{elastic}_{1-2}} = \left(\frac{\Delta f_c}{E_c} \right)_{1-2} \qquad \text{Eqn. 1-11}$$

$$\varepsilon_2 = (\varepsilon_{\text{creep}} + \varepsilon_{\text{shrinkage}} + \Delta\varepsilon_{\text{elastic}})_{1-2} \qquad \text{Eqn. 1-12}$$

13. Use the stresses found in steps 9 and 12 as initial stresses for a time increment t_2 to t_3 and repeat steps 5 through 12, making proper changes in subscripts of time designations. This process is repeated until the total time duration is covered.

Step 13 ends the method for predicting creep. Deflection calculations use the information developed in the steps above, and continues with step 14 for each element. Symmetry about midspan is assumed in deflection calculations below.

14. Compute the rotation between the end sections of each element over each interval of time using strains computed in step 12.

$$\alpha_t = \frac{\varepsilon_t - \varepsilon_{t-\Delta t}}{d} \qquad \text{Eqn. 1-13}$$

15. Multiply increment rotation by distance from the end support to the center of the incremental length to find incremental deflection at midspan due to rotation of the element during the time interval.

$$\Delta_i = (\alpha_t x)_i \qquad \text{Eqn. 1-14}$$

16. Sum the incremental deflections at midspan over one-half the beam length to obtain total deflection.

Steps 17 through 29 must be added when the composite action of the prestressed beam with the cast-in-place slab is to be accounted for. In those steps, segmental lengths are used just as in the steps above, and the computations are based on strain per unit length of segment -- not total length of segment. Creep and shrinkage strains are kept separate, as are stresses from those causes, so that their individual effects may be studied later.

These steps assume that the modulus of elasticity of the slab concrete is known. The timing of events may be chosen to fit actual conditions because computations can be made to fit those conditions.

17. Develop shrinkage and unit curves for slab concrete in the

same way as was done for beam concrete; see step 1 above.

$$\varepsilon_{s(slab)} = \alpha(t) \qquad \text{Eqn. 1-15}$$

$$\varepsilon^{u}_{c(slab)} = \beta(t) \qquad \text{Eqn. 1-16}$$

18. Compute changes in stresses and in strains in the beam concrete brought about by the dead load moment of the slab.

19. Compute the change in elastic steel stress due to dead load moment of the slab by multiplying the strain at cgs by the steel modulus. Then, compute change in prestress force as the product of the change in stress computed above and the area of prestress steel.

    Reverse the change in prestress steel force in step 19, applying it as an eccentric axial external force on the element at cgs.

20. Compute changes in beam stresses and strains caused by the force of step 19.

21. Sum the changes in beam and steel stresses and strains from steps 18 through 20 and add them to corresponding values at time t_o to produce stress and strains at the beginning of the new time increment (the first after casting of the slab).

22. Compute free shrinkage in the slab, and shrinkage and creep in the beam for the time interval Δt per unit length of the element.

23. Compute the difference in free shrinkage (differential shrinkage) between the slab and the beam over time increment Δt per unit length of the element.

24. Force compatibility of strains at the interface by applying equal and opposite longitudinal forces on the slab and beam at their interface.

25. Compute stress change in beam and in slab due to the action in step 24.

26. Compute the change in elastic steel stress, as in step 19, due to stress changes from step 25.

27. Compute changes in beam stresses and strains caused by the force of step 26.

28. Sum changes in strains and stresses from steps 22 through 27.

29. Compute the difference in creep (differential creep) between the bottom of the slab and top of beam for the time increment Δt . The procedure of step 5 is followed, keeping in mind that the beam concrete and the slab concrete each has its unit creep curve.

30. Perform the operations of Steps 24-28 for differential creep from step 29.

31. Determine the stress and strain in beam and slab (the composite section) at the beginning of the next time increment by summing those values at the beginning of the present time increment with those occurring previously.

32. Compute the rotation between end sections of the segmental lengths over each time interval using strains, from steps 28 and 30, at top and bottom of beam. (This compares with the operations of step 14.)

33. Perform the operations of steps 15 and 16 to find mid-span deflection.

1.4 Test Program

A. The general program

The overall program consists of four test programs of which the first three, Parts 1, 2, and 3, were designed to develop methods and techniques to be followed in Part 4. The last test, Part 4, is the main series of the program and is the part toward which all others are directed. A large portion of Part 4 is concerned with checking theoretical methods developed earlier against field measurements on a full scale highway bridge.

The four series are described briefly below and in more detail later in Chapters II through V.

Part 1, reported in Chapter II, developed the numerical program for predicting creep and prestress loss, and tested it against laboratory model beams.

Part 2, reported in Chapter III, developed procedures for field instrumentation and tests for a full size highway bridge beam and slab.

Part 3, reported in Chapter IV, extended the program developed in Part 1 to cover the composite action of a prestressed beam with cast-in-place reinforced concrete slab. Small laboratory beams were made for the purpose.

Part 4, reported in Chapter V, is in progress at the time of this writing. It has as its primary objective the develop-

ment of the prediction method to cover full size bridge beams made of prestressed concrete and cast-in-place reinforced concrete deck slab. The interaction of the beam and deck slab is of interest, and the prestress loss in the beams is of concern. The deck was being placed when this report was in preparation, and only the prestressed beams are reported here.

Each of the four parts of the program are reported in a separate section because of the almost independent nature of each. In order to avoid undue repetition, one common section, Section 1.4-B, describes specimens and tests that were common to each of the four series.

Although Parts 2 and 3 were valuable in contributing to the knowledge needed for executing tests on the full size beams and slabs, it is not necessary for the reader to follow them in this report in order to understand the more important Parts 1 and 4.

B. Shrinkage, creep, and cylinder tests on laboratory specimens

Descriptions given in this section apply equally well to each of the major tests of this program because they describe specimens and tests that were essentially identical in each of the major parts.

Strength and stress-strain tests were made on standard size

cylinders, shrinkage tests were made on non-loaded prisms, and creep tests were made on prisms loaded by compressed helical springs. The shrinkage and creep prisms are described in tables and figures given in later sections.

(1) Cylinders

Standard size 6 x 12 inch cylinders were cast from concrete batched for the prestressed test beam specimens and the slab specimens. Both steel and waxed paper molds were used, and compaction was by rodding and mechanical vibration. They were cured throughout their test life by the side of the test beams. They were capped with commercial sulphur capping compound, and tested in a 300,000 pound capacity, screw type, universal testing machine.

Stress-strain cylinders were preloaded three times to approximately 25% of their strengths before strain data were recorded.

Strains were read from 0.0001 inch dial gages mounted in each of 4 quadrants of the compressometer. Simultaneous readings of load and strain were taken to approximately 75% of ultimate load. Load was applied continuously, after the record run was begun, until the cylinder broke. Stress strain data plots were made, and the secant modulii were determined from those plots.

(2) Shrinkage prism tests

Shrinkage prisms in Part 1 were 3 x 4 x 16 inch in size; all others were 3 x 3 x 16 inch specimens. The steel molds were fitted with hexagonal brass inserts centrally located 10 inches apart on

each side of the 3 x 16 vertical faces. Temporary screws placed through drilled holes in the steel side forms held the inserts in place until the prisms were ready for removal from the mold.

The concrete used in these specimens was taken from batches made for the main test articles. It was rodded and mechanically vibrated in the forms.

After the prisms were removed from the molds, center drilled stainless steel screws were screwed into the brass inserts to serve as gaging points.

Strains were read from a 0.0001 inch dial gage mounted in a cast aluminum frame. Conical points at ends of the measuring gage engaged the holes in the gage points for dial readings. An invar bar was used as the standard, and readings were taken from it at frequent intervals during every series of strain measurements. All gage readings were referred to the standard length of the invar bar which served as the datum.

The first strain reading was taken when the prism was removed from its mold. Readings were normally taken daily thereafter for at least a week, then they were spaced at longer time intervals from a few days early in the test to a month or so in the later stages.

(3) Spring loaded prism creep tests

Creep prisms were identical in size and in preparation to the shrinkage prisms described above. They were mounted between flat plates in a steel frame and were axially loaded by heavy helical

springs confined in the frame. Load was applied by a hydraulic universal testing machine and was maintained by running down tie-rod nuts to hold the spring in a compressed condition. The springs had modulii of 10 or 20 kips per inch depending on the amount of of the load applied. The loaded test specimens are shown in figures later in the report.

Strain readings were taken in the same way and on the same schedule as given above for shrinkage specimens.

(4) Reduction of shrinkage and creep data

Strain gage readings were taken from two opposite sides of each specimen, and the strains computed from those readings were later averaged. Strains were determined in the following way:

$$\Delta G = G - S \qquad \text{Eqn. 1-17}$$

where ΔG = gage difference; G = gage reading from specimen; and S = gage reading from the standard invar bar.

$$\text{Strain} = \Delta L = \Delta G_o - \Delta G_i \qquad \text{Eqn. 1-18}$$

where ΔG_o = gage difference at initial reading, and ΔG_i = gage difference on day i.

The strain, ΔL, includes all effects measurable by the strain gage, and those effects include the length changes in the gage itself. The difference in the coefficient of thermal expansion of the gage and the specimen would account for a portion of ΔL.

Creep strains were determined by subtracting strain for the non-loaded shrinkage specimen from strain for the loaded specimen for the corresponding day. Those specimens were stored side by

side, and readings were taken at the same time. In that way, temperature effects were cancelled out of the resulting creep strain.

CHAPTER II

CREEP OF PRESTRESSED RECTANGULAR LABORATORY BEAMS MADE OF LIGHTWEIGHT AGGREGATE

2.1 Introduction

The first step in proving the method for predicting creep in prestressed beams, as outlined in Chapter I, was to construct small laboratory beams, collect creep and shrinkage data from those beams, and test the prediction method against the measured results. This chapter gives details of that first step.

2.2 Objectives

A. to develop creep and shrinkage curves for small laboratory prestressed beams.

B. To develop a computational method for predicting creep in prestressed beams and to test that method against data collected from the beams of part A.

C. To determine the prestress loss in the beams of part A.

2.3 Test Specimens

A. Details of test cylinders are given in Section 1.4-B, and shrinkage and prism specimen details are given in the same section and in Fig. 2.1 and Table 2-1.

B. Beams - Both plain and prestressed beams 5 x 8 x 8 ft were used in the tests, Fig. 2.1 and Table 2-1. The non-prestressed beam was used for shrinkage, and the prestressed beams were used for creep.

Prestressing strands were 29 ft long between anchorage seats, and they were positioned by steel templates at each end. The stretch of strands required for stress plus 1/8 inch for take-up was marked on each strand by tape, and the strand was then stretched individually by a hydraulic jack on the day before casting. All strands for any one beam were equally stressed, and each line of strands accommodated two identical beams. Gage inserts were mounted on the two side and bottom forms at midspan, whereas top gage inserts were attached to a jig which was fastened to the form and held until the concrete was cast and hardened.

Forms were plastic-coated plywood, and they were mounted on wood blocks shimmed up to the correct elevation before casting. Concrete from the same batch was used for all beams, prisms, and cylinders for each pour, and it was compacted in the beam forms by an internal vibrator.

All specimens were set by the side of the prestressed beams after casting, and the entire casting was covered with an impervious plastic sheet. The floor beneath the sheet was flooded with water and the concrete was left in that condition to cure in the forms for one day. Forms were removed the day after casting, and the moist cure was continued under the plastic sheet until the concrete was six days old for the first casting and five days old for the second casting.

The concrete tested out at about 6000 psi at six and five day ages, respectively, for the two pours, then the moist cure was discontinued and the prestress anchorage was released. Strands were cut with an acetylene torch by slowly heating and cutting them in patterns to prevent overstressing any section. About two weeks after release, the beams were stood vertically on end and stored in a frame where they remained for the duration of the test.

2.4 Materials

Concrete was made of Type III cement, Stafford[a] lightweight

a. A product of Texas Industries, Arlington, Texas. The aggregate is an expanded clay and is manufactured at Stafford, Texas.

coarse aggregate, natural sand fines from the vicinity of Hearne, Texas, with the following mix per cubic yard of concrete: cement, 816 lb; water, 525 lb; sand, 1330 lb; coarse aggregate, 810 lb; no admix was used. It was mixed in a 6 yard transmit mixer which was charged at the casting site. Some properties of the concrete are given in Table 2-2.

Prestressing steel was 3/8 inch diameter 7 wire strand[b] with properties as listed in Fig. 2.3.

2.5 Tests

Shrinkage, creep, strength, and stress strain tests are described in Section 1.4-B, and there were no deviations from those procedures in this series of tests.

Strain readings were taken from the beam specimens in the same way and on the same schedule as those from the prisms. Each beam had gages at midspan on top, bottom, and the two opposite vertical sides. The four sets of readings taken from the shrinkage beam were averaged, as were the two sets from the sides of the prestressed beams. The stressed beam strains were reduced to creep by subtracting shrinkage of the companion non-stressed beam, and plots of strains versus time were produced for each beam.

2.6 Test Results and Discussion

A. Mechanical properties - Figs. 2.2 and 2.3 show stress-strain curves for concrete cylinders and prestressing strands, and

b. 1 x 7 Tufwire Strand, TW 906, Sheffield Div., Armco Steel Corp., Kansas City, Missouri.

properties are tabulated in Table 2-2. There is good agreement between strengths of batches cast on the two different dates, and the secant modulii are in good agreement except for the 40 day age tests of the batch of April 23, 1964.

B. Shrinkage - Strains in non-loaded specimens include the effects of all factors influencing dimensional changes in the stressed specimens of these tests. Drying shrinkage at early age caused most of the change, but temperature changes, and possibly other things too, had some effect. Assuming that creep and shrinkage specimens react in the same way to those things, it is not of primary concern in these tests what causes the shrinkage. Since shrinkage is deducted from total strains in order to get the value for creep, the net result is to remove all effects except creep, whatever might be their causes or magnitudes, from the test. It is known, of course, that some effects are not independent of stress, therefore the treatment given here might produce values that are in error because of that dependence.

Fig. 2.4 displays the variation of shrinkage of a 3 x 4 prism and Fig. 2.5 presents corresponding information for the 5 x 8 beam. The dates of castings of these two specimens differ by two weeks, but other conditions are the same. The curves show that the smaller specimen had the higher rate of shrinkage during the first three months but after that the changes were largely seasonal. At about six month age, a plateau of shrinkage was reached and only seasonal variations changed the magnitude of the shrinkage for the remainder of the test. The larger specimen was much more stable than the smaller one.

The same kind of plateau as mentioned above is evident in several curves of shrinkage in non-controlled environment in the work of Jones, Hirsch, and Stephenson (4). In that work, sand-and-gravel concrete stored in laboratory air leveled off at about 400 days, Ranger lightweight aggregate concrete at about 180 days, and Stafford lightweight aggregate concrete at about 240 to 300 days for some mixes. Specimens under exposed conditions in those tests showed marked changes in strain with the seasons. Hatt (11) reported work at a much earlier date which showed some effect of air storage on strains in non-loaded specimens.

C. Spring loaded creep - Creep in spring loaded specimens was computed by deducting shrinkage, Fig. 2.4, from total strains measured in the loaded prisms. Fig. 2.6 shows strain versus time for specimens 15-1 and 15-2 which were loaded with an initial compression stress of 1250 psi. The curve of measured strains shows the same pattern of variation with time as are found in Fig. 2.4. When the shrinkage strains were deducted, most of the seasonal variation vanished, but not all.

It has been shown by Davis (15) and by Neville and Meyers (13) that creep is not independent of storage conditions and by Ali and Kessler (1) that shrinkage is not independent of stress. The residual change displayed in Fig. 2.6 after deduction of shrinkage, is probably due to the interdependence of these factors.

Creep behavior of other specimens was similar to that displayed in Fig. 2.6 and are not shown for that reason.

It is shown in Appendix B that the losses of spring load due to elastic straining of the steel frame and creep plus shrinkage of the concrete are 1.52, 2.57, and 2.73 percentage, respectively, of the initial loads of 10, 15, and 20 kips. That small loss accumulated during the time of duration of load was considered to be negligible in determining ordinates for the unit creep curve.

Creep strain from the three spring loaded specimen pairs are reduced to creep per unit stress in Fig. 2.7. That curve represents the average of the three sets of specimens under 10, 15, and 20 kip loads, respectively. The 10 kip values are a little lower than those for the 15 and 20 kip loads where the latter two are in good agreement. Although there are questions as to the validity of a unit creep expression covering a wide range of stress values, these stresses are low and, for the purpose of these tests, the unit creep curve worked out well. Roll (12) cites a number of references limiting linearity of creep-to-stress to stress levels below some 20 to 40 percent of ultimate. Neville and Meyers (13) on the other hand support linearity within the range of working stresses. The highest stress to strength ratio in the spring loaded creep tests was less than 0.30, well within working stress ranges.

The unit creep curve developed from the results of this test series was used in predicting creep strain in prestressed beams discussed in the next section.

D. Prestressed beam creep - Creep strains in prestressed beams were determined in the same way as those in the spring loaded specimens. Those strains computed from measurements of strains in five prestressed beams and in one non-loaded companion control specimen are shown in Figs. 2.9 through 2.11. Five pairs of prestressed beamswere tested for approximately two years, and the strains were compared at the end of that time. Details of the beam sections are shown in Fig. 2.8, and initial prestress, prestress loss, and final prestress are given in Table 2-3.

Strains of beams of the same pair were found to be in excellent agreement, and the second beam of each pair was then withdrawn from the test. Each of those withdrawn beams was sawed into two pieces at mid-length for purposes of checking positions of prestressing steel. Some departures of actual position of the centroid of the prestressing steel from the design values were found, and the corrections were made and included in calculations for initial stress at release and for creep predictions. Since all beams were prestressed with straight strands and, after stressing, were stored vertically to rest on one end, the stress magnitude and distribution was theoretically constant throughout each pair of identical specimens.

In the search for a method that would predict creep in prestressed beams at any age after prestress release and after transverse loading, it was felt that all factors that influenced creep should be taken into account in the method. There are a

number of those factors, and they have been discussed by many who have investigated creep of concrete. One of the latest works presenting a comprehensive discussion of those factors is that of Neville and Meyers (13) in which the following factors are discussed:

1. Mix constituents
2. Mix proportions
3. The mixing and placing operation
4. Age of specimen
5. Stress level
6. Temperature
7. Humidity
8. Size of member

All of the factors that influence strains in the concrete under its conditions of service can be partially accounted for by using data from test specimens which conform as nearly as possible to the prototype. In this series of tests, the prestressed beam might be considered as the prototype and the prisms as the test specimens. Since all test articles -- the prototype as well as the test specimens -- come from the same batch, the first three items in the above list were satisfied. Item 4 is satisfied in that dates of mixing and ages of loading are the same, or essentially so; see Table 2-1. Items 6 and 7 were identical in the cases of both the beams and prisms. The remaining items 5, stress level, and 8, size of member, were not the same in beam and prism.

There does not appear to be any question that shrinkage of members of a given shape in a constant environment of say 70°F and 50% relative humidity will occur at a faster rate for a member with a large surface area-to-volume ratio than one with a small such ratio. Thus, it should be expected that the prism, 3 x 4 section, would shrink at a faster rate than the beam, 5 x 8 section, in such a controlled environment, up to the time that the volume is stabilized.

On the other hand, shrinkage in a non-controlled environment where temperature and relative humidity fluctuate from day to day is far different than that in the controlled environment. The ratio of surface area-to-volume acts in a similar way in absorbing moisture as it does in giving off moisture to atmospheres with relative humidity differing from the moisture content of the specimen. In Figs. 2.4 and 2.5, it will be noted that although the magnitude of shrinkage of the smaller specimen is greater than the larger specimen, the seasonal fluctuations, too are larger, especially at early age. Thus, the small specimen, with the larger ratio of surface area to volume, gains volume in moist air at a faster rate than the larger specimen just as it loses it at a faster rate in dry air.

The shrinkage of the beam and prism specimens stabilized at about six months age to some 600 and 800 micro inches per inch, respectively, and played about those general values depending on seasonal changes.

From the values that developed in the shrinkage specimens, it appears that a shrinkage specimen of approximately the same size and shape as the prototype should be used to determine the shrinkage component of strains in the prototype. In the computations made for predicting creep strains of beams in these tests, the shrinkage component was taken from measurements on a non-loaded specimen identical to the prestressed beam in all respects except that of stress.

Prestressed beam stresses at release, the maximum during test, ranged from 94 psi tension in the top of beam 5 to 1933 psi compression in the bottom of the same beam. At release, the concrete had a breaking strength of 6050 psi and the maximum stress to strength ratio at release was slightly less than 0.30.

The creep in spring loaded specimens of these tests was linear with stress within the ranges treated. Those specimens had stress-to-strength ratios of slightly below 30%, which was about the same as that of the prestressed beams. On the basis of those tests and the reports of Roll (12) and Neville and Meyers (13), the use of a linear creep to stress relationship is justified for the stress range of these tests.

Both exponential and hyperbolic functions (13) have been used for expressing creep and shrinkage of concrete. Shrinkage and unit creep from these tests were plotted on semi-log paper, Fig. 2.12, using the expression that was successfully used by Hanson (14). It may be seen from that figure that these data did not fit a linear

logarithmic curve. After much experimentation with the data, it was found that they would fit reasonably well a higher order logarithmic expression of the type:

$$\varepsilon = C_1 \text{Ln}(t + 1)^2 + C_2 \text{Ln}(t + 1) + C_3 \quad \text{Eqn. 2-1}$$

where ε is strain, t is age in days, and C_1, C_2, and C_3 are constants. Those constants were determined by using the least square method of fit to measured values. Such an expression was necessary to get a reasonable fit at early and at late ages.

It was found that the hyperbolic expression (24)

$$\varepsilon = (\varepsilon^{\infty} t)/(n + t) \quad \text{Eqn. 2-2}$$

would fit the data well over the entire range. In that expression, ε is strain, ε^{∞} is strain at time equal to infinity, t is age, and n is age at which strain of 1/2 ε^{∞} occurs.

To evaluate the ultimate strain ε^{∞} and the constant n, it is convenient to rewrite the above equation as follows:

$$t = \varepsilon^{\infty} \frac{t}{\varepsilon} - n \quad \text{Eqn. 2-3}$$

The slope of this linear function is ε^{∞} and its time intercept is n, both of which are constants.

In general, the hyperbolic function tends to underestimate the strains at earlier ages, and specially when the data are taken from a specimen subjected to low humidities and temperatures for a long period of time.

Predictions of creep were made for beams 1 through 5 using both the logarithmic and hyperbolic expressions for unit creep and for shrinkage. Better results were developed from the

hyperbolic fit and those results are shown in Figs. 2.9 through 2.11.

Predicted creep was computed by the method outlined step-by-step in Chapter I. Detailed steps of the method in Fortran IV for IBM 7094 computer and the results are given in Appendix C. Each beam required only a few seconds of machine time for computation.

Measured creep and computed creep are shown for beam 1 in Fig. 2.9. The prestress in this beam was constant across the section, and the fit between the computed and the measured creep is good. Measured creep reached a plateau at about six month age and stayed there for almost a year. The rise in strains that begin at about 500 days is due to shrinkage, see Fig. 2.5.

Beam 2 was prestressed by straight eccentric strands to produce a little more initial prestress in the bottom fibers than in the top. The measured creep was so nearly the same in the top and bottom, however, that only the average curve is shown in Fig. 2.9. A perfect fit would arrange the computed curves symmetrically about the measured curve, but up to about four months age the computed values are high. For the remaining period, the agreement between measured and predicted creep is good.

Measured and computed creeps for beam 3 are compared in Fig. 2.10 and the agreement is rather poor throughout the test. A careful check of all data failed to disclose any reason for that poor agreement. Measured strains are higher than predicted strains

throughout the test. The evidence on the curves indicates that a mistake was made in locating the steel or in initial prestress. Measurements in the beam that was cut into two pieces showed that the steel was positioned correctly, and each steel strand was carefully checked at initial tensioning to be sure that equal strain was put in all strands.

The curves for beam 4, Fig. 2.10, behave in the same way as those for beam 3 at about 1 1/2 year age, although they are in good agreement up to about one year age. Computed top strains are a little low throughout, but middle and bottom strains agree fairly well.

There is greater stress gradient in beam 5 than in any other beam and the strains in Fig. 2.11 bear that out. There is excellent agreement at mid-depth throughout, fair agreement in bottom fiber strains, and rather poor agreement in top fiber strains where stress was very low.

Eccentricity of strands in the companion beam 5, when it was cut in two at midspan, was found to be about 1/8 of an inch greater than called for in the design. The design eccentricity has been corrected in the curves of Fig. 2.11. Laboratory records of measured strand load were closely checked and were found to agree with design values.

Prestress losses, Figs. 2.13 to 2.15, are high but this would be expected because of the high shrinkage of the concrete and because of the relatively high creep. Yang (7) in similar

tests, but using a different mix of the same aggregates, obtained prestress losses of about 25 to 35% of initial prestress. Furr (8) in tests of small uniformly stressed prestressed slabs found prestress losses of about 25 to 30% with the same aggregates but the concrete mix was different than that used in these tests. The prestress loss curves show good agreement between measured and predicted values. The measured values represent the product of total strain multiplied by the modulus of elasticity of the steel strands, and predicted values were found by computations in the step-by-step method outlined for computing creep. The agreement between prestress loss curves corresponds to the agreement between measured and predicted strains for any given beam. This is as should be expected because computational methods were similar.

2.7 Conclusions

On the basis of test results from this series, the following conclusions are drawn:

1. With the support of shrinkage and unit creep data, the rate-of-creep method as outlined in this report provides reasonably accurate predictions of creep in small laboratory prestressed beams.
2. Prestress losses from creep and shrinkage can be computed along with predicted creep values. Those prestress losses in beams of these tests ranged from 30 to 36% of initial prestress.

3. The experience with the rate-of-creep method for predicting creep in specimens of these tests indicates that the method would be applicable to full size prestressed concrete structures.

Table 2-1 Specimens for Laboratory Rectangular Beams

Designation	Size (in.)	Type	Date Cast	Date Loaded	Stress at loading (psi)		Prestress force lbs. after release Computed	Prestress force lbs. after release Measured[3]
0-1	3x4x16	Shrinkage	4/23/64					
10-1&2	3x4x16	Spring Loaded	4/23/64	4/30/64	833			
15-1&2	3x4x16	Spring Loaded	4/23/64	4/30/64	1250			
20-1&2	3x4x16	Spring Loaded	4/23/64	4/30/64	1667			
C-1	5x8x8ft	Shrinkage	5/07/64					
1	5x8x8ft	Prestress	5/07/64	5/12/64	1780[1]	1780[2]		
2	5x8x8ft	Prestress	4/23/64	4/30/64	1377	1793	63400	62600
3	5x8x8ft	Prestress	5/07/64	5/12/64	501	1789	45800	-
4	5x8x8ft	Prestress	4/23/64	4/30/64	784	1518	46040	46500
5	5x8x8ft	Prestress	4/23/64	4/30/64	-94	1933	36800	36300

[1]Stress at top of beam (f^{top}), (-) tension, (+) compression.

[2]Stress at bottom of beam (f^{bot}), (-) tension, (+) compression.

[3]Measured strain at release $x(E_s A_s)$ = Measured prestress force.

Table 2-2 Concrete Properties

Batch date	Age of Test (days)	Strength "f'_c" (psi)	Secant Modulus at $1/4f'_c$ (ksi)	Secant Modulus at $1/2\ f'_c$ (ksi)
4/23/64	4	5860	2870	2690
	7	6050	3020	2780
	40	6230	4210	3580
	114	6080	3600	3200
5/07/64	4	6140	3270	2820
	7	6050	3690	3060
	35	6410	3410	2920
	100	6270	3410	3040

Table 2-3 Concrete Stresses in 5x8x8 Beams

at Release and at end of 660 Days

Beam	Stress at release (psi)			Stress at 660 days (psi)		
	top	bot.	cgs	top	bot.	cgs
1	1780	1780	1780	1252	1252	1252
2	1377	1793	1594	1013	1320	1173
3	501	1789	1266	370	1322	935
4	784	1518	1190	586	1134	889
5	-94	1933	1292	-71	1455	973

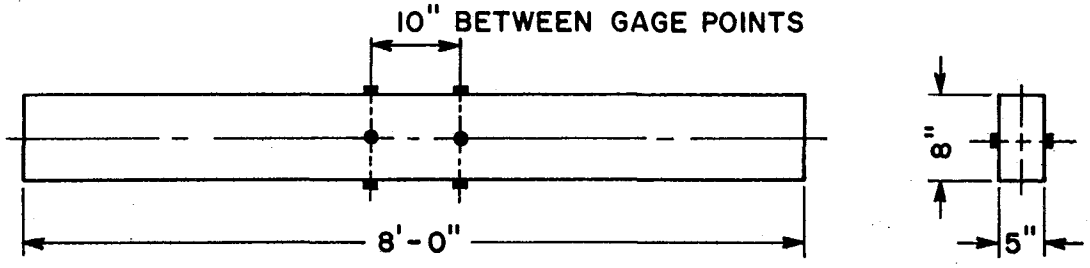

(a) BEAM

NOTE: IN ALL SPECIMENS GAGE POINT INSERTS WERE CAST IN THE CONCRETE. GAGE POINTS WERE INSERTED AFTER REMOVAL OF FORMS.

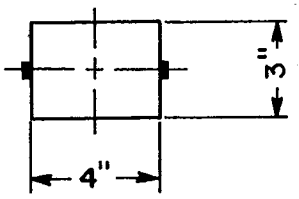

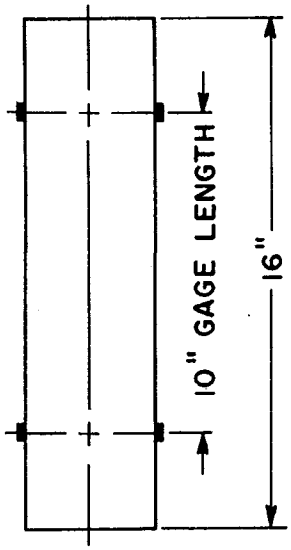

(b) SHRINKAGE PRISM

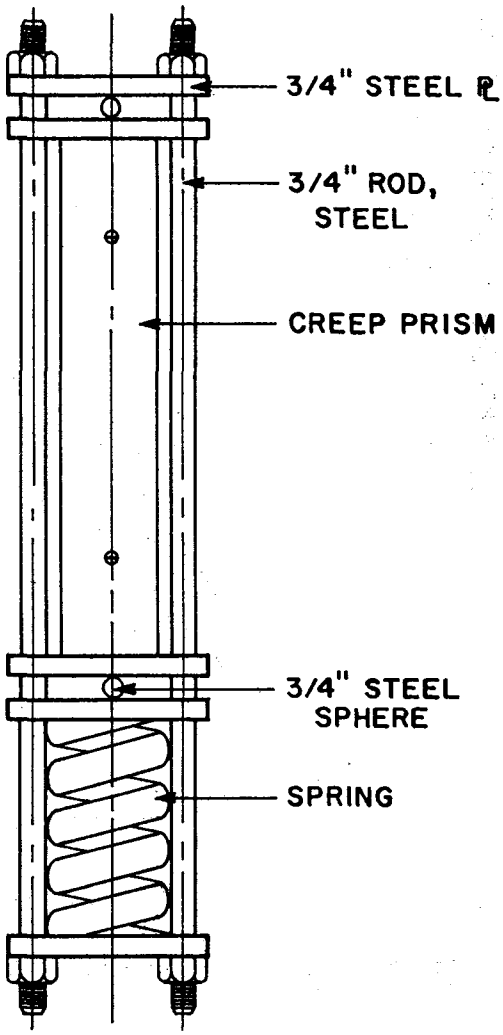

(c) SPRING LOADED CREEP PRISM

FIGURE 2.1 TEST SPECIMENS

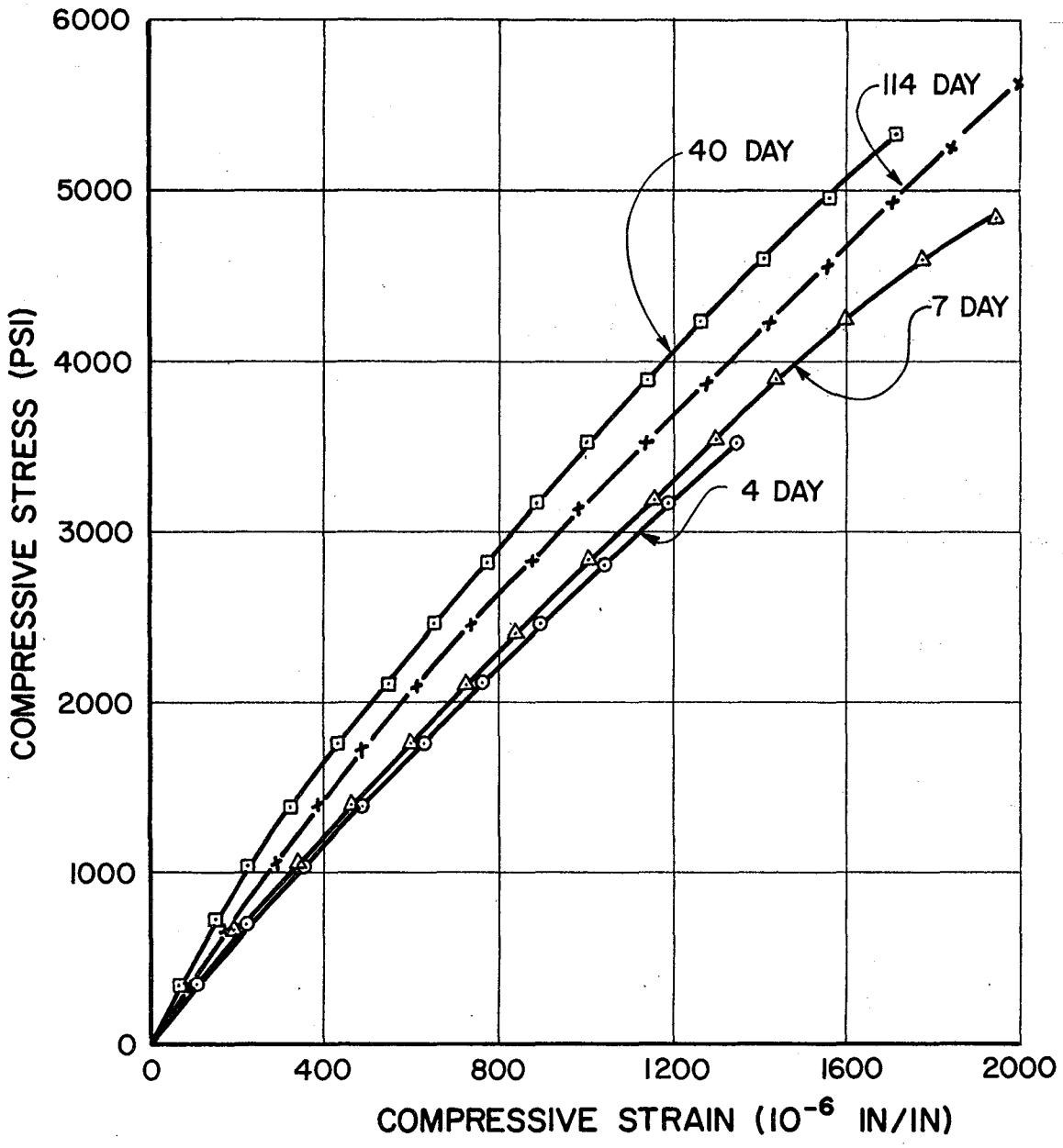

FIGURE 2-2 CYLINDER STRESS-STRAIN DIAGRAM FOR BATCH OF APRIL 23, 1964.

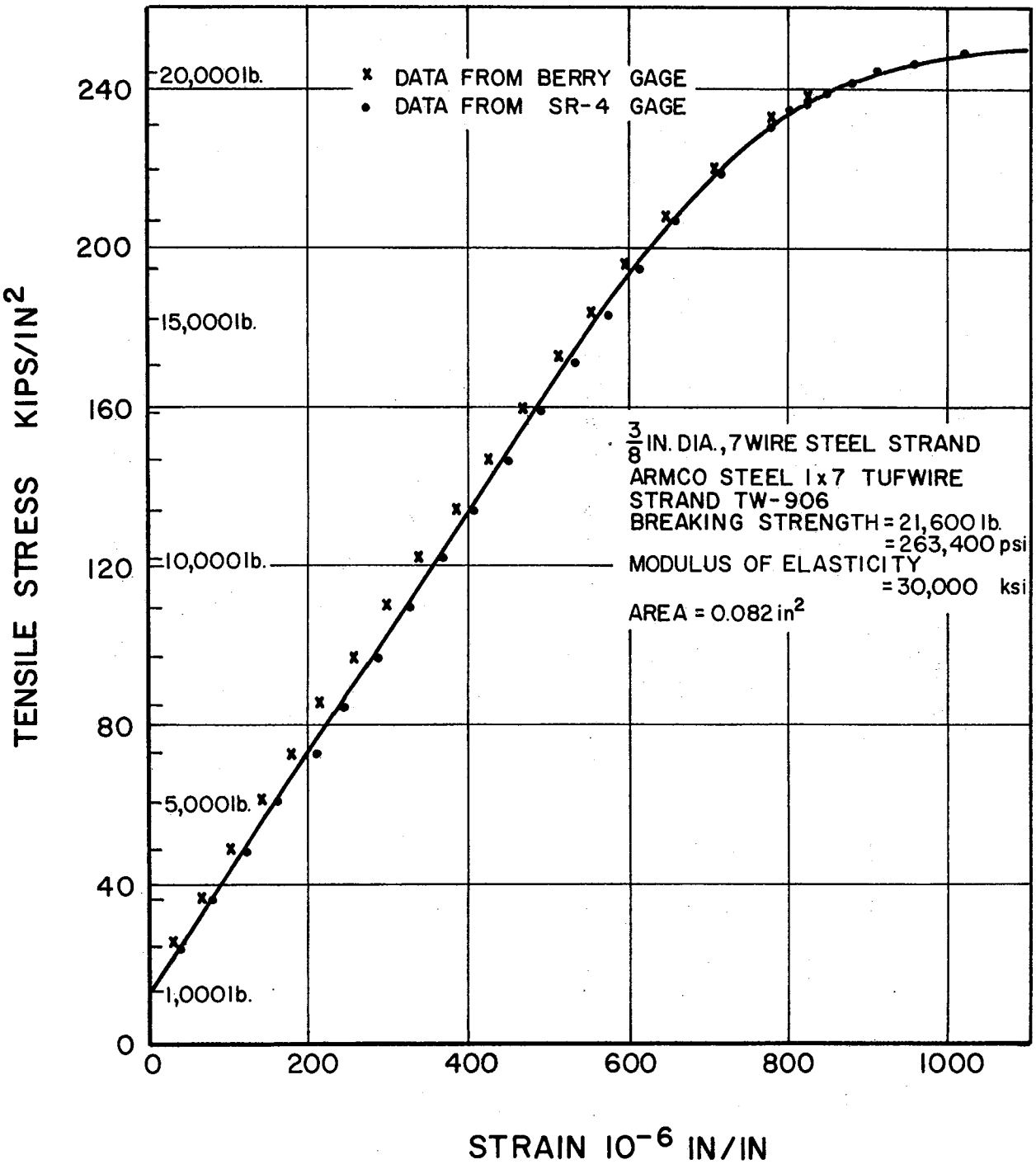

FIGURE 2.3 TENSILE STRESS STRAIN CURVE FOR PRESTRESSING STRAND

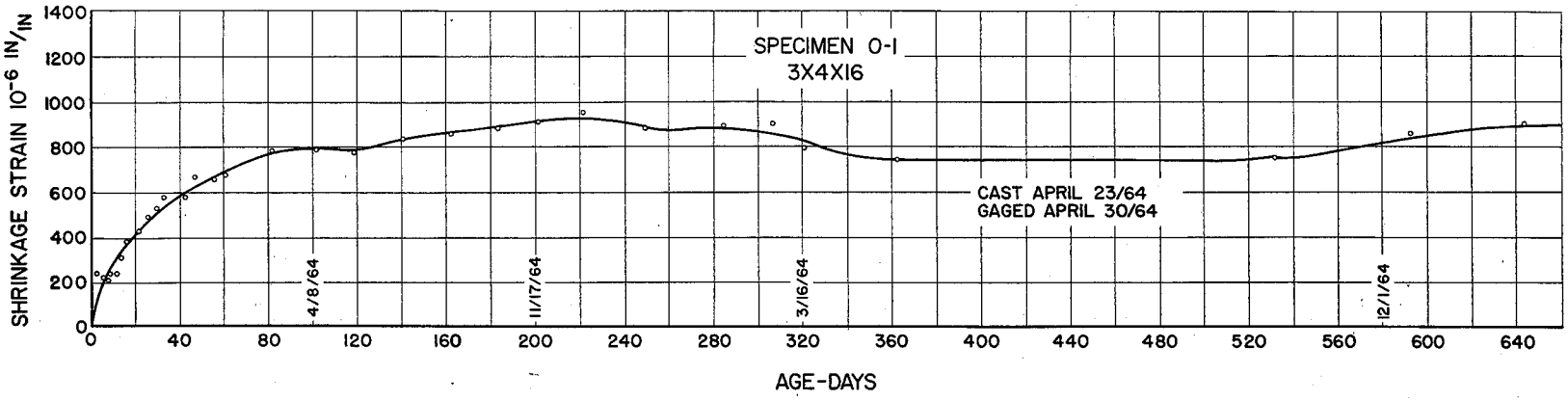

FIGURE 2.4 SHRINKAGE OF 3X4X16 SPECIMENS

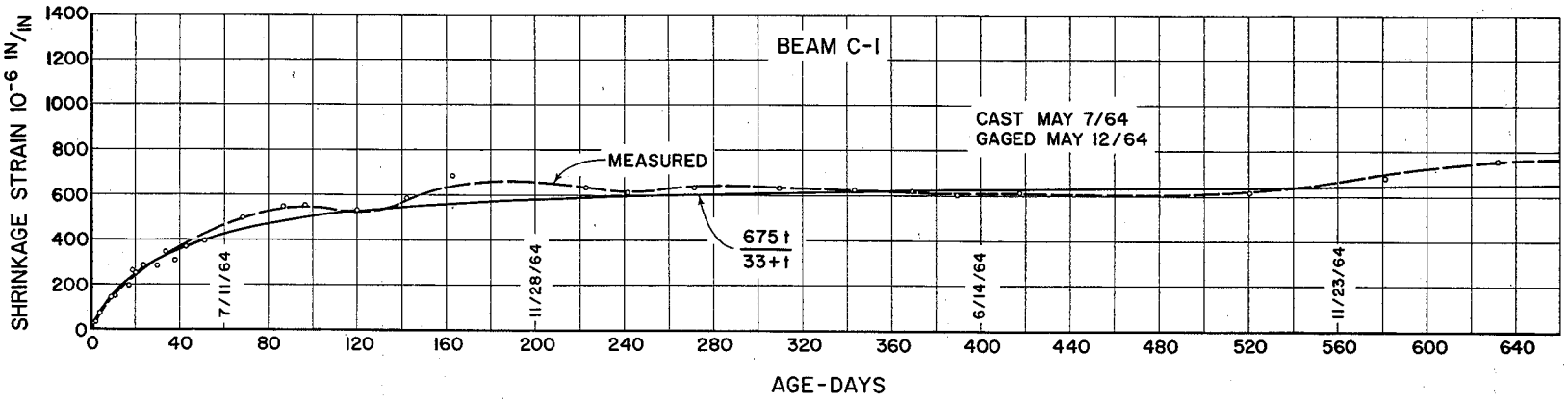

FIGURE 2.5 SHRINKAGE OF 5X8 BEAMS

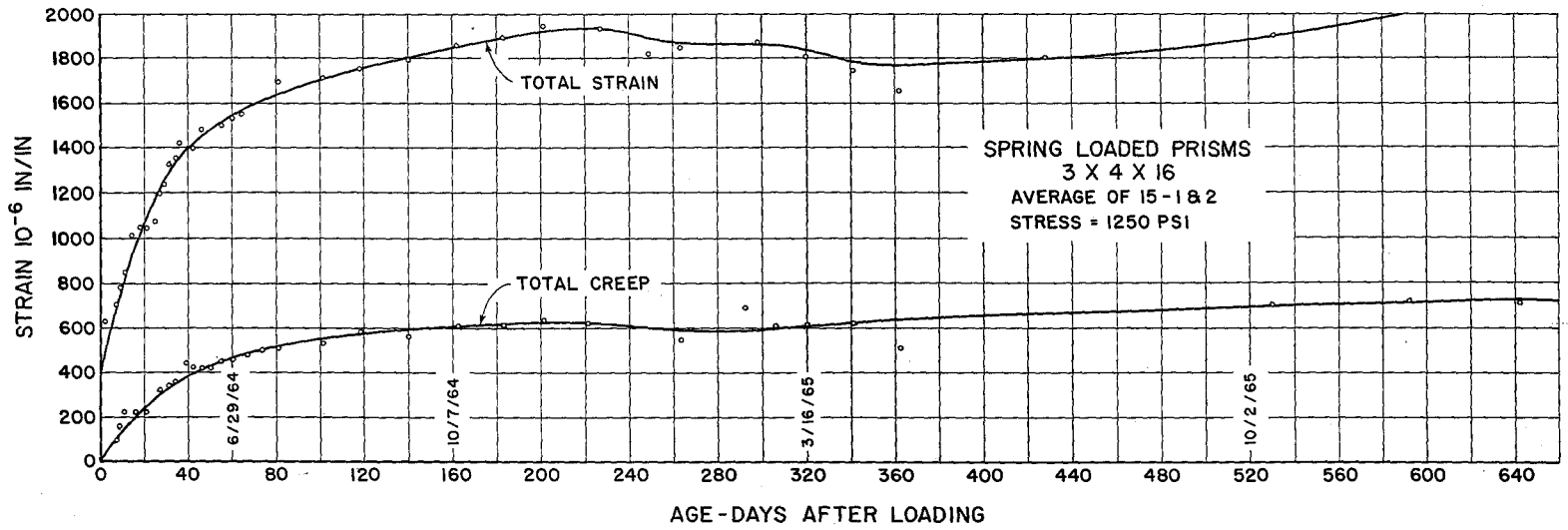

FIGURE 2.6 TOTAL STRAIN AND CREEP UNDER CONSTANT STRESS

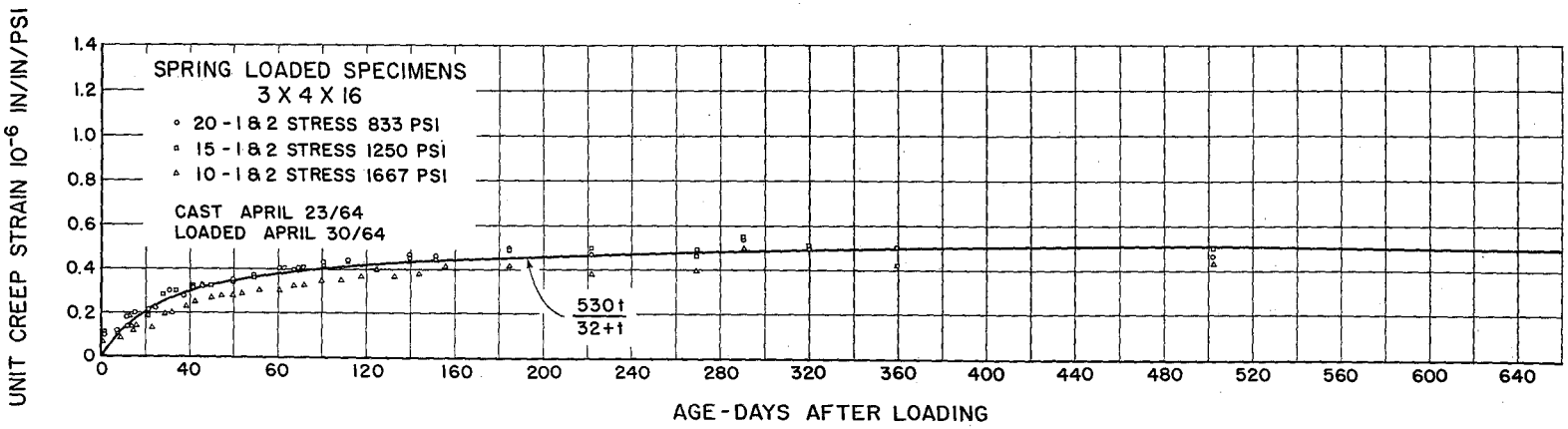

FIGURE 2.7 UNIT CREEP CURVE

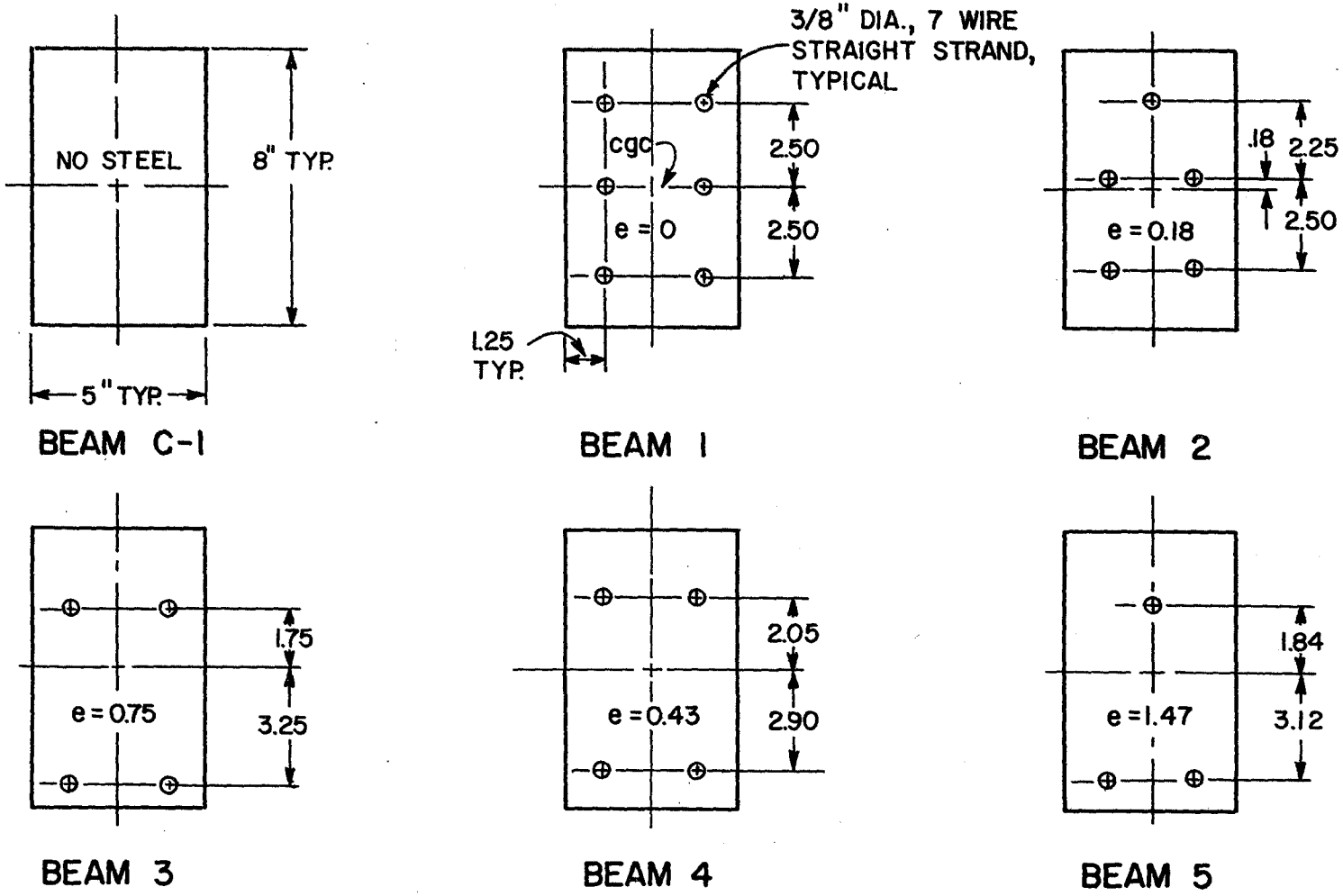

FIGURE 2.8 STEEL LAYOUT

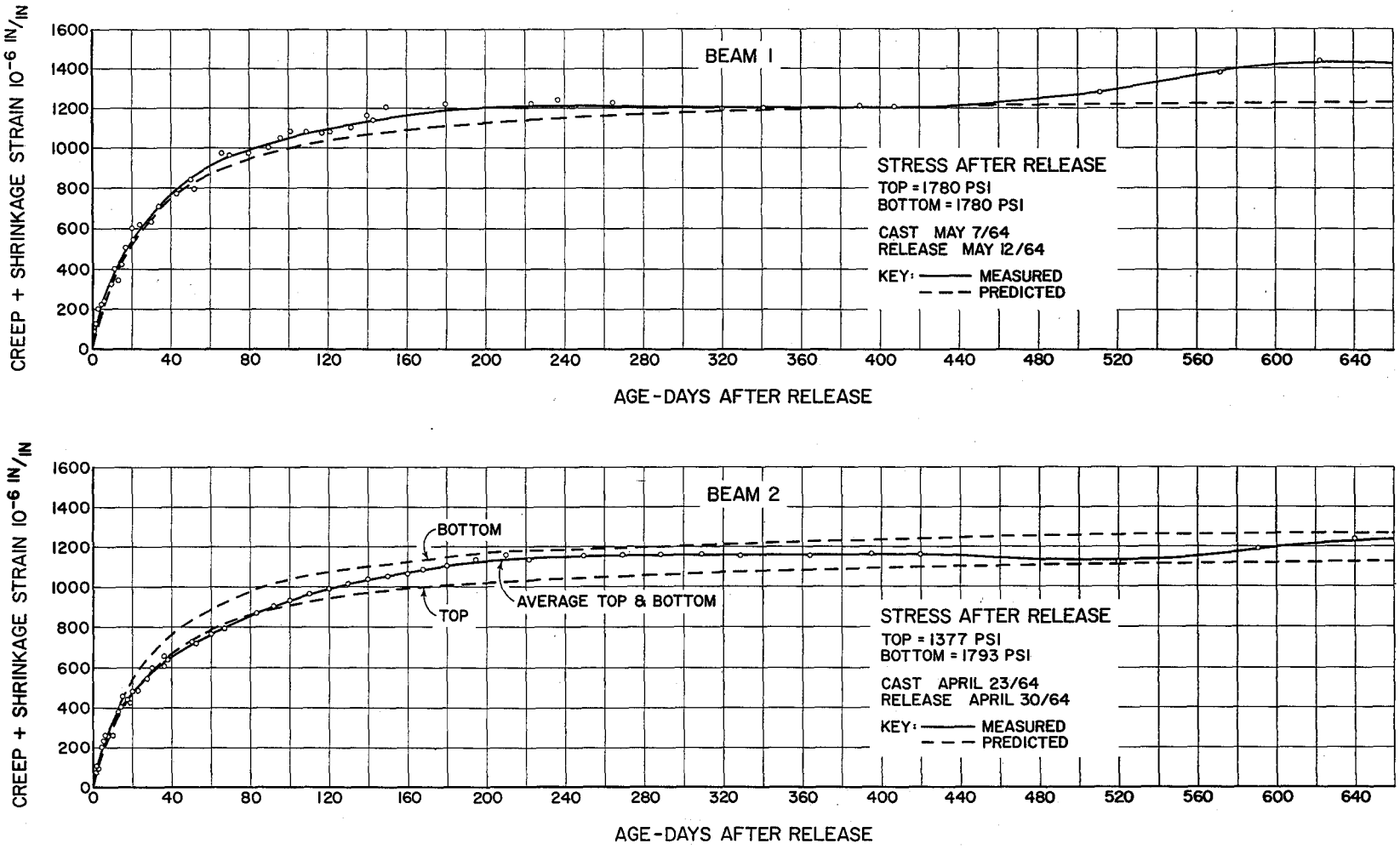

FIGURE 2.9 STRAINS IN 5 X 8 PRESTRESS BEAMS 1&2

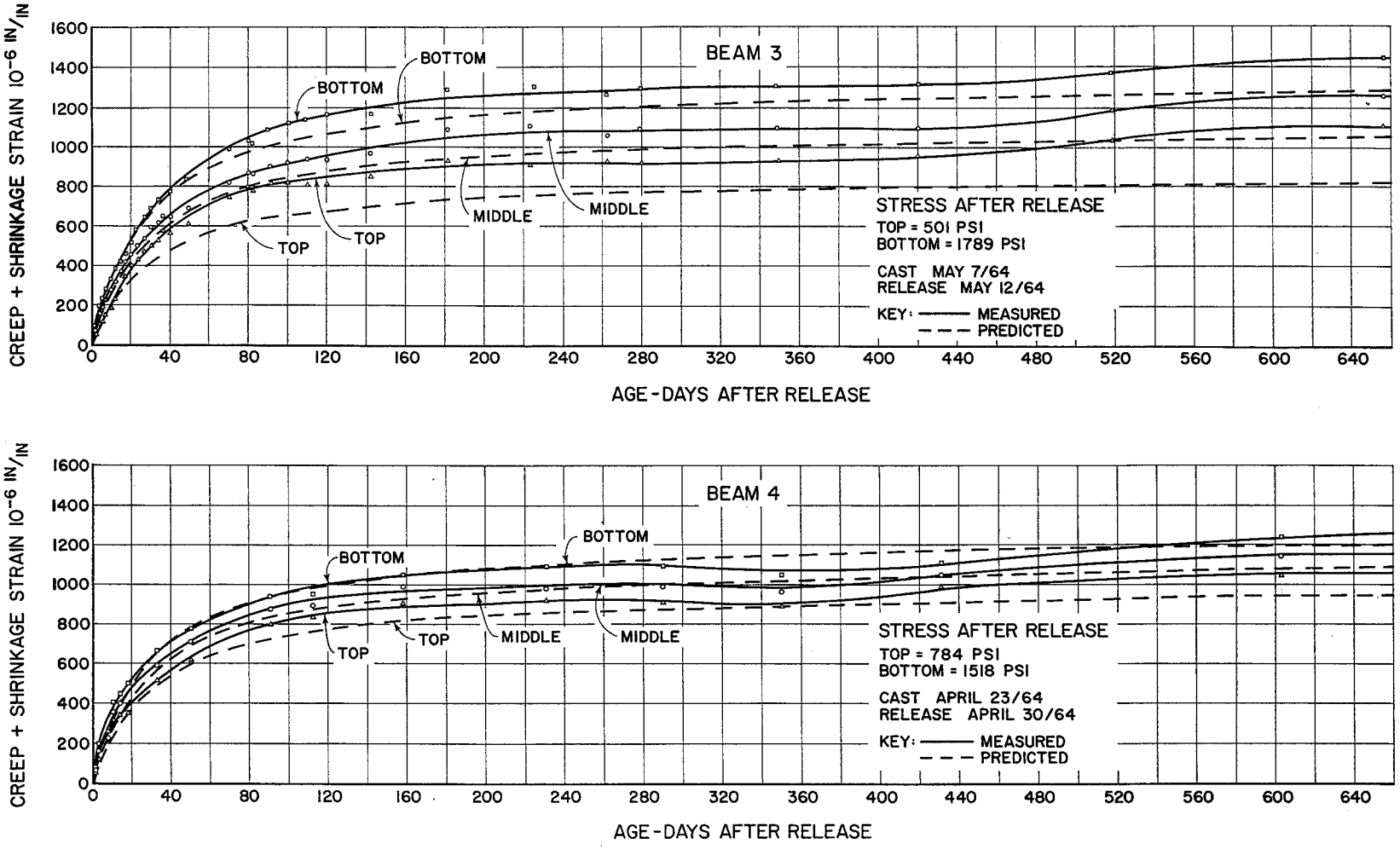

FIGURE 2.10 STRAINS IN 5 X 8 PRESTRESS BEAMS 3 & 4

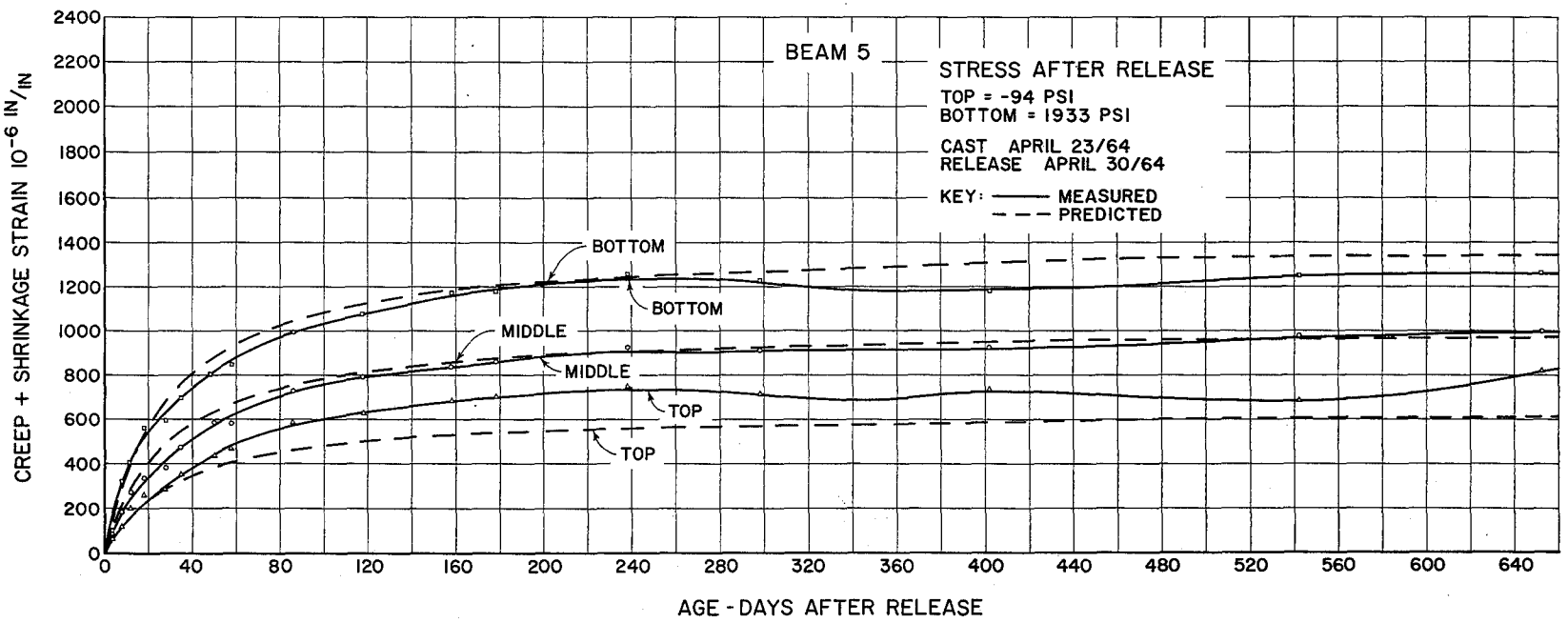

FIGURE 2.11 STRAINS IN 5X8 PRESTRESS BEAM 5

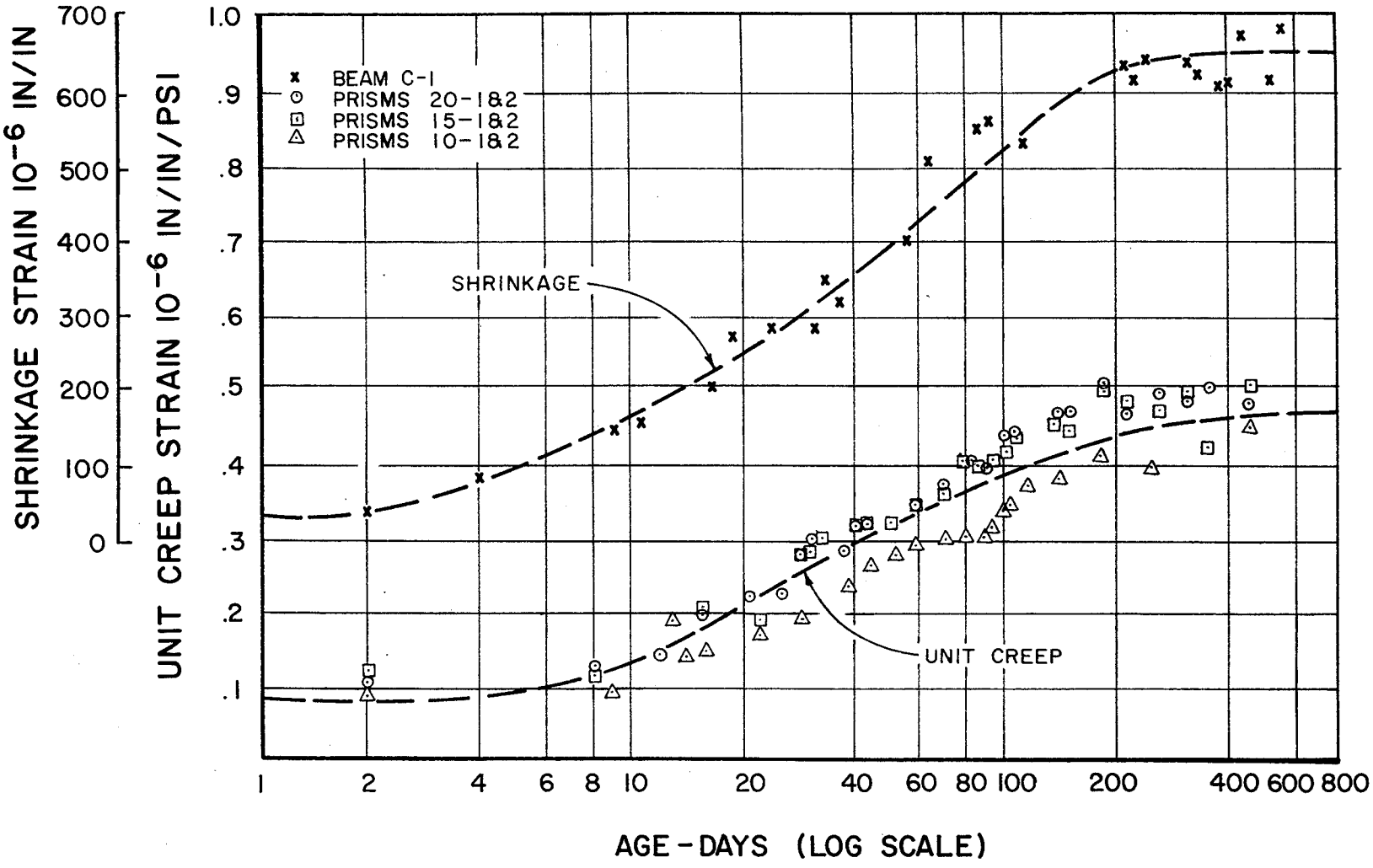

FIGURE 2-12 SHRINKAGE AND UNIT CREEP STRAIN VERSUS TIME

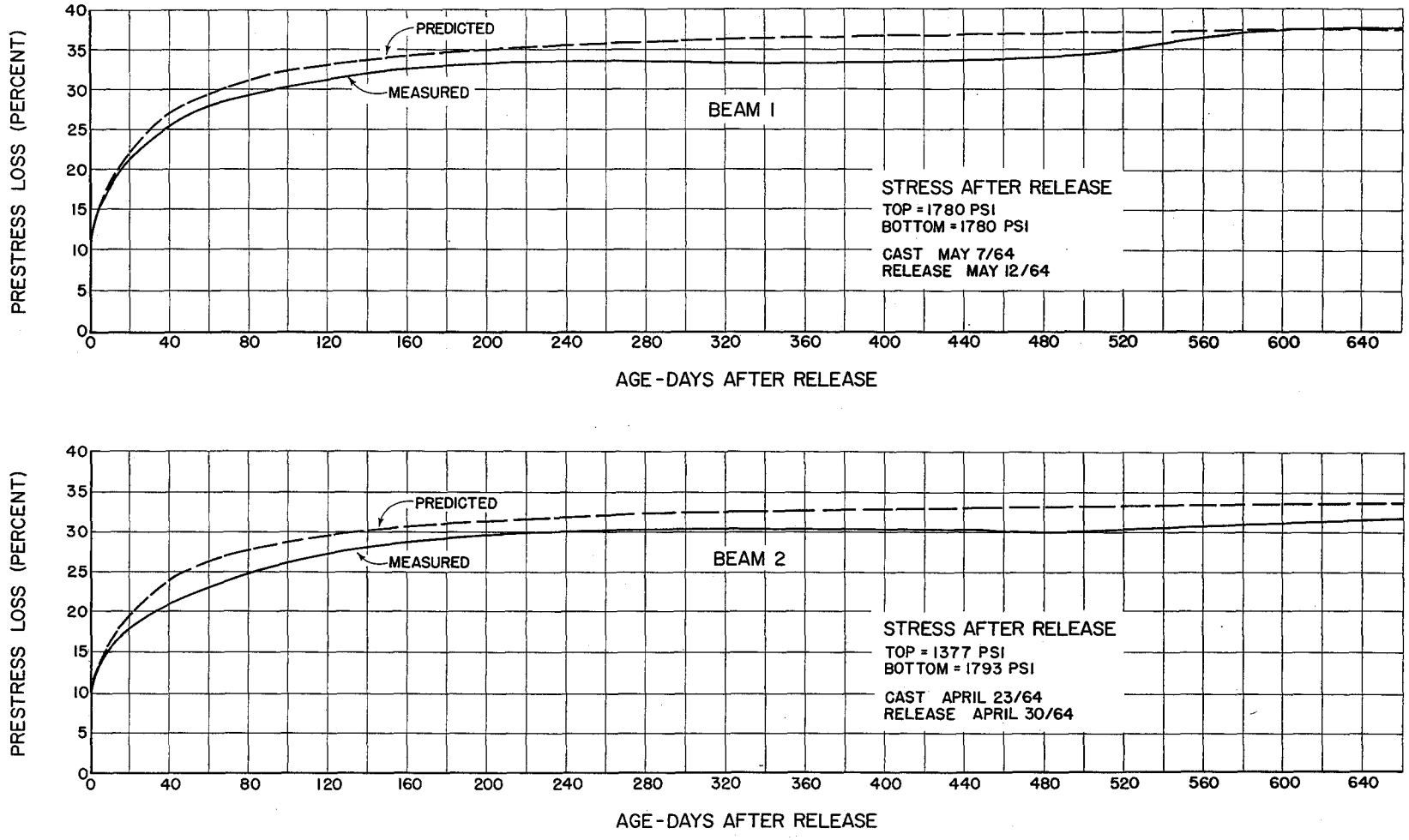

FIGURE 2.13 PRESTRESS LOSS IN 5X8 PRESTRESS BEAMS 1&2

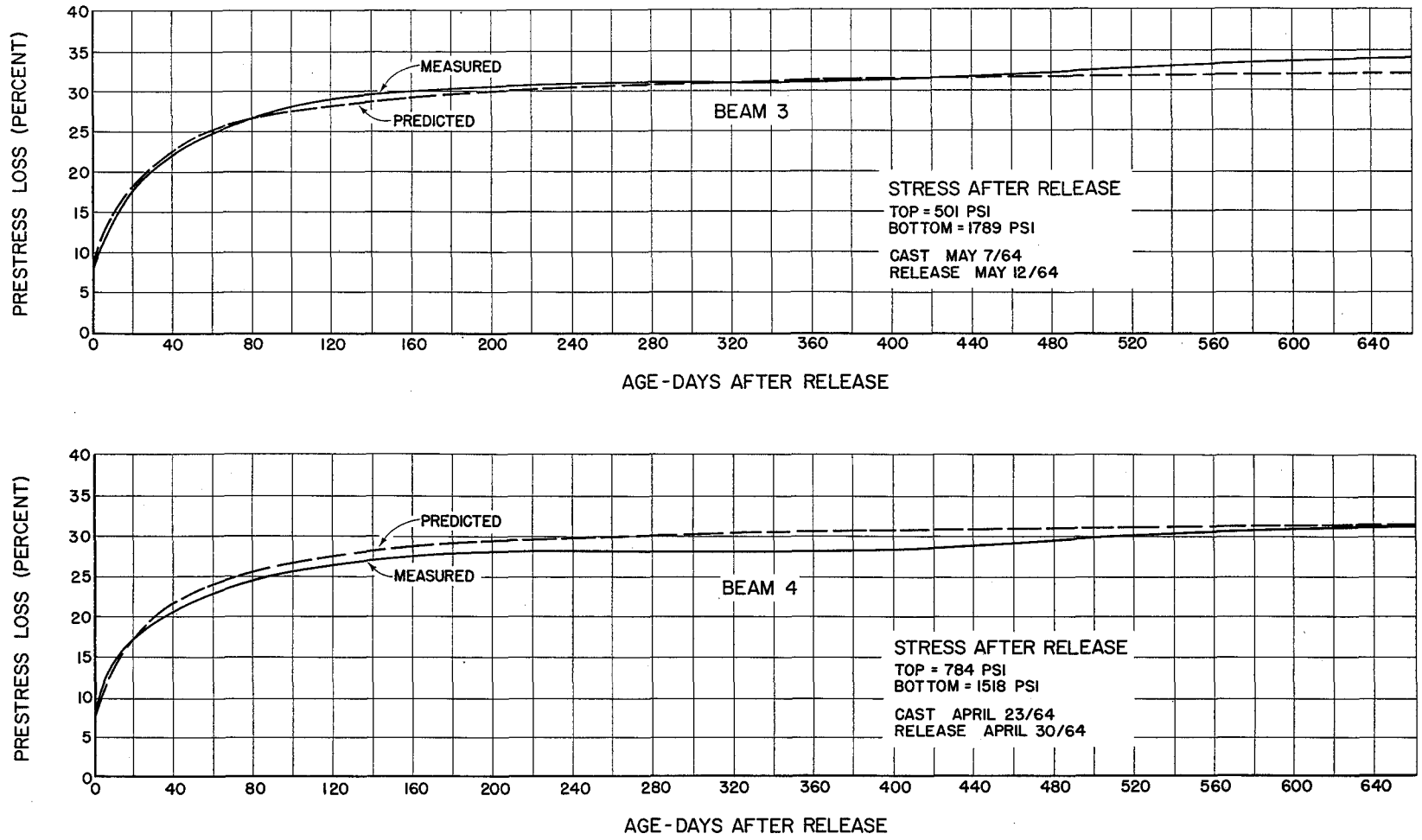

FIGURE 2.14 PRESTRESS LOSS IN 5X8 PRESTRESS BEAMS 3&4

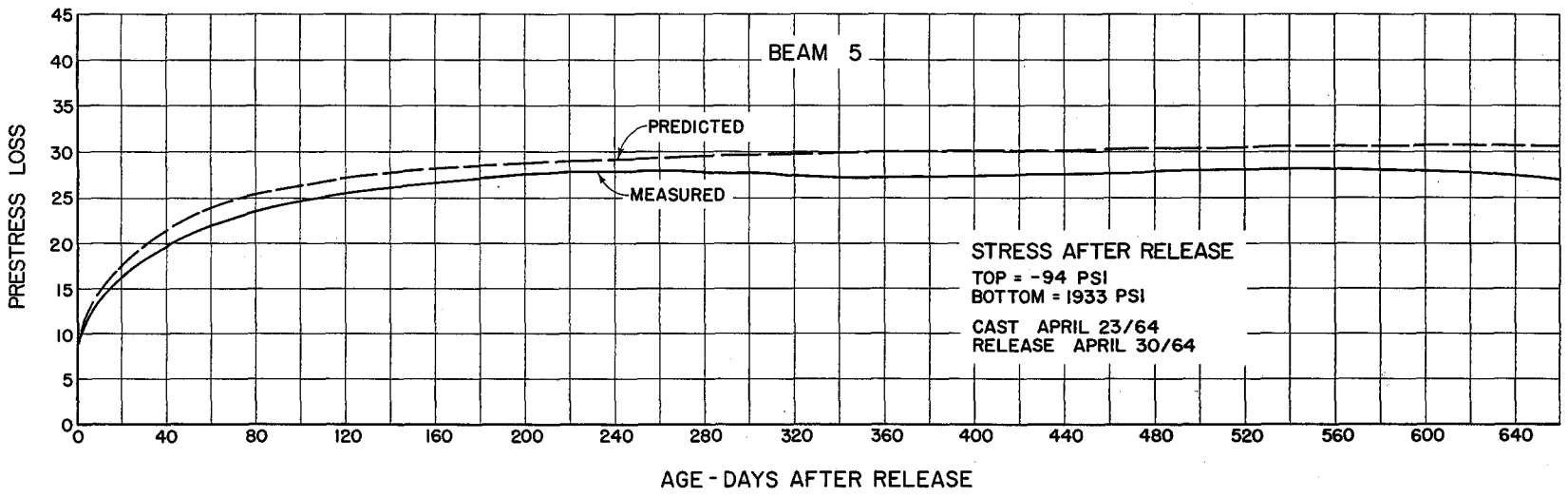

FIGURE 2.15 PRESTRESS LOSS IN 5X8 PRESTRESS BEAM 5

CHAPTER III

LITTLE WALNUT CREEK BRIDGE

3.1 Introduction

The Little Walnut Creek bridge in U. S. Highway 290, just east of Austin, Texas, was selected as a test structure for instrumentation and testing of techniques because of its type, location, and time of construction. That two-lane, three span, H 20-S16 bridge was to carry two lanes of eastbound traffic on a cast-in-place deck carried by prestressed concrete beams.*

One prestressed beam and portions of the slab adjacent to that beam were instrumented, Fig. 3-1, along with small prismatic specimens, Fig. 3-2.

3.2 Objectives

A. To instrument and collect creep and shrinkage data from a full size prestressed bridge beam and reinforced concrete deck slab.

B. To use the processed data on creep and shrinkage, from paragraph A above, in developing a criterion for predicting creep deflection of prestressed bridge beams.

C. To test the instrumentation plan and the techniques used on this set of test specimens for application on a more completely instrumented bridge.

---

*Texas Highway Department Type C., Texas Highway Department, Bridge Division Drwgs. Title Prestressed Concrete Beams, GpA1, GpA2, GpC1, and GpC2.

3.3 Test Specimens

A. One full-size prestressed beam, Fig. 3-1, was one of the main test articles. Brass inserts were cast in the concrete, and stainless steel gage points were installed when forms were removed.

The instrumented beam was the middle one of five beams set 8'-9" on centers, and it was designed by the Texas Highway Department. The design initial prestress at midspan was 339 psi top fiber compression and 2411 psi bottom fiber compression. That prestress was provided by 40-7/16 inch diameter 7-wire straight strands. The beam was cast on March 31, 1965 in Austin, Texas, and prestress was released on April 2. The concrete was compacted by internal vibrators.

B. The reinforced cast-in-place concrete slab panel adjacent to the test beam was the other main test article. That slab was cast on May 24, 1965 on which date the beam was 54 days old. Brass inserts for later installation of stainless steel gaging points were fastened to the wood bottom forms at the same stations that were gaged on the beam. Those inserts were cast in the concrete when it was placed. Top-of-slab gage inserts were to have been placed with a jig immediately after the surface was screeded to a finish, but the concrete was so stiff at that time that the inserts would not seat firmly. They were set into small holes dug into the slab before it hardened, and epoxied into place.

C. Standard size cylinders were cast from both beam and slab concretes for strength and stress-strain specimens.

D. Standard size 6 x 6 x 18 inch plain concrete beams were cast from both beam and slab concretes for shrinkage specimens. Those specimens were gaged in the same way as the smaller 3 x 3 x 16 inch shrinkage prisms.

E. Plain concrete 3 x 3 x 16 inch prisms were cast from both beam and slab concretes for spring loaded creep specimens and for shrinkage control of those specimens. This type of specimen is described in paragraphs 1.4-B (2 and 3). The spring loaded creep specimens, Fig. 3-2, were loaded to 1000, 1500, 2000, and 2500 psi for beam concrete, and to 1000, 1500, and 2000 psi for the slab concrete. The small specimens were cured under wet mat along with the large test articles.

3.4 Materials

The prestressing steel was 7/16 inch diameter 7-wire high strength steel. No tests were made to determine its properties.

Concrete mix data appears below in Table 3-1. Properties are given in Figs. 3-3 and 3-4.

3.5 Tests

A. Instrumentation - Creep and shrinkage strain and stress-strain data were collected and processed as described in paragraph 1.4-B.

Elevations along the beam and slab were taken with a precise engineer level from a target rod reading to 1/1000 ft. Tops of selected stirrups served as elevation points on the beam before the slab was cast. Before the slab was in place, elevation readings were transferred to the bottom of the beam and afterwards, to the top surface of the slab at points directly above the beam elevation points. These were then correlated to the previous readings, and thereafter elevations were taken from the top surface of the slab only.

B. Strength and stress-strain tests - Stress-strain data were taken from 6 x 12 inch cylinders of beam concrete on day of prestress release, 3 day age, and at 60 day age. Slab concrete was similarly tested at 22 and 55 day ages. Details of this type of test are given in paragraph 1.4-B (1).

C. Shrinkage - In addition to 3 x 3 x 16 inch shrinkage prisms described in paragraph 1.4-B (2), 6 x 6 x 18 inch beams were cast and instrumented for shrinkage. Those specimens, cast in steel standard beam forms, served as companion specimens to the beam and the slab. They were cast with the bridge beams and slab and were instrumented in the same way as the smaller prisms.

D. Spring loaded creep specimens - The 3 x 3 x 16 inch prism creep specimens were loaded in pairs by the procedure described in paragraph 1.4-B (3). They were gaged one day after casting and loaded on the day of release of prestress.

E. Prestressed beam and cast-in-place slab strains - Details of gage points on the beam and slab are shown in Fig. 3-1. Gage

readings were first made just before release of the beam. It was again gaged just after release, then daily for five days, then weekly until the slab was cast; after thant, beam strains were taken on the same schedule as the slab.

The slab gages were read on the day after casting, daily for five days thereafter, and then weekly for the duration of the test.

F. Bridge camber - The beam and slab cambers were determined from elevation readings taken from points shown in Fig. 3-1. The straight line joining the two end elevation points, A and E, served as the elevation datum, and all points were referrred to it. Readings were taken just before release, just after release, and thereafter on the same schedule as strain readings.

3.6 Test Results and Discussion

A. Mechanical properties - Figs. 3-3 and 3-4 show stress-strain curves for beam and slab concretes.

B. Shrinkage, spring load creep, beam, and slab strains - All specimens were stored unguarded in the open at the bridge site. They were frequently found moved about on the ground; and, on two occasions, the creep and shrinkage prisms were retrieved from creek water where they had been thrown by meddlers. Some small specimens were broken, and the stainless steel screws were loosened and some were lost. Strain data taken from those specimens were so erratic that it was impossible to present as orderly results. Datta would plot for possibly three or four weeks in an orderly way,

then specimens would be thrown about and the data would scatter wildly. It is for those reasons that the completely meaningless data on strains is not presented. The results of this series proved that specimens must be protected if good data is to be forthcoming.

C. Bridge camber - The plots of relative elevations shown in Fig. 3-5 give the camber history of the beam and the bridge from the time just before prestress to the end of the test some five months later. Fig. 3-6 shows the camber profile during that time at major events in the history.

The figures show good agreement between the two quarter point elevation, and Fig. 3-6 graphically shows the parabolic nature of the camber.

Fig. 3-5 clearly shows the effect on camber of the various construction phases in the project. There was a disturbance when the beams were moved from yard storage to the bridge site, and the effect of diaphragm placement is clearly discernable at about six weeks age. The shift in the elevation reading after moving could have been caused by bending the steel stirrup that served as an elevation reference point. For this reason, it was deemed best to provide fixed elevation bolts in the full-size test bridge, Chapter V.

The placement of the deck slab caused a relatively large deflection at quarter points and at mid-span. The slow transition from pre-slab creep to post-slab creep lasted some 10 days, and then the upward camber growth began again, but at a very slow rate as compared with that of the pre-slab period.

There can be no comparison here of actual camber with predicted camber because of ineffective data from small specimens due to causes discussed earlier.

3.7 Conclusions

A. The plan developed and executed in tests of the series works well with a few modifications in tests of this kind.

B. The techniques adapted for collection of data by use of mechanical strain gage and engineers level is workable. No improvements in the handling of that equipment developed during the tests.

C. Specimens must be protected from vandals and they should be stored in a way that makes collection of data as simple as possible.

Table 3-1. Concrete Mix Data

		Beam Concrete	Slab Concrete
Mix: lb/cy	Cement	611 Type III	470 Type I
	Sand	1137	1118
	Coarse Agg.	1926	2084
	Water	221	242
	Admix	6 qts. Pozzolith #8	5 qts. Pozzolith #8
			2 oz. Darex

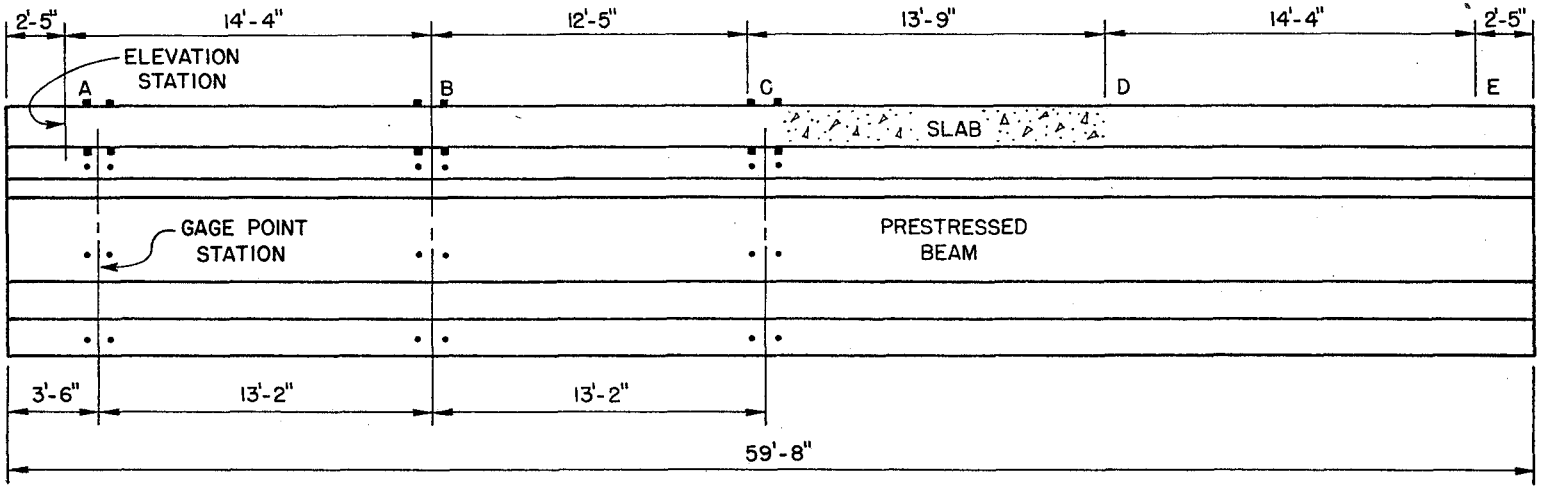

DATA:

PRESTRESSING STEEL:
40-7/16 DIA, 7 WIRE STRAIGHT STRANDS,
e = 8.87 in.

NOTE:
CENTER OF SUPPORT BEARINGS ARE LOCATED 5 1/2" FROM ENDS OF THE BEAM

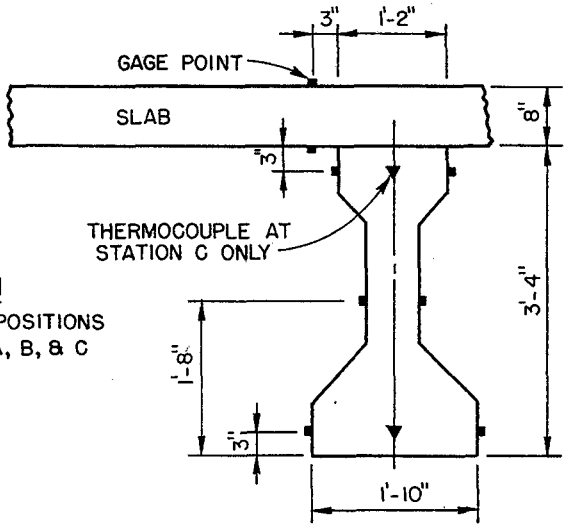

SECTION
SHOWING GAGE POSITIONS AT STATIONS A, B, & C

FIGURE 3-1 TEST BEAM

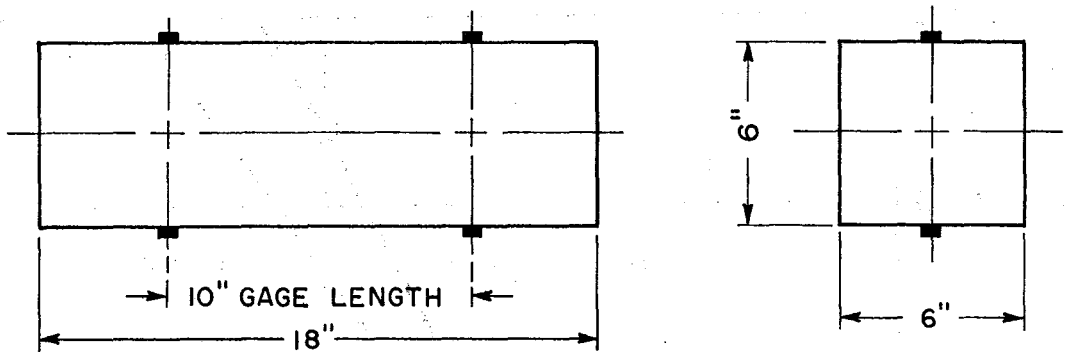

(a) SHRINKAGE BEAM

NOTE: IN ALL SPECIMENS GAGE POINT INSERTS WERE CAST IN THE CONCRETE GAGE POINTS WERE INSERTED AFTER REMOVAL OF FORMS

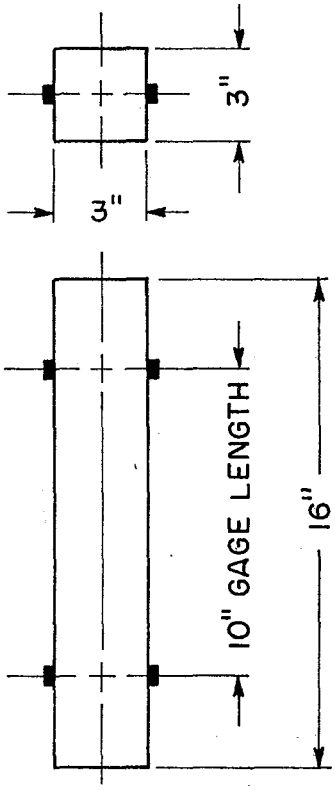

(b) SHRINKAGE PRISM

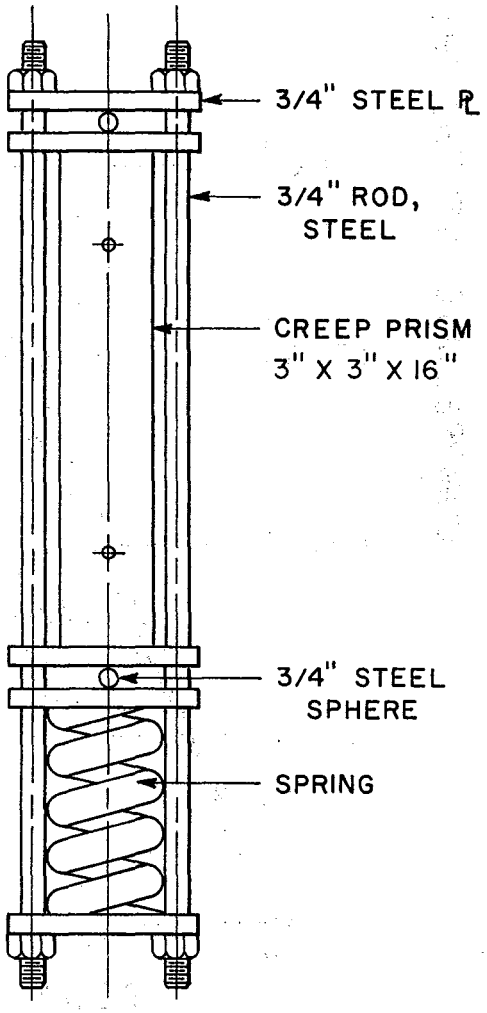

(c) SPRING LOADED CREEP PRISM

FIGURE 3-2 TEST SPECIMENS

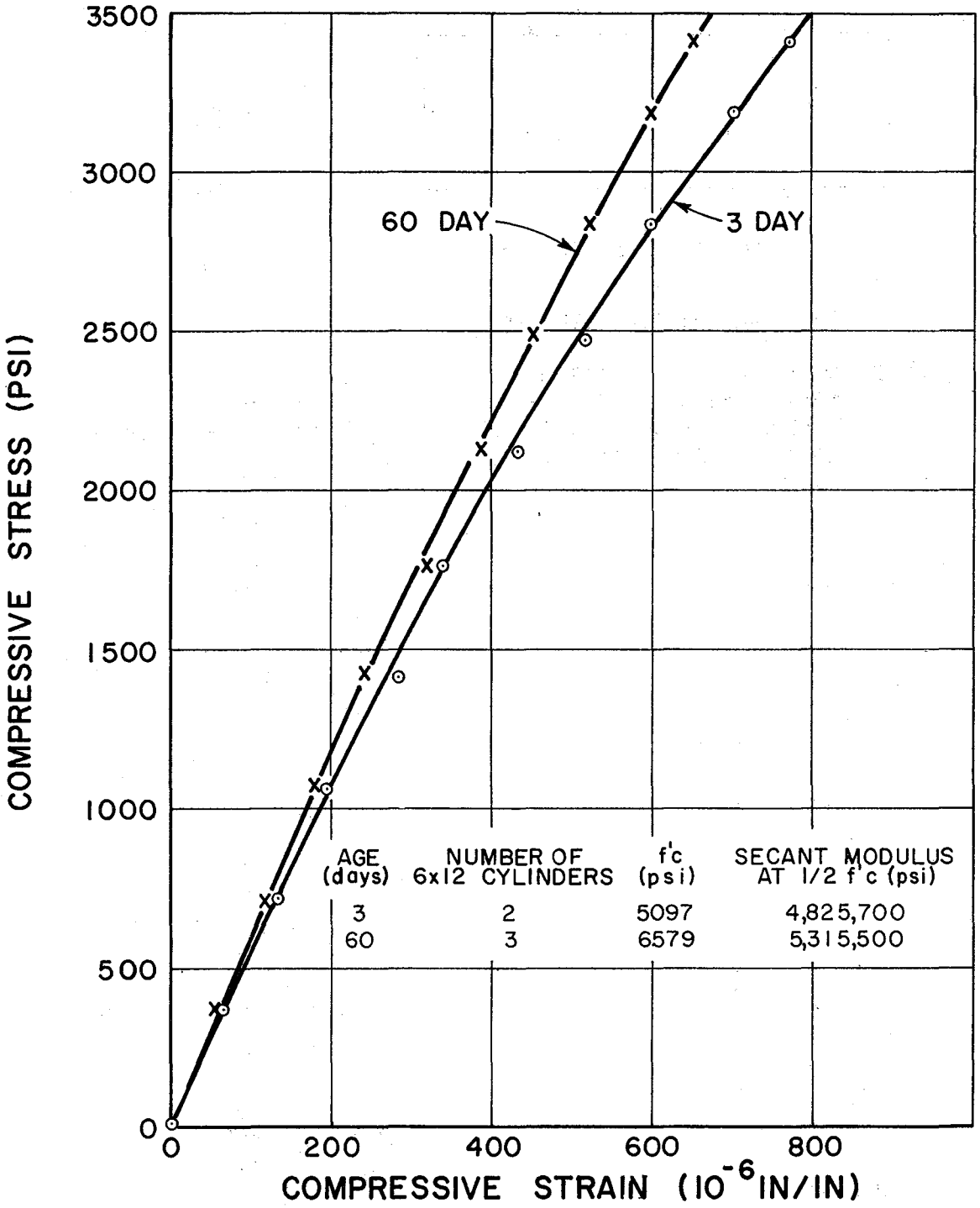

FIGURE 3-3 STRESS-STRAIN RELATIONSHIP FOR WALNUT CREEK BRIDGE BEAM CONCRETE

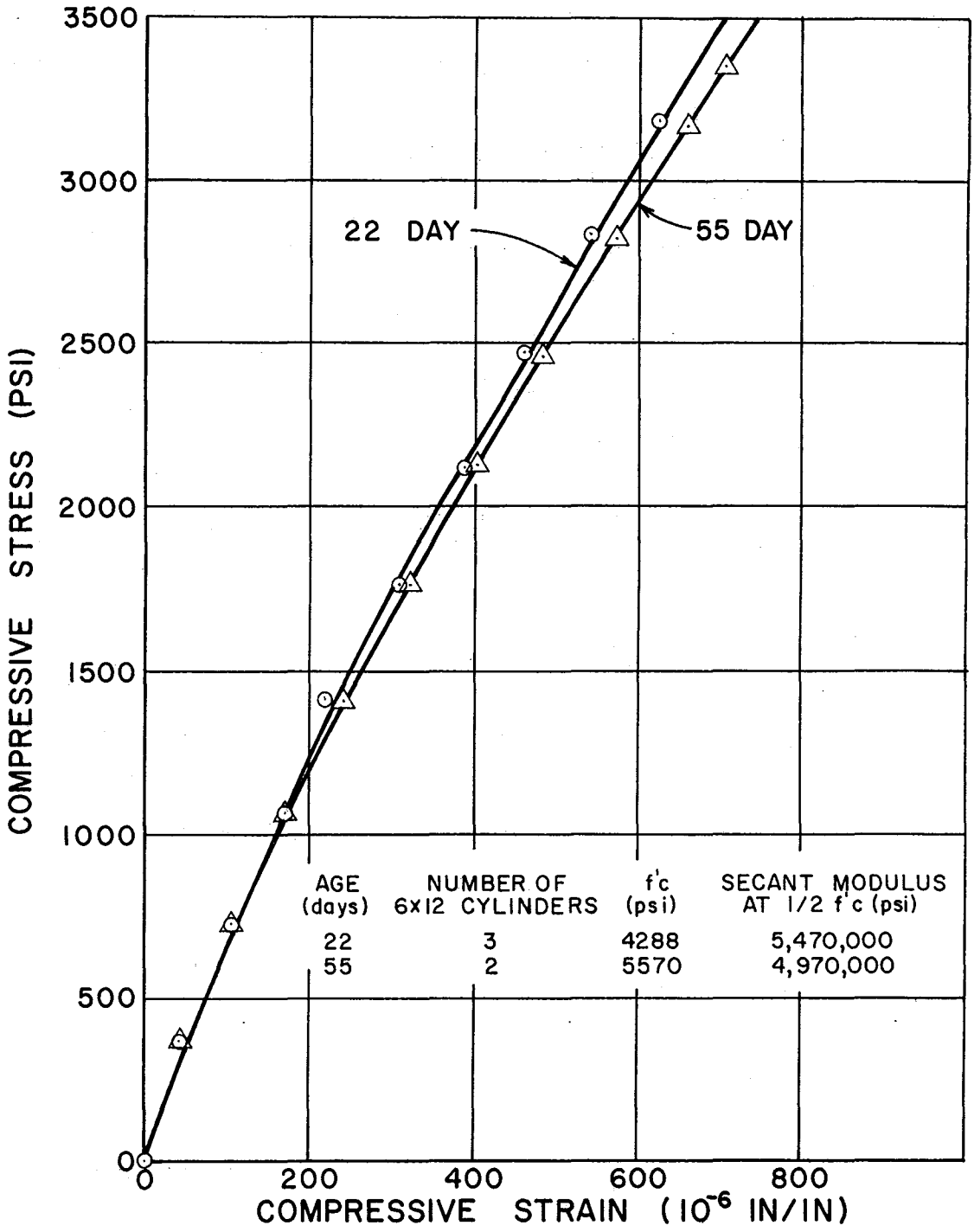

FIGURE 3-4 STRESS-STRAIN RELATIONSHIP FOR WALNUT CREEK BRIDGE SLAB CONCRETE

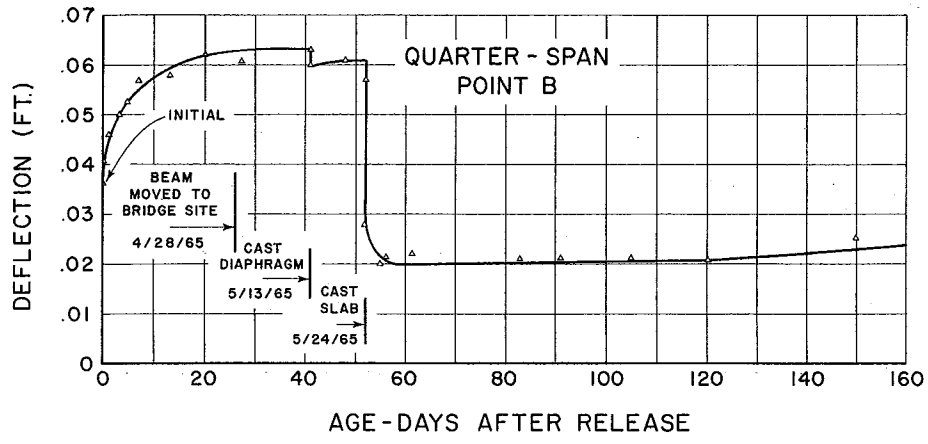

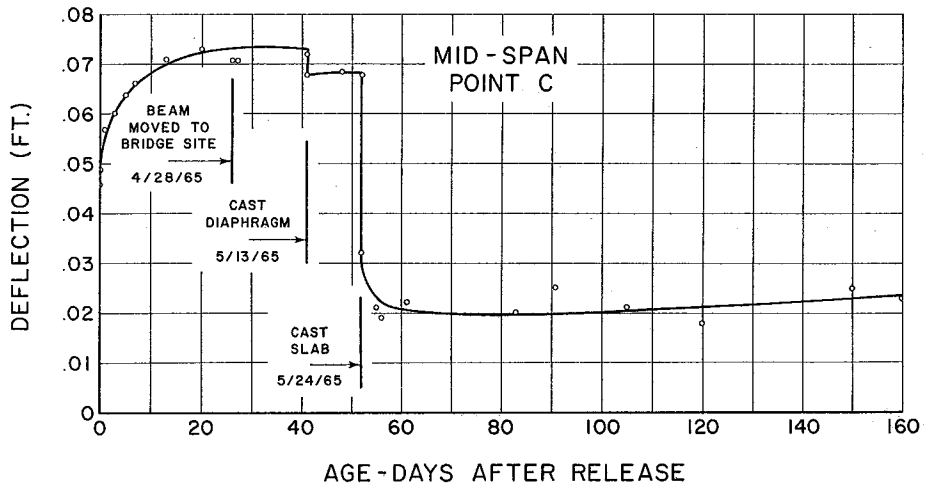

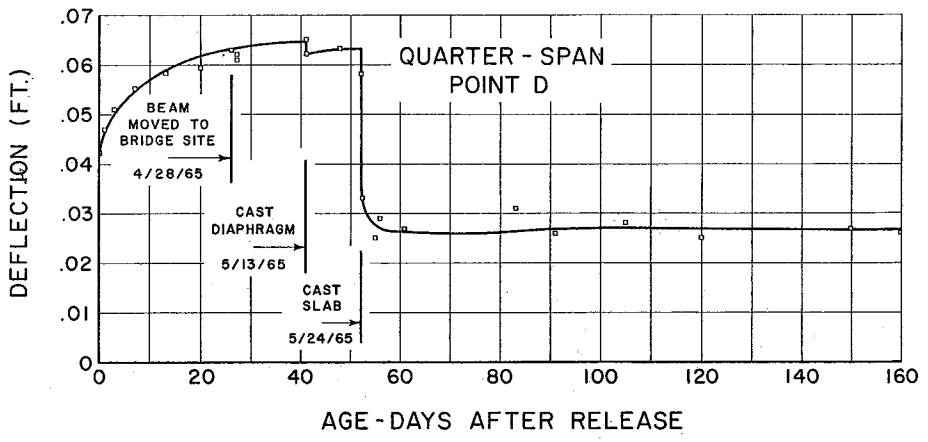

FIGURE 3-5 DEFLECTIONS OF TEST BEAM

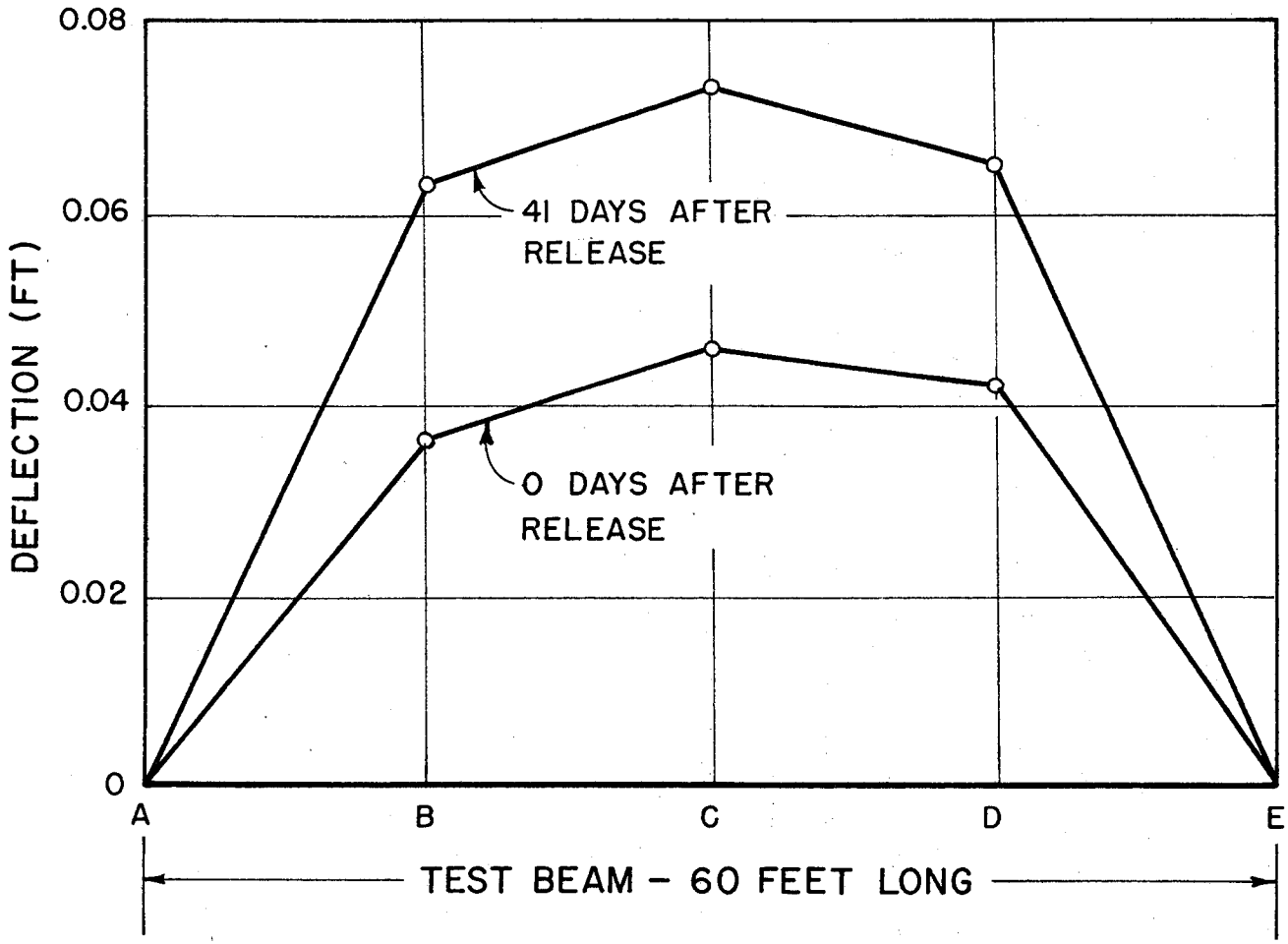

FIGURE 3-6 DEFLECTION PROFILE

CHAPTER IV

LABORATORY T-BEAMS

4.1 Introduction

The strains resulting from the interaction of a prestressed beam and the cast-in-place reinforced concrete slab are of concern in the study reported in this chapter.

The prestressed beam is usually cast many days before it is installed in the structure, and it is usually stored in the casting yard area until it is hauled to the bridge site. The time lapse between casting and erection varies from about 30 days to several months, depending on the highway specification and the construction requirements.

The beam concrete is generally not the same mix as the slab concrete, and curing conditions for the two are sometimes different. Differences in mixes, curing, and ages contribute to differences in free shrinkage rates of the beam and slab concretes at the time when they become composite.

The beam will have lost a considerable amount of its excess mixing water before the slab-is-cast, and its free shrinkage rate will probably be much smaller than that of the slab. Too, the beam, being under stress from action of the prestressing steel, will have a rate of unrestrained creep different than that of the slab which carries no load at the time. After the slab is cast, there is some indefinite period during which there is an exchange of moisture from the fresh slab to the top of the beam on which

it is cast. There is probably very little, if any, shrinkage in the slab during its wet cure period.

Restraint to free strain is developed shortly after the slab is cast because of the bonding together of the two structural elements. The resulting composite action causes the beam and the slab to strain equally at their interface, assuming complete bonding, and strains at all other levels in a section are influenced by that bonding.

The benefits derived from composite action in ability to carry loads are great, but there are problems in creep and shrinkage which are different from those encountered in the unrestrained action of the elements. Those problems have been recognized and have been treated by a number of writers in discussing warping in concrete, reinforced concrete, and composite steel beam-concrete deck bridge (16-23). Branson (21), and Branson and Ozell (22) have reported significant work on differential shrinkage in composite reinforced concrete and prestressed concrete beams.

The method referred to by Branson (21) as the "separate section method", which had been advanced by others, is used in the analysis of this chapter in developing predicted strains and camber for a composite prestressed beam. That method computes the difference in free strains at the interface of slab and beam over a certain period. The two elements are then forced to be longitudinally compatible by the action of tangential forces on the slab and beam at the interface. Stresses caused by those forces cause creep in the materials, and that creep is accompanied

by camber of the composite beam.

As a second step in the development of a method for predicting creep camber in prestressed concrete bridges a short laboratory program in testing of small composite beams was carried out. In that test two beams, each with a precast prestressed stem and a cast-in-place concrete flange slab were constructed and instrumented. The objectives of the program and details of its execution appear in the following sections.

4.2 Objectives

A. To extend the method of predicting creep in prestressed beams, see Chapter II, to cover the prediction of creep in composite prestressed concrete beams.

B. To evaluate the validity of the method by comparing its results against values of strain measured from laboratory beams constructed for the purpose of producing such strain data.

4.3 Test Specimens

A. Details of all test specimens are given in Figs. 4-1, 4-2, and Table 4-1.

B. Two identical prestressed beam stems, 3 in. x 9 in. x 10 ft., with two 3/8 in. diameter, 7 wire straight strands were made. In later tests, one served as an unloaded specimen and the other served as a load carrying beam.

The prestressing strands were individually tensioned in one line, and the next day concrete for the two stems was cast around them, Fig. 4-3(a). Plastic coated plywood forms were fitted with

brass inserts, Fig. 4-3(b), for gaging points near the top and bottom of the stems at midspan. Closed vertical stirrups of number 3 deformed bars were spaced 3 in. apart near the ends and 8 in. over the remainder of the length. The top loop of the stirrups extended 1¼ in. above the surface for later bonding to the cast-in-place slab.

The concrete was vibrated in the forms with an internal vibrator, and the beams were covered with a plastic sheet for curing. All specimens were stored under the sheet with the beams.

Forms were removed the day after casting and gage points were inserted. The stems were then left to cure under a plastic sheet for 7 days. Gage readings were taken from all gages, beams and small specimens at 7 day age just prior to prestress release, and from beam gages just after release.

After release, the stems were mounted on end supports, and wood forms for the flange slab were later attached, Fig. 4-3(c). Those forms were supported by the stems, as in unshored bridge slab construction. They were fitted with brass inserts at midspan, and at 24 day age of stems, the slabs were cast.

Flange slab reinforcement consisted of transverse number 3 rods, 24 in. long, spaced on 12 in. center. They were set at mid-depth of the slab.

The top of the stem was cleaned and moistened just prior to casting the flange. The flange concrete was vibrated in the form, and top gage inserts were installed with a jig while the concrete was plastic. The beams and small specimens were cured for

9 days under plastic sheet at which age the sheet and the wood forms were removed. Gage points were then inserted, and the beams were water sprayed once daily until they were 20 days old.

After curing, the beams were transported 12 miles by truck to laboratory storage where they were set on end supports. The laboratory was generally open during the summer and it was closed and heated during winter.

C. A 3 x 9 x 14 in. shrinkage block was made from stem concrete, and fitted with centrally located 10 in. gage points in each 9x14 face. That block served as shrinkage control for the prestressed stems.

D. A shrinkage slab, 2 1/2 x 24x 24 in., was made from slab concrete. That slab was fitted with one set of 10 in. gage points centrally located in each 24 in. square face. It served as shrinkage control for the slab concrete.

4.4 Materials

A. The concrete mix for all specimens was the same except that Type I cement was used for flange concrete and Type III for stem concrete. Mix quantities per cubic yard of concrete were as follows: cement 672 lb., water 333 lb., sand 1152 lb., Stafford lightweight coarse aggregate (see Chapter 2) 950 lb., plastiment 7 lb., and Sika AER 81 cc. Slump was 2 1/2 in., air content by pressure meter was 7.5% and by Rollometer 3.0%. The plastic mix weighed 114.8 pcf for the stem concrete and 115.1 pcf for the slab concrete. Mechanical properties are given in Table 4-2, and Figs. 4-4 and 4-5.

B. Prestressing steel was 3/8 in. diameter, 7 wire strand[a] with properties as listed in Table 4-2.

4.5 Tests

A. Instrumentation

Creep and shrinkage strains and stress-strain data were collected and processed as described in paragraph 1.4-B.

Elevations at quarter-points along the beams were read from an engineers scale with a precise engineers level. No elevation readings were taken before the slabs were cast.

B. Strength and Stress-Strain Tests

Stress-strain data were taken from 6x12 cylinders of beam concrete on the day of release of prestress, 7 day age, and at 93 day age. Slab concrete was similarly tested at 28 day and at 73 day age. The tests followed the procedures given in paragraph 1.4-B(1).

C. Shrinkage

The 3 x 3 x 16 shrinkage specimens served as control to the companion 3 x 3 x 16 spring loaded specimens. These were prepared for both stem and slab concretes. The 3 x 9 x 14 specimen served as control for the stem, and the 2 1/2 x 24 x 24 specimen served as shrinkage control for the slab concrete. Strains were taken from these specimens at each gaging of the main test articles, the beams.

---

a. 1x7 Tufwire Strand, TW906, Sheffield Div., Armco Steel Corp., Kansas City, Kansas.

D. Spring Loaded Creep Specimens

One spring loaded creep specimen for the stem was stressed to 2000 psi on the day of release of prestress. It was gaged just before and just after loading and thereafter on the same schedule as the beam gaging.

One slab prism was spring loaded to 1000 psi on the same day that transverse load was applied to the loaded beam. Strain gage readings were taken just before and just after loading, and thereafter on the same schedule as the loaded beam.

E. Beams

Strain and elevation readings were taken from the stems periodically after prestress release, 7 days after casting, and from the day of removal of forms for slabs, 9 days age.

One of the beams was stored on end supports and carried only its own weight throughout the test, Fig. 4-3(d). The other beam was mounted on end supports on a loading frame, and at 93 day age it was loaded with 2130 pounds at each of its 1/3 points, see Fig. 4.3(e). The load was applied through compressing calibrated helical springs by running the nuts down on tie rods which confined the system. The springs were deflected to a predetermined value, and the deflections were measured during the process by 0.001 inch dial gages.

At 275 day age, after 6 months under load, the transverse load was removed by reversing the loading process.

Strain and elevation measurements were made just before and just after loading and unloading and at frequent intervals between those events.

4.6 Test Results and Discussion

A. Mechanical Properties

Stress-strain curves for the concrete are shown in Figs. 4-4 and 4-5 and properties are tabulated in Table 4-2. The concrete mix was designed for a strength of 5000 psi and that strength was attained in the stem concrete at 7 days using Type III cement. At 28 day age the slab concrete, using Type I cement, had reached 4100 psi strength and only a little higher at 73 days. The secant modulii increased only a little between 28 and 73 day ages for slab concrete, and it was only a little higher for stem concrete between 7 and 93 day ages.

B. Shrinkage

The effect of warm, humid spring weather is evident in Figs. 4-6, 4-9, and 4-10 where shrinkage shows a marked change beginning at about 200 days. The specimens began expanding when humid weather set in and the specimens never returned to their earlier dimensions before tests were terminated. The rapid rate of shrinkage at early age of TS-2, Fig. 4-6 compared with that of TS-1, Fig. 4-9, emphasizes the effect of specimen size on the rate of moisture lost. Curing and storage of the two specimens were identical, only the size was different. Although the smaller specimen shrank faster, the shrinkage at termination of testing was about the same for both. A similar influence of size is noted in Figs. 4-9 and 4-10 where the thinner specimen SS-1, 2 1/2 in. thick, shows a greater expansion beginning at about 200 days, than is shown in the

slightly thicker 3 in. thick specimen TS-1.

C. Spring Loaded Creep Prisms

The strain behavior of both spring loaded specimens is shown in Fig. 4-6. That behavior is of interest here because strains from these specimens were used in prediction of strains in the prestressed beams.

The spring loaded prisms and their companion shrinkage specimens were all of the same size, 3 x 3 x 16. Stem concrete prism, TC-1, was loaded to 2000 psi at 7 day age, and slab concrete prism, SC-1, was loaded to 1000 psi at 28 day age. They were handled in the same manner except that duration of cure of the slab concrete was longer than that of stem concrete.

It is of interest to note that TC-1 underwent a high rate of creep at early age when compared to SC-1, which was loaded at an older age. The unit creep rate of TC-1 gradually reduced until at about 60 day age, 23 days after its loading, it was about the same as that of SC-1 at 80 day age, 52 days after its loading. This is seen from the slope of those curves. Thus, there is strong indication here that age of loading has a great influence on rate of creep, and, as the curves show, on the magnitude of unit creep. This is in agreement with findings reported in the literature. Although the strength of the flange concrete was lower than stem concrete, its secant modulus was somewhat higher. The higher modulus possible has an influence on the lower creep rate.

D. Beams

Figures 4-11 through 4-14 display strains in stems and slabs as measured and as predicted. The predicted curves follow the trend of events well, the greatest disagreements showing up at early age, before the transverse load was applied to T-2, and near the end of the test after removal of the load.

The early differences are almost certain to be differences in strain rates of the main test articles and the small shrinkage specimens. Some of the difference might be attributed to a shifting of the neutral plane with creep, which would make values of elastic strains computed by conventional elastic methods to be off somewhat.

The deflections of beam T-2 are shown in Fig. 4-15 where the events of loading and unloading are clearly marked. It will be noted that deflection under the load became almost stable fairly quickly after the load was applied. The rebound when the load was removed was noticeably smaller than the deflection when the load was first applied. The beams were recovering, however, and eventually they might have come back up near their elevation before loading.

The beam stresses shown in Table 4-3 are very low at the top of the beam, and they are never great in the slab. The stresses were computed by conventional elastic methods and do not reflect non-linear changes.

The computer program for this series had to account for changes in loading and the corresponding stress changes, the added element of the cast-in-place slab which was not encountered in the previous work, different concretes in the stem and slab, and different shrinkage and creep functions. The program traced out the changes at different events during the test period and it did it rather well. It would, no doubt, provide a better agreement with measured values under more rigid control of variables.

4.7 Conclusions

Creep in composite beams made of prestressed concrete beam and cast-in-place concrete slab can be predicted by the rate of creep method. That method must be modified to account for changes in loads, beam section, and material properties.

TABLE 4-1

SPECIMENS FOR LABORATORY T-BEAM

Designation	Kind of Concrete	Size	Kind of Test	Date Cast
TS-1	Stem	3x9x14	Shrinkage	Aug. 7/65
TS-2	Stem	3x3x16	Shrinkage	Aug. 7/65
TC-1	Stem	3x3x16	Creep (18^k spring load)	Aug. 7/65
T-1	Prestr. Stem	Fig. 4-2	Strain & Camber	Aug. 7/65
T-2	Prestr. Stem	Fig. 4-2	Strain & Camber	Aug. 7/65
SC-1	Slab	3x3x16	Creep (9^k spring load)	Aug. 31/65
SC-2	Slab	3x3x16	Shrinkage	Aug. 31/65
SS-1	Slab	2½x24x24	Shrinkage	Aug. 31/65
TF-1	Slab	2½x26½x10'	Slab for T-1	Aug. 31/65
TF-2	Slab	2½x26½x10'	Slab for T-2	Aug. 31/65

TABLE 4-2

PROPERTIES OF MATERIALS

CONCRETE

Date Cast	Age At Test (days)	f'_c psi	$E\frac{1}{2}f'_c$ ksi
Aug. 7, 1965	7	5050	2,775
	93	4609	3,115
Aug. 31, 1965	28	4100	3,250
	73	4233	3,418

STEEL PRESTRESSING STRAND

Area = 0.082 sq. in.
E = 30,000,000 psi
Breaking Strength = 21,600 pounds

TABLE 4-3

BEAM COMPUTED STRESSES AND STRAINS, AT MIDSPAN, DUE TO ONLY ELASTIC STRESSES: NO CREEP NOR SHRINKAGE INVOLVED. THE POSITIVE SIGN SIGNIFIES TENSION; THE NEGATIVE, COMPRESSION.

Item	Event	Secant Modulus (ksi)		f(psi) due to the event				(in/in) due to the event			
				Slab		Stem		Slab		Slab	
		Slab	Stem	Top	Bot	Top	Bot	Top	Bot	Top	Bot
T-1	Cast Stem	----	----	----	----	(-67)[b]	(+67)[b]	----	----	0	0
T-2		----	----			(-67)[b]	(+67)[b]	----	----	0	0
T-1	Release	----	2775	----	----	+3	-2017	----	----	0 (-120)	-726[c] (-710)[d]
T-2			2775	----	----	+3	-2017	----	----	0 (-80)	-726 (-610)
T-1	Cast Slab		3000[a]	----	----	-165	+165	----	----	-55	+55
T-2			3000[a]	----	----	-165	+165	----	----	-55	+55
T-2	Load	3418	3115	-247	-35	-35	+730	-72 (-60)	-10 (0)	-11 (+10)	+234 (+220)
T-2	Unload	3418[a]	3115[a]	+247	+35	+35	-730	+72 (+90)	+10 (+50)	+10 (+110)	-234 (-70)

a Estimated value
b Zero reading was taken when this stress, due to self weight, was acting.
c Computed strain values not bracketed
d Measured strain values bracketed

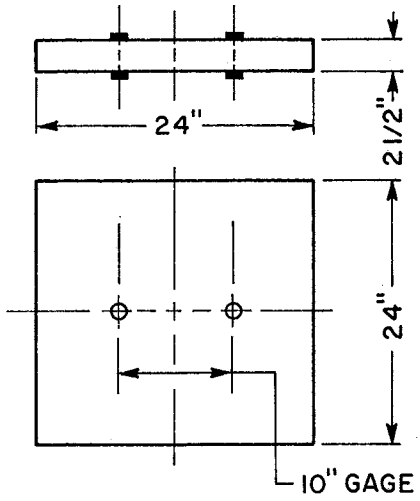

(a) SLAB SHRINKAGE BLOCK

NOTE IN ALL SPECIMENS GAGE POINT INSERTS WERE CAST IN THE CONCRETE. GAGE POINTS WERE INSERTED AFTER REMOVAL OF FORMS

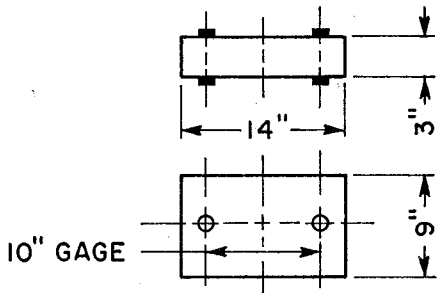

(b) STEM SHRINKAGE BLOCK

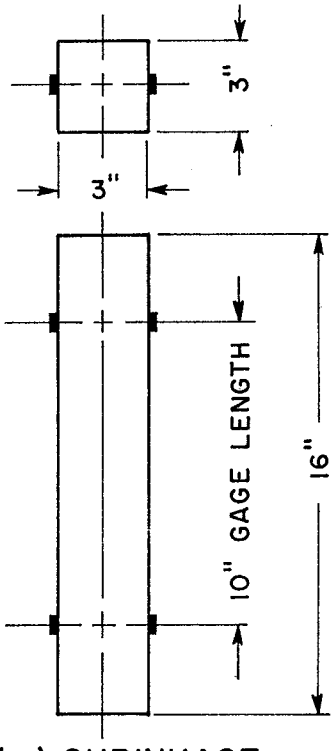

(c) SHRINKAGE PRISM

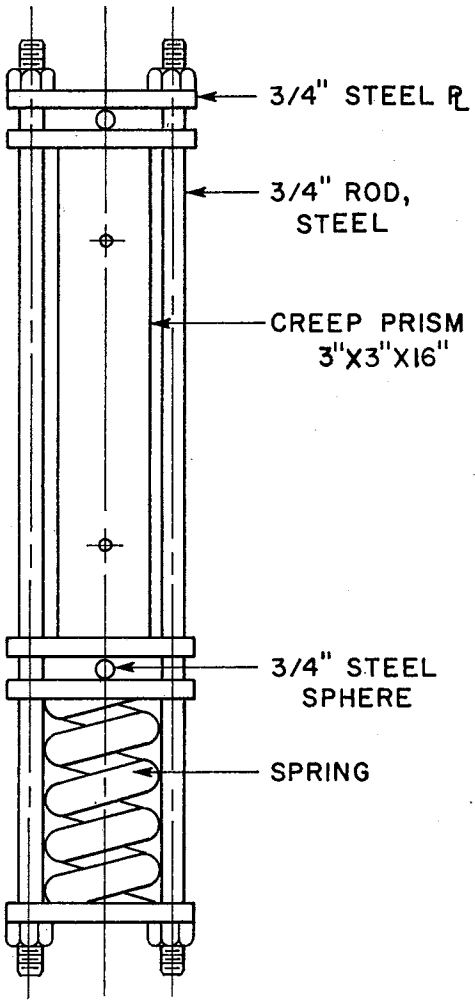

(d) SPRING LOADED CREEP PRISM

FIGURE 4-1 TEST SPECIMENS

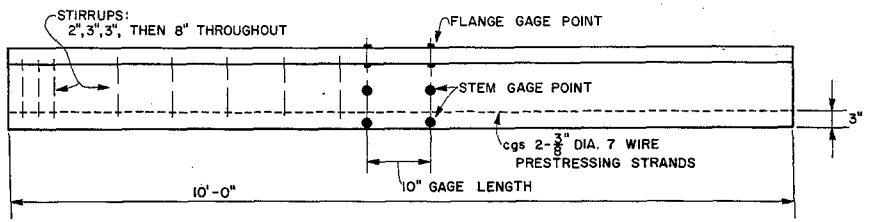

(a) BEAM DETAILS - SIDE

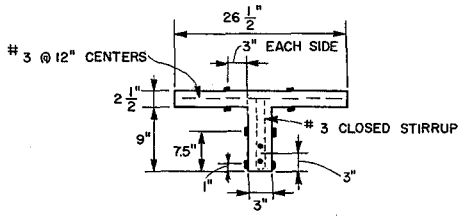

(b) BEAM DETAILS - END

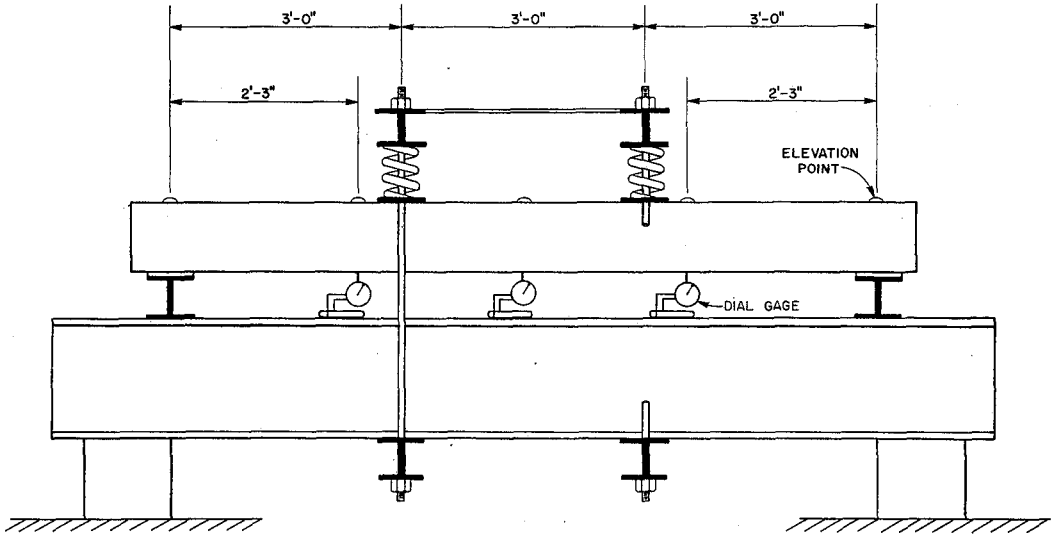

(c) LOADING FRAME AND GAGING - SIDE VIEW

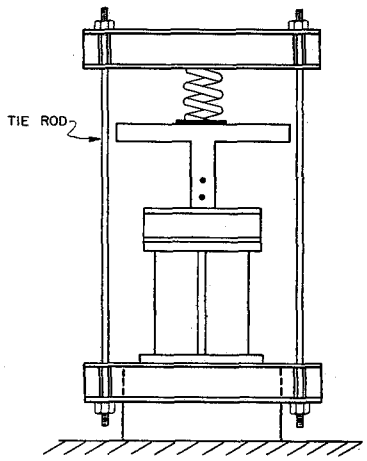

(d) LOADING FRAME - END VIEW

FIGURE 4-2 BEAM DETAILS AND LOADING FRAME

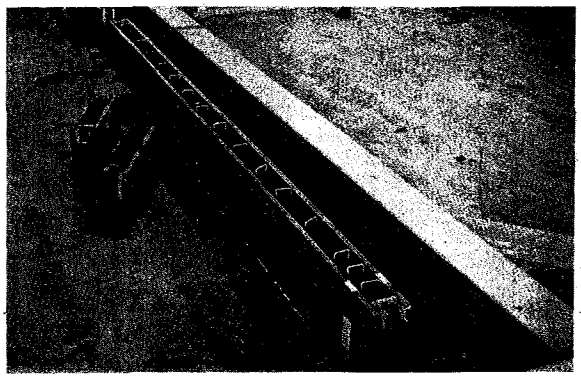

(a) FORMS IN LINE READY FOR CASTING

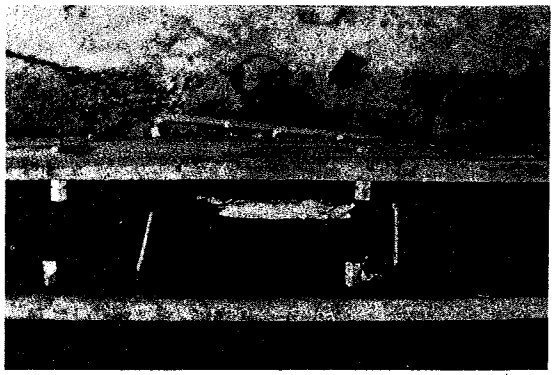

(b) GAGE INSERTS NEAR TOP OF FORM

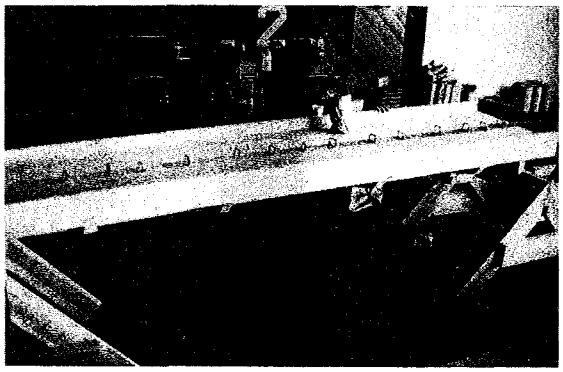

(c) FORMS IN PLACE FOR FLANGE SLAB

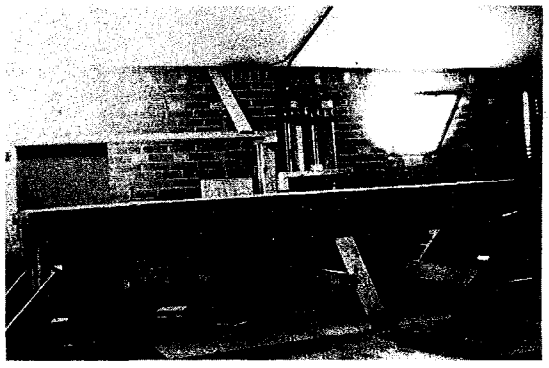

(d) NON-LOADED BEAM

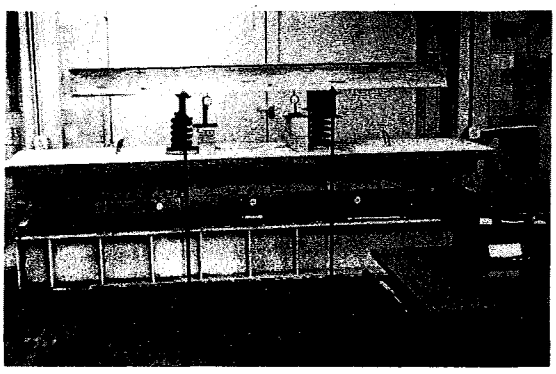

(e) LOADED BEAM

FIGURE 4-3 PHOTOGRAPHS OF BEAMS

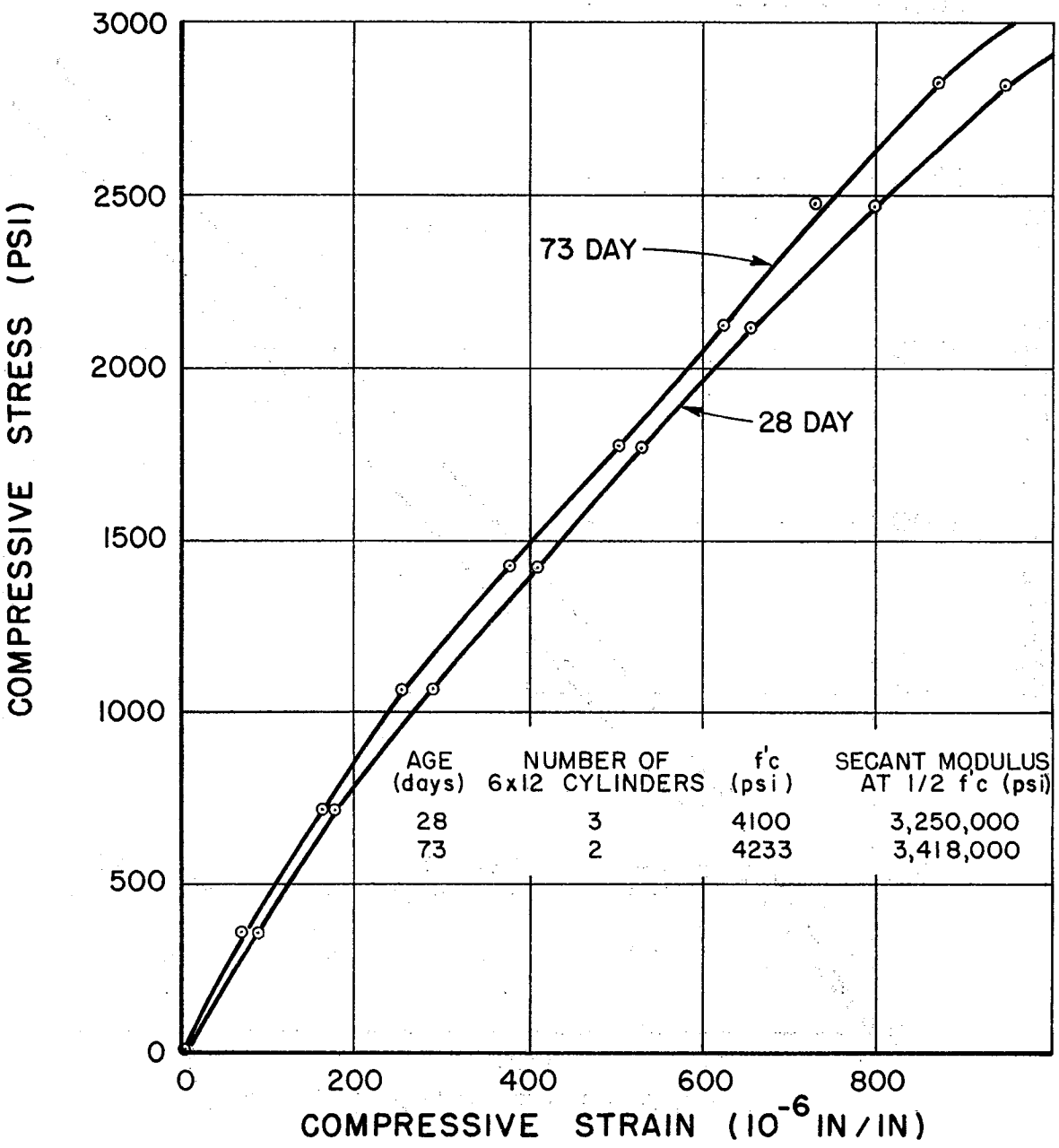

FIGURE 4-4 STRESS-STRAIN RELATIONSHIP FOR SLAB CONCRETE OF LABORATORY COMPOSITE BEAM

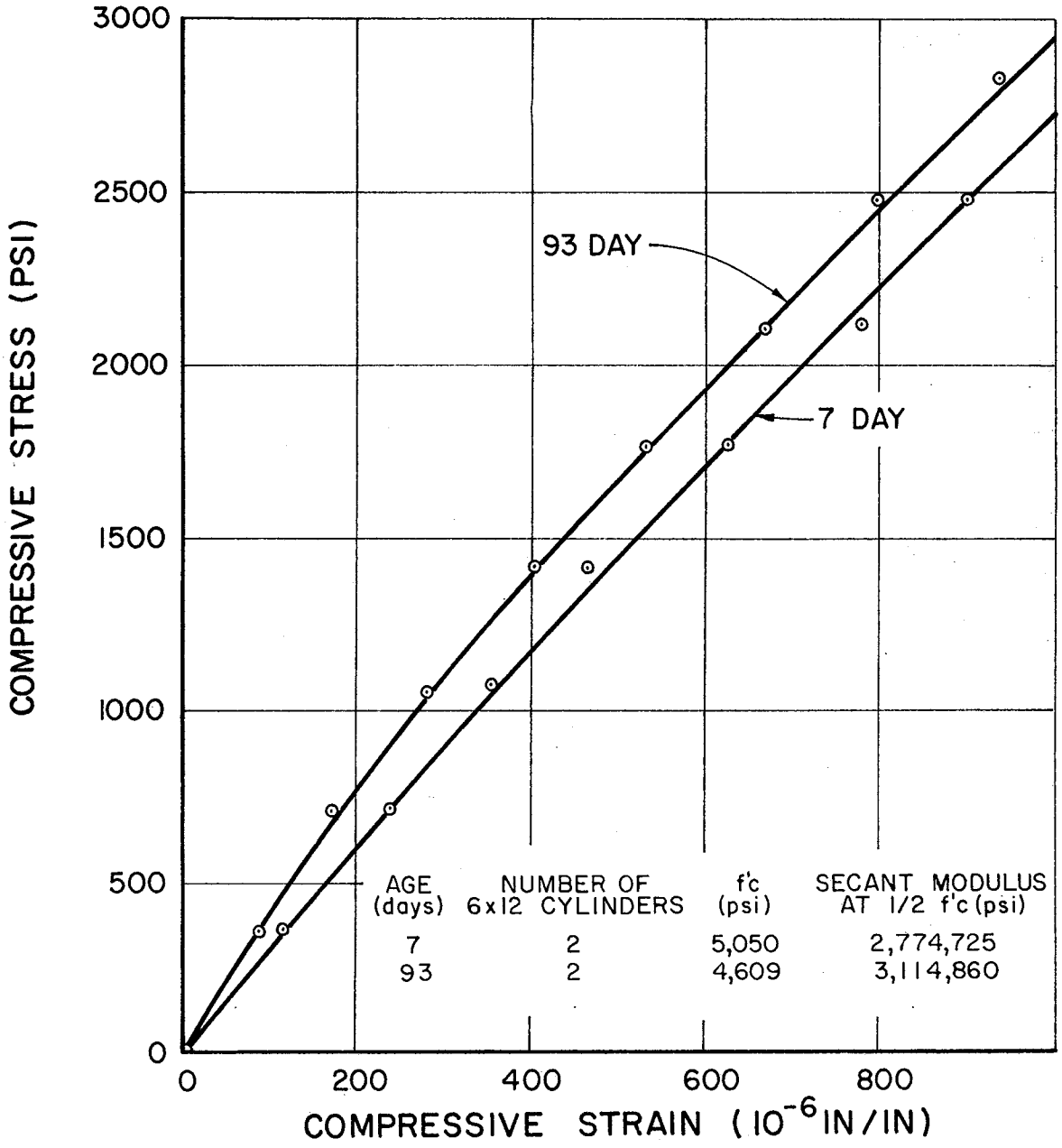

FIGURE 4-5 STRESS-STRAIN RELATIONSHIP FOR STEM CONCRETE OF LABORATORY COMPOSITE BEAM

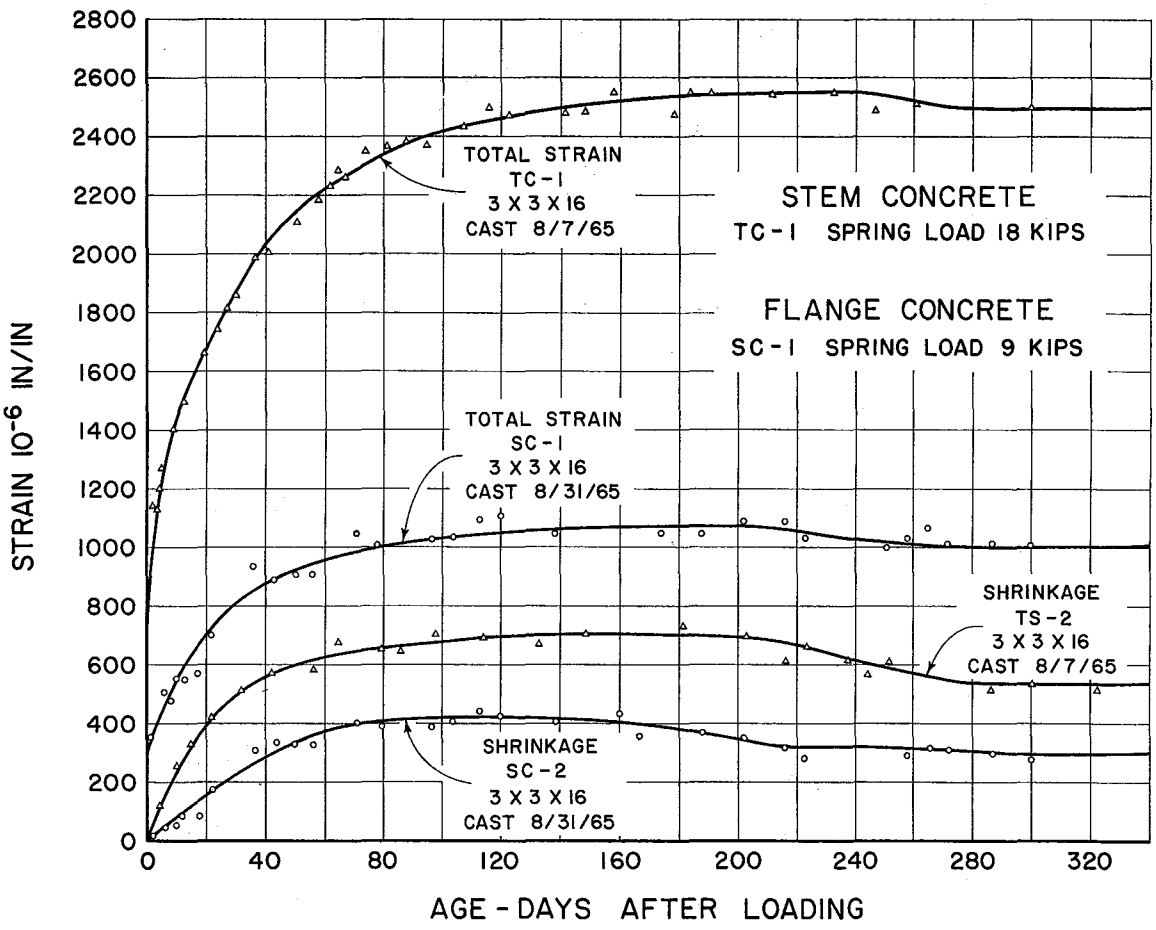

FIGURE 4-6 CREEP SPECIMENS FOR LABORATORY BEAM T-1 & T-2

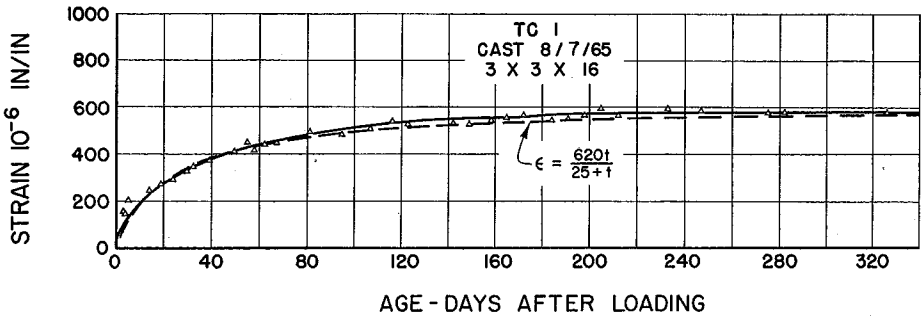

FIGURE 4-7 UNIT CREEP FOR STEM CONCRETE OF LABRATORY BEAMS

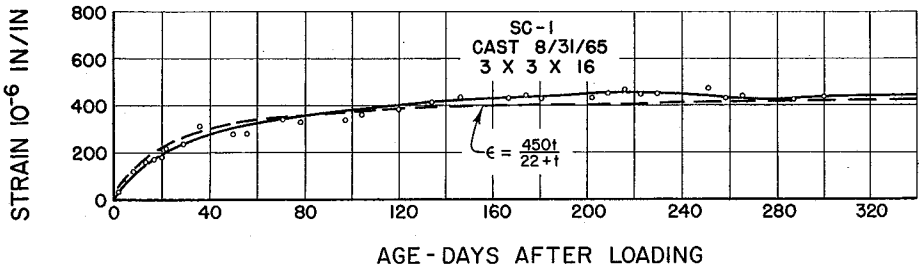

FIGURE 4-8 UNIT CREEP FOR SLAB CONCRETE OF LABRATORY BEAMS

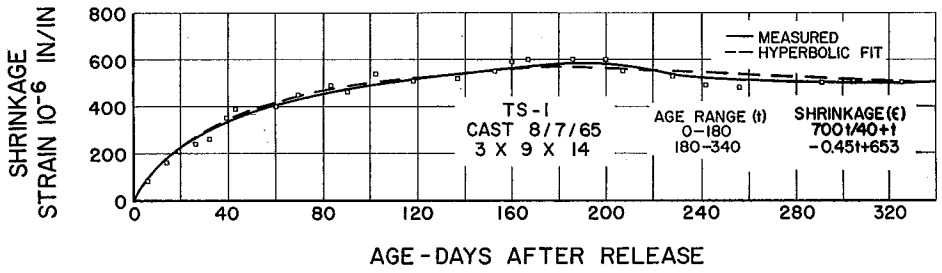

FIGURE 4-9 SHRINKAGE OF STEM CONCRETE OF LABRATORY BEAMS

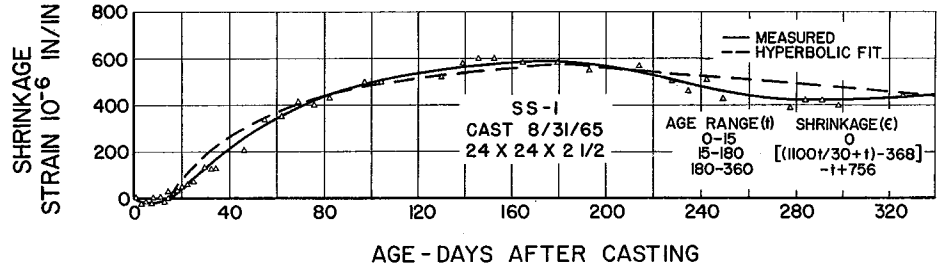

FIGURE 4-10 SHRINKAGE OF SLAB CONCRETE OF LABRATORY BEAMS

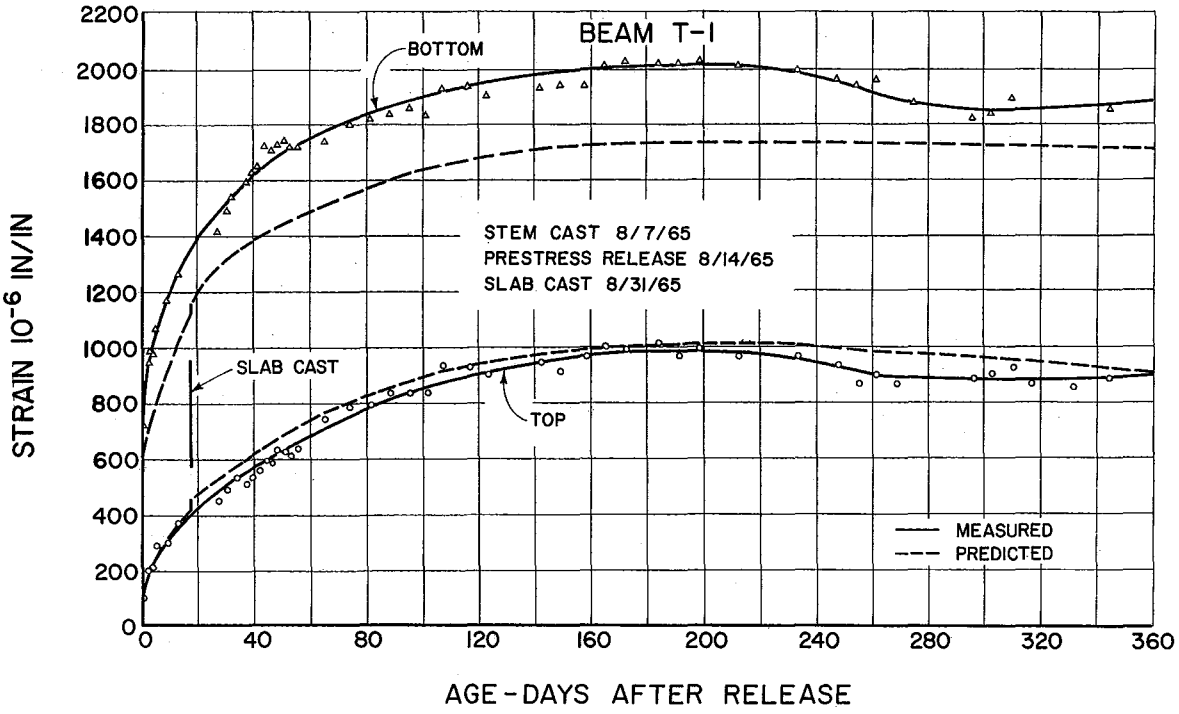

FIGURE 4-11 STRAIN IN STEM OF LABORATORY BEAM T-1

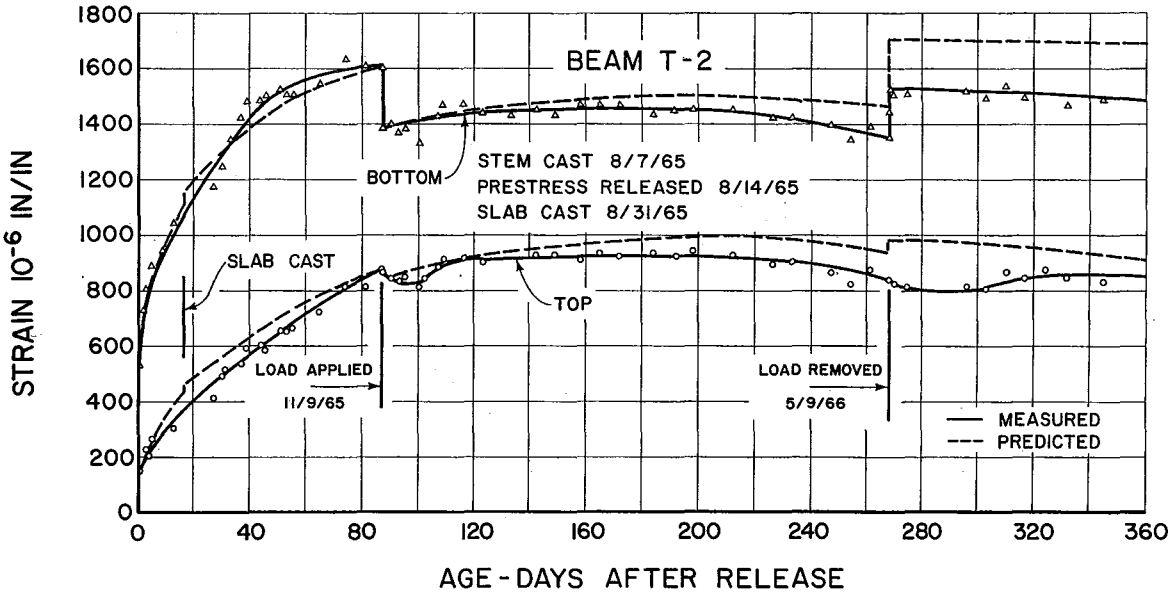

FIGURE 4-12 STRAIN IN STEM OF LABORATORY BEAM T-2

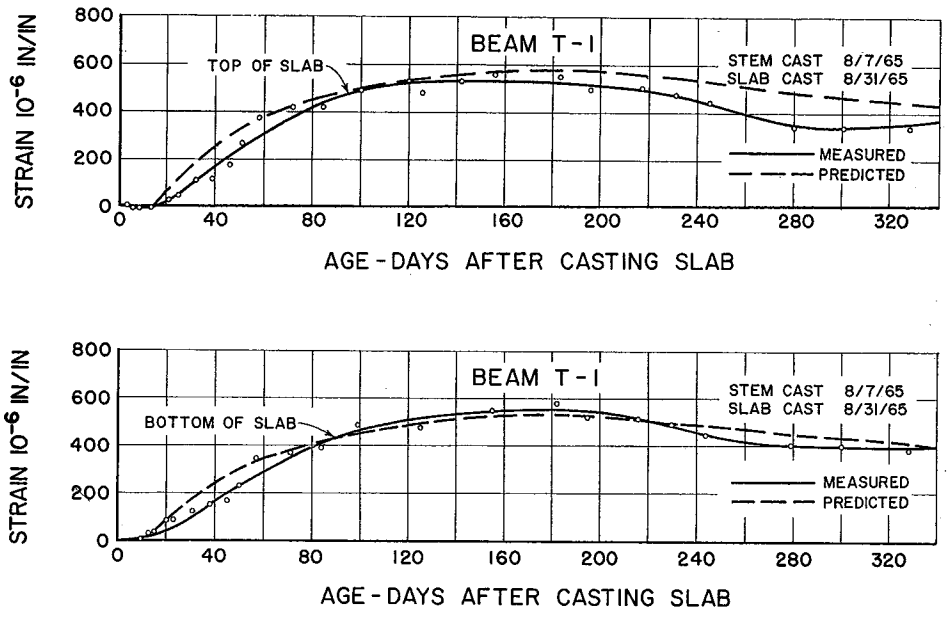

FIGURE 4-13 STRAIN IN TOP AND BOTTOM OF SLAB - LABORATORY BEAM T-1

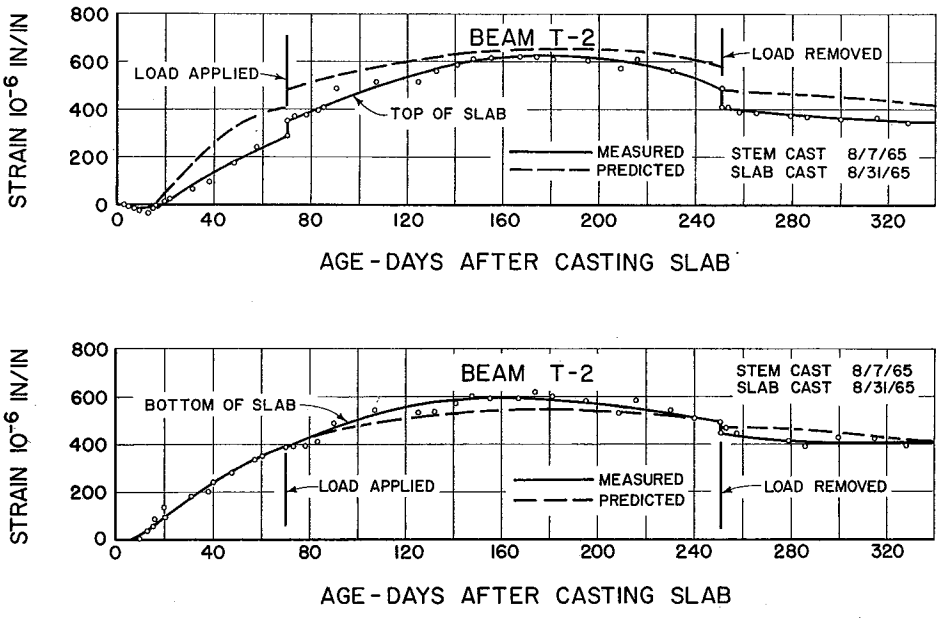

FIGURE 4-14 STRAIN IN TOP AND BOTTOM OF SLAB - LABORATORY BEAM T-2

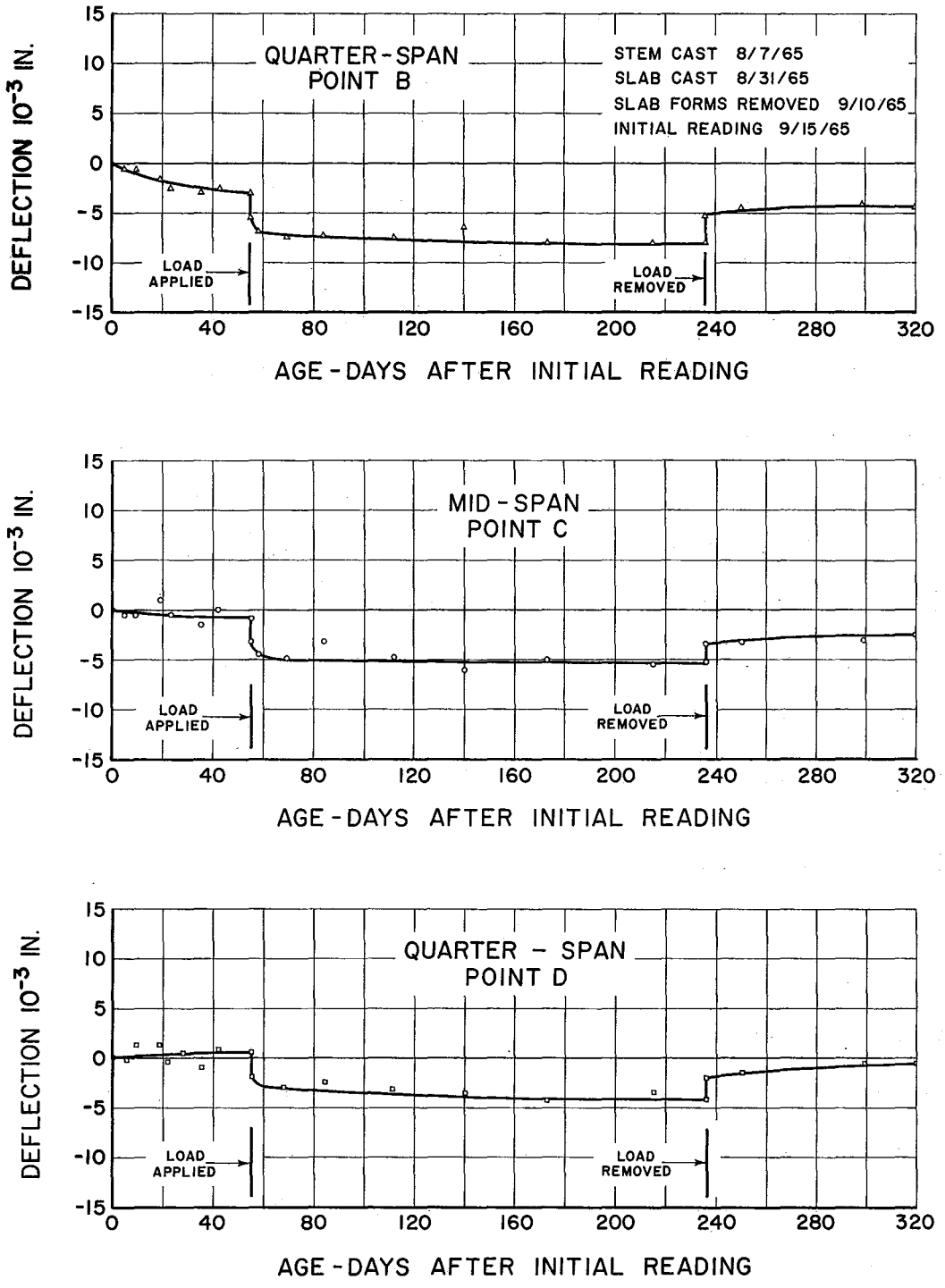

FIGURE 4-15 DEFLECTIONS OF LABORATORY BEAM T-2

CHAPTER V

CREEP AND CAMBER OF A FULL SIZE HIGHWAY BRIDGE

5-1 Introduction

The proof of methods for predicting creep, explained in earlier chapters, depends on agreement of results with creep developed in a full size structure of the type intended in its development. A highway bridge designed by the Texas State Highway Department for the Urban Expressway System in Houston, Texas, was selected as the test bridge for that purpose.

Construction of the bridge was not complete at the time of this writing, and only the period from casting of the beams to their erection on the bents, about 300 days, is covered in this report. The final report will cover the entire construction and possibly a period of service of the structure.

5-2 Description of the Bridge

The test bridge, Figure 5-1, is being constructed to carry traffic on Interstate Route 610 over South Park Boulevard in Houston, Texas. It is located on the South Loop of the expressway surrounding the central part of the city. Four traffic lanes are provided each way for east and west bound traffic over four simple spans, one of 40 feet and three of 56 feet. The beams are pre-cast prestressed concrete, and the deck is reinforced concrete, Figure 5-2.

Lightweight and normal weight concrete beams and deck slabs

are used in various combinations in order to determine the different behavior patterns.

The structure was designed and supervised in all construction phases by the Texas Highway Department. The beams were fabricated by Trinity Concrete Products Company at its Houston, Texas plant. Construction at the bridge site is by George Consolidated, Inc.

Instrumentation and collection of test data were carried out by personnel of the Texas Transportation Institute, Texas A&M University with the assistance of Texas Highway Department personnel.

Details of the beams and of gage locations are given in Tables 5-1 and 5-2.

5-3 Objectives

The overall objective of the entire program is to develop a method for predicting creep in prestressed concrete. The specific objectives of the part treated in this chapter are:

A. Instrumentation of a highway bridge for strain and elevation measurements, and to collect data from that bridge by making such measurements.

B. To develop and test a method for predicting creep and camber of prestressed concrete highway bridges.

C. To determine camber and prestress losses in normal weight and lightweight prestressed concrete beams used in a highway bridge.

5-4 Test specimens

A. Test specimens consisted of standard size cylinders for

stress-strain and strength information; 3 x 3 x 16 inch prisms for creep and shrinkage data; shrinkage specimens of full size beam section by 4 feet long; and full size beams. Details of all, except the cylinders, are given in Figure 5-3 and Table 5-2.

B. Seventy-two prestressed beams, Texas Highway Department Type B, were used on the job. Among those, five were instrumented with elevation points, strain gage points, and thermocouples. Those five beams are the main test articles. Fourteen additional beams were fitted with elevation points only. Five beams originally instrumented for elevation measurements were not included in the tests because the prestress was released before measurements of elevation could be taken.

Copper-constantan thermocouples were installed in the five main test beams at midspan near the bottom and mid-depth of the beams. Those thermocouples were installed for purposes of comparing slab and beam temperatures in the finished structure. The leads were brought out at the tops of beams, and Figure 5-6 shows a photograph of the wires done up in waterproof plastic and tied to the top of beam stirrups.

Brass inserts were fixed on the inside of the steel sideforms of the five main test beams before casting, Figures 5-3(d) and 5-7. Stainless steel gage points were installed in the inserts when the forms were pulled away.

Elevation points, 1/2 inch diameter bolts, were set into steel inserts cast flush with the top surfaces, Figure 5-3(e), of nineteen of the beams. The bolt threads were dipped in epoxy

resin before being screwed down tightly in the inserts. The heads of the bolts, which later served as the seat for the level rod, extended seven inches above the top of the beam. When the slab is cast the top of the bolt will be just under the slab surface, and will be uncovered before the concrete sets up. Locations of elevation points are shown in Table 5-2.

The 40 ft. beams were prestressed with straight strands; all others used depressed strands. Some of the beams were steamed in the line and some were not. All were cured under wet mat until removed from the line, and they were then cured under an impervious blanket for a minimum of three days.

C. Two four foot long shrinkage beam specimens, Figures 5-3(c) and 5-4, of the same section as the bridge beams were cast in line with the prestressed beams. One was made of lightweight concrete and the other of normal weight. Plastic tubing was threaded over each strand for the full four foot length of each of those specimens to prevent bonding of concrete to prestressing steel. All of the strands were easily withdrawn from one specimen, but the other, having large beads of metal at ends of the strands left from the burning operation, retained about half of those unbonded strands. The ends of these shrinkage beams were smoothed over with a layer of mortar which filled the ends of the holes left when the strands were removed, and that mortar cover was then coated with a thin bituminous cover. Gage points were installed in the same way as for

the main beams, and the specimens were cured in the same way as the main beams.

D. Test cylinders, shrinkage prisms, and creep prisms were made as explained in Section 1-4 B from one batch each of light-weight and normal weight concretes. Two prisms of each concrete were spring loaded to 2000 psi and two to 3000 psi. Figure 5-3 (b) gives details of the spring loaded specimens, and Figure 5-5 shows a photograph of them in yard storage.

5-5 Materials

A. Prestressing steel was specified as 7/16 inch diameter high strength, stress relieved 250K, seven wire strand meeting ASTM A-416 with minimum ultimate strength of 27,000 pounds per strand.

B. The concrete mixes are given in Table 5-3. All concrete was batched in a central batching plant in the casting yard, and was transported to the forms by overhead crane, Figure 5-8. Internal vibrators were used for compacting the concrete in the forms. The steam cure schedule called for a temperature rise of 20° F per hour to 140°, hold it at 140° for four hours, then lower at the rate of 20° per hour. The beams that were steamed were then cured under wet mat until released, and they were then stored three more days under an impervious mat. The beams that

were not steam cured remained in the prestressing line under wet mat until released after which time they were treated in the same way as the other beams.

5-6 Instrumentation

A. Shrinkage and creep measurements and reductions followed the method outlined in Section 1-4 B. Strain and elevation measurements were taken from each instrumented beam just before and just after release, and daily for five days thereafter. Subsequent readings were taken at intervals of one to three weeks.

B. Thermocouple readings were taken for a few days after casting. It was found that the beam temperatures were essentially the same as ambient temperatures after curing, and thermocouple readings were then discontinued.

5-7 Test Results and Discussion

A. Stress-strain tests

Specimens from one batch each of lightweight and normal weight concretes were tested for stress-strain data. The secant moduli at 1/2 f'_c determined from those tests were used in computations of strain and camber. The age at test of those specimens did not coincide in all cases with the release age of the test beams.

The original plans called for release of prestress at one day age in all cases except for those beams which were cast on weekends, in which cases release was to be at two day age.

As it developed, strength sufficient for release was not reached in all cases on the schedule originally anticipated, therefore some beams remained in the forms longer than anticipated. Lightweight specimens were collected from the casting of beam R2-5, which was steam cured and released at one day age. The normal weight prism specimens were collected from the casting of beam L3-5, cured under wet mat and released at two day age, and the normal weight shrinkage beam was collected from the casting of beam L3-2, steam cured and released at one day age.

All beams were released at either one or two day ages except those cast with R1-5, three-day release, and those cast with R4-5, seven-day release. For these two castings, one should expect differences in shrinkage and modulus of elasticity between the test articles and the small specimens. This was recognized at the time of release, but it was too late, then, to prepare specimens with the same history as the beams.

B. Shrinkage

Shrinkage of small sprisms made of normal weight and lightweight concretes, Figures 5-9 and 5-11, are about equal up to an age of about six weeks. The influence of seasonal rains which began at about that age is evident, but the normal weight concrete prisms expanded more than the lightweight during that wet season. At 300 day age, the net shrinkage of lightweight prisms was almost 50% higher than the normal weight prisms.

Shrinkage of non-stressed beams, four foot long

specimens, Figures 5-13 and 5-14, was much greater in the normal weight concrete than in the companion lightweight specimen. Seasonal changes are evident in those specimens, too, at about six months age. At that age, the beam and prism of normal weight concrete had about the same shrinkage, but the lightweight prism had shrunk about twice as much as the lightweight beam. There is the indication here that size effect is more pronounced in the lightweight specimens than in the normal weight.

At the time of this writing, 300 day age, the 4 ft. long beam specimens were still shrinking, but they will probably stabilize to some 200 to 300 microinches, and vary seasonally about that range of values.

Hyperbolic function curves fitted to shrinkage of the four foot beams are shown with measured shrinkage in Figures 5-13 and 5-14. Those functions are used later in calculations for predicting creep and camber in the prestressed beams. That type of function fits the data well over a long test run, and it has proved to be of value in earlier chapters in providing reasonable agreement between measured and predicted strains. It has the very powerful advantages of being simple, continuous, and compatible with measured values.

C. Creep in small specimens

Creep in prisms was found by deducting shrinkage from total strains, Figures 5-9 and 5-11. Sustained stresses, 2000 and 3000 psi, from spring load divided into creep produced the

average unit creep values plotted in Figures 5-10 and 5-12. Hyperbolic functions fit those curves well, too, and they are used later for predictions of creep and camber in the bridge beams.

The difference in properties of normal weight and lightweight concretes shows up clearly in Figures 5-10 and 5-12 in the unit creep curves. At three weeks age, the unit creep of lightweight concrete is about 2 1/3 times that of the normal weight concrete, whereas at 300 days it is about 1 2/3 times as great. The early age ratio compares favorably with the ratio of secant moduli of approximately 2 1/4 taken at 1/2 f'_c. In these tests there is no question about which concrete has the greater creep; throughout the test history the lightweight creep per unit of stress surpasses that of the normal weight concrete.

D. Strains in beams

Prestressed beam strains are plotted in Figures 5-15 to 5-19. On each plot the measured strains are compared graphically with the predicted values computed by the method outlined in Chapter I.

Strains are shown at three stations for points near the top, mid-depth, and bottom of five beams. Each data point represents the average values on the two sides of the beam. Station A is located from the end of the beam a distance equal to the depth of the beam in order that local end effects be smoothed out before gaging. Station B is located at or near the quarter span, and Station C at or near mid-span.

In elevation, gage points are nominally three inches from the top, three inches from the bottom, and at mid-depth.

Strains from Station A are predominately those of prestress, whereas those from Stations B and C are influenced more by dead load bending -- Stations C moreso than Station B. Mid-span release stresses are listed in Table 5-1.

Beams L1-5 and R1-5 are identical, 40 foot span, lightweight concrete, except that the former was released at two day age after steam cure, whereas the latter was released at three day age after curing under wet mat. Figures 5-15 and 5-16 show strains in those beams, and it may be seen in those figures that L1-5 strains are higher than those in R1-5, and that the difference begins with the release strains. The lower modulus of the less mature concrete of L1-5 caused greater initial strains in that beam; at 300 days the strains have leveled off to almost stability in both of those beams.

Beams L4-5 and R4-5, both lightweight 56 foot spans, have different histories in the prestress line. L4 beams were released on the day after casting whereas R4 beams were held in the line seven days before release because the concrete was slow in gaining strength; both were steam cured. Release strains are greater in L4-5, released at one day age, probably because of a lower modulus corresponding to the age at release. The bottom strains, where compressive stresses are highest, are greater in L4-5 than in R4-5, but mid-depth strains, where stress is

comparatively low, are almost the same in the two beams. The strains developed at top gages in R4-5 after release are greater than in L4-5, and in R4-5 they continue to increase throughout the period, whereas they level off at about one month age in L4-5. The stress at release, Table 5-1, being tension in the former beam and compression in the latter would be responsible for that type of behavior.

Strains in the normal weight beam L3-5 in Figure 5-19 are much lower than those of corresponding lightweight beams L4-5, Figure 5-17 and R4-5, Figure 5-18. It will be noted, too, that the normal weight beam strains appear to be stabilized after about six months age whereas the lightweight beams continue to strain, especially in bottom concrete, at 300 day age.

Good agreement may be seen between predicted strains and measured strains in all of the beams, except those which remained in the prestress line so long. Shrinkage and unit creeps were taken from specimens which were removed with their companion prestressed beams, having cured in the prestress line one or two days. Recalling that R1-5 remained in the line three days before release, and that R4-5 remained seven days before release, the difference between predicted and measured strains which are shown in Figures 5-16 and 5-18 are as one might expect. There is good agreement between measured strains and predicted strains where conditons of the small models agree closely with those of the full size beams.

E. Deflections

Deflections versus time are shown for mid-span and quarter-span stations in Figures 5-20 to 5-29, and information is tabulated in Table 5-4. Deflections for at least one beam in each span, except span L2, were collected. In the left bridge, five beams in each of spans 1, 3, and 4 were studied, and one beam in each of the four right bridge spans, for a total of nineteen beams. As was mentioned earlier, span L2 beams were instrumented for deflection measurements, but the field crew was not able to take the readings just before and just after release, therefore those beams were excluded from tests.

Generally speaking, the 56 foot normal weight concrete beams deflected upward at mid-span about 5/8 of an inch on release compared with about 1 3/8 inches for the lighter beams, Table 5-4. The ratio of those deflections compares roughly with the initial moduli of the concretes. The initial prestress was different for the different concretes, and for the different spans, and those differences would have a bearing on the deflections and strains. Beams L1-5 and R1-5, discussed above in paragraph 5-7 D, may be compared for deflections by referring to Table 5-4. There it is seen that the release camber of R1-5 is a little lower than its steam cured companion, and its camber at 300 day age is, too, a little less. The one extra day of curing before release had a greater influence on camber than did the stram cure with one day less of curing.

It is interesting to compare deflections of these beams over a period of time to determine relative camber growth.

Table 5-4 shows a greater ratio of 300 day camber to release camber for the normal weight beam, L3-5, than for the 56 foot lightweight beam, R4-5. This indicates that the normal weight beam has a greater percentage of creep than the lightweight beam although its magnitude is considerably less.

With the exceptions of lightweight beam L1-5 and normal weight beam L3-5, the deflections predicted by the methods of this paper are consistently a little greater than the measured values. This disagreement is greater than that found between measured and predicted strains, which leads to a search for variables or procedures used in deflection calculations that were not used in strain calculations.

Going back to the step-by-step procedure outlined in Chapter I, it is seen that strains are computed and compared at only three stations per beam whereas deflections are found by summing products of angle changes and distances for many sections in each beam. A possible cause, or causes, then, of overestimating deflections is excessive angle change per unit of length, deficiency in number of segments into which the beams are divided, or both. It was pointed out by Corley *et al.*,[10] that predictions would be high because the value of unit creep at the beginning of each time interval is used as a constant value over the interval when, in reality, it decreases as the time increases within each interval. Such a treatment of unit creep will result in excessive deflection, computed by this method if the time intervals are excessively long. The five-day time intervals used in this work are short, and if discrepancies result from such short intervals, those discrepancies

will be developed at an early age.

The search for the cause, or causes, of overestimation of deflection has not yet been successful in establishing the causes. Any discoveries that lead to a reduction of differences will be given in the final report on this study.

F. Prestress loss

Changes in prestress are computed over each interval of time, and the adjusted prestress is found for the beginning of each time period. The loss of stress in the prestressing steel as a percentage of the pre-release stress is shown in Table 5-5 and in Figures 5-30 to 5-34. The elastic loss at release appears as a sudden change at the beginning of each curve, and the loss rate gradually diminishes with the passage of time. In most cases there is very little loss after 60 days age measured from date of release.

Identical beams, L1-5, Figure 5-30, and R1-5, Figure 5-31, were prestressed to 1460 and 1400 psi respectively, mid-span, bottom fiber stress. The curing condition of these two beams has been discussed earlier in paragraph 5-7 D. L1-5 prestress loss at 300 day age was about 15%, and excellent agreement is shown between measured and predicted prestress loss, especially at Station C. The loss in R1-5 at Station C was about 12.5% at 300 days, with somewhat poorer agreement between predicted and measured.

It should be said by way of explanation here that measured prestress loss was found as the product of measured strain at the level of the prestress steel and the modulus of elasticity

of the prestress steel. Strains at the centroid of the prestressing steel were found by interpolating between strains measured at top and bottom gage points.

The lack of excellent agreement between measured and predicted losses in R1-5 can be attributed, at least in part, to reasons already mentioned -- differences in treatment of small specimens, from which parameters were evaluated, and the large beams to which the parameters were applied in computing losses, strains, and cambers.

Lightweight beams L4-5 and R4-5 may be compared on the basis of equal spans, but other variables are different. L4-5 was made with a 7 1/2 sack mix whereas R4-5 used a 7 sack mix; both were steamed before release. L4-5 remained in the line one day before release whereas R4-5 was not released until seven days old. Because of the greater age at release of R4-5, it would be expected that prestress loss would be less than that of L4-5, and Figures 5-32 and 5-33 show that to be the case. The loss in beam L4-5 was about 23%, and that of R4-5 was about 21%, not a great difference.

The mid-span, bottom fiber stress in L4-5 was 2520 psi, Table 5-1, and in R4-5 it was 2790 psi. The greater age of the latter beam at release appears to have overcome its lower cement content and higher stress, as compared to L4-5, in prestress loss.

Normal weight beam L3-5, Figure 5-34, lost about 14% of its pre-release steel stress, having mid-span, bottom fiber stress

at release of 2730 psi.

All of these beams lost approximately 50% of their 300 day prestress loss upon release. The normal weight concrete beam loss at release and at 300 day age was almost 67% of that of corresponding lightweight concrete beams.

Losses, taking 300 day as the datum, 100% at 300 days, were nearly complete at 30 day age, Table 5-5. At 90 day age, 93% to 97% of the 300 day losses had developed.

The general agreement between measured and predicted prestress loss was good in all cases.

G. Thermocouples

Thermocouple data, not presented here, indicated that beam temperature was essentially the same as ambient temperature when readings began about a week after casting.

5-8 Conclusions

A. The details for instrumentation and the techniques for collecting and processing data that were developed in earlier tests were successfully applied in the test of a full size bridge.

B. The method developed for predicting creep and camber of prestressed beams produces good agreement between predicted and measured values provided that the small specimens and the prototype beam are of the same materials and are treated alike. Reasonable agreement may be had if there are no differences in curing conditions and if there are minor differences in materials.

C. Prestress steel stress losses in the materials of these tests varied from 14% of pre-release stress in normal weight concrete to 23% (nominal values) in lightweight concrete at 300 day age. At 90 day age prestress loss has, for all practical purposes, stabilized under the field conditions of these tests.

TABLE 5-1 DESIGN DETAILS OF BRIDGE BEAMS

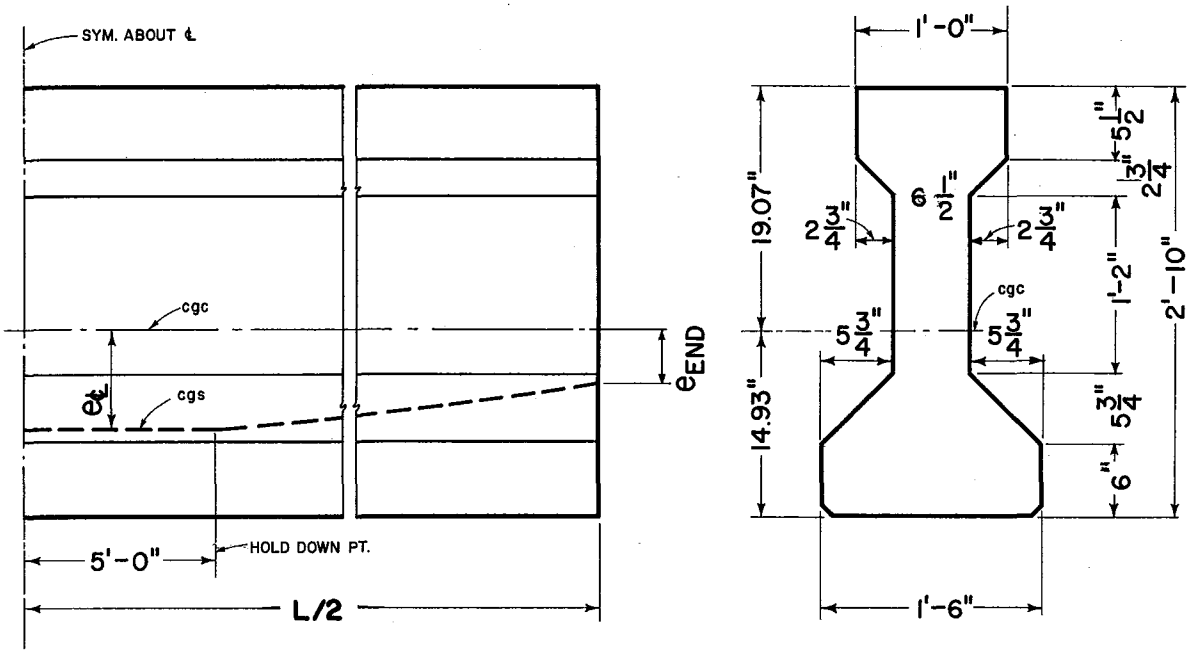

SPAN	LENGTH "L" (FT)	BEAM CONC. (TYPE)	DECK CONC. (TYPE)	NUMBER OF STRANDS (7/16 IN)	e AT ℄ (IN)	e AT END (IN)	INITIAL TENSION K/strand	RELEASE STRESSES AT ℄ OF BEAM[1] (psi)	
								TOP	BOTTOM
L1	40	LIGHT WEIGHT	LIGHT WEIGHT	16	9.19	9.19	19.00	-80	1460
L2	56	LIGHT WEIGHT	NORMAL WEIGHT	36	7.82	5.82	19.00	160	2830
L3	56	NORMAL WEIGHT	LIGHT WEIGHT	32	9.05	5.55	18.90	80	2730
L4	56	LIGHT WEIGHT	LIGHT WEIGHT	30	9.60	7.20	18.80	-130	2520
R1	40	LIGHT WEIGHT	LIGHT WEIGHT	16	9.19	9.19	18.30	-60	1400
R2	56	LIGHT WEIGHT	LIGHT WEIGHT	30	9.60	7.20	18.80	-130	2520
R3	56	NORMAL WEIGHT	LIGHT WEIGHT	32	9.05	5.55	18.90	80	2730
R4	56	LIGHT WEIGHT	NORMAL WEIGHT	36	7.82	5.82	18.60	180	2790

[1](-) TENSION, (+) COMPRESSION

TABLE 5-2 LOCATION OF GAGE AND ELEVATION POINTS IN BRIDGE BEAMS

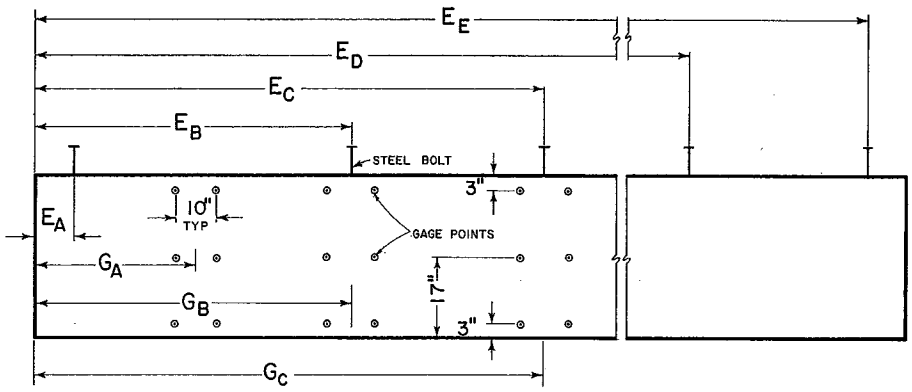

BEAM	LGTH. (FT)	G_A (FT)	G_B (FT)	G_C (FT)	E_A (FT)	E_B (FT)	E_C (FT)	E_D (FT)	E_E (FT)
L1-1	40				0.67		19.25		39.00
L1-3	40				0.67		20.58		39.08
L1-5	40	3.33	12.33	22.33	0.67	9.75	20.46	30.25	39.00
L1-6	40				0.75		20.33		39.08
L1-8	40				0.67		20.08		39.00
L2-1	56				0.71		28.04		54.71
L2-3	56				0.75		27.50		55.04
L2-5	56				1.04	13.75	28.75	41.88	55.04
L2-6	56				0.70		27.83		55.08
L2-8	56				1.00		27.67		54.96
L3-1	56				0.77		27.92		55.08
L3-3	56				0.69		27.92		54.62
L3-5	56	3.25	14.25	28.17	0.71	14.12	27.83	41.75	55.04
L3-6	56				0.74		28.00		55.08
L3-8	56				0.67		27.75		55.04
L4-1	56				0.75		27.12		55.04
L4-3	56				0.71		26.75		55.25
L4-5	56	3.33	14.33	28.33	0.69	14.52	27.33	40.62	55.17
L4-6	56				0.71		28.25		54.67
L4-8	56				1.08		27.25		55.08
R1-5	40	3.25	12.25	22.25	0.67	12.25	21.83	30.12	39.00
R2-5	56				0.79	14.04	29.02	41.88	55.08
R3-5	56				0.71	14.17	28.21	42.71	55.12
R4-5	56	3.25	14.17	28.17	0.70	14.46	27.85	41.92	55.10

TABLE 5-3 CONCRETE MIX AND PROPERTIES

Quantities Per Cubic Yard of Concrete:			
	Light Wgt. Mix 1 (Spans L1, R1, R4)	Light Wgt Mix 2 (Span L4, L2, R2)	Normal Wgt. (Spans L3 & R3)
Cement (Type III)	7 sacks	7 1/2 sacks	7 sacks
Water	332 lb.	356 lb.	298 lb.
Sand	1305 lb.	1243 lb.	1218 lb.
Coarse Aggregate	877 (Featherlite Ranger)	907 (Featherlite Ranger)	2016 (Crushed Stone)
Pozzolith (#8,Dbl.Str.)	112 oz.	112 oz.	112 oz.
Air (MB-VC)	1 oz./sack	1 oz./sack	(Unknown)
Properties			
f'_c (psi)	Not tested	3430 (1 day) 7138 (219 day)	3520 (2 day) 4016 (4 day) 4092 (223 day)
E at $\frac{1}{2}f'_c$ (ksi)		2950 (1 day) 3600 (156 day) 3220 (219 day)	6896 (2 day) 6500 (4 day) 5882 (223 day)

TABLE 5-4. MID-SPAN CAMBER (UPWARD DEFLECTION)
(Determined from Field Measurements)

BEAM	SPAN (ft)	TYPE OF CONCRETE	AGE AT RELEASE (Days)	TYPE OF EARLY CURE	CEMENT CONTENT (Sacks/cy)	MID-SPAN STRESS AT RELEASE		MID-SPAN CAMBER, Δ			
						TOP (psi)	BOTTOM (psi)	RELEASE (in)	300 DAY (in)	$\left(\frac{\Delta 300}{\Delta RELEASE}\right)$	AVG. RATIO
L1-1	40	LW	2	Steam	7	-80	1460	0.38	0.72	1.89)	
L1-3	40	LW	2	Steam	7	-80	1460	0.40	0.74	1.85)	
L1-5	40	LW	2	Steam	7	-80	1460	0.43	0.81	1.88)	1.86
L1-6	40	LW	2	Steam	7	-80	1460	0.38	0.70	1.84)	
L1-8	40	LW	2	Steam	7	-80	1460	0.40	0.73	1.83)	
L3-1	56	NW	2	Wet Mat	7	80	2730	0.65	1.14	1.75)	
L3-3	56	NW	2	Wet Mat	7	80	2730	0.58	1.10	1.92)	
L3-5	56	NW	2	Wet Mat	7	80	2730	0.62	1.12	1.81)	1.77
L3-6	56	NW	2	Wet Mat	7	80	2730	0.62	1.05	1.70)	
L3-8	56	NW	2	Wet Mat	7	80	2730	0.65	1.08	1.66)	
L4-1	56	LW	1	Steam	7	-130	2520	1.31	2.03	1.55)	
L4-3	56	LW	1	Steam	7	-130	2520	1.32	2.06	1.56)	
L4-5	56	LW	1	Steam	7	-130	2520	1.37	2.24	1.64)	1.59
L4-6	56	LW	1	Steam	7	-130	2520	1.26	2.10	1.67)	
L4-8	56	LW	1	Steam	7	-130	2520	1.36	2.10	1.55)	
R1-5	40	LW	3	Wet Mat	7	-60	1400	0.33	0.53	1.61	
R2-5	56	LW	1	Steam	7 $\frac{1}{2}$	-130	2520	1.30	2.06	1.59	
R3-5	56	NW	2	Steam	7	80	2730	0.64	1.17	1.83	
R4-5	56	LW	7	Steam	7	180	2790	1.12	1.73	1.55	

TABLE 5-5. LOSS OF INITIAL (PRE-RELEASE) STEEL-STRESS
(Nominal Load on $\frac{7}{16}$ Diameter Strand = 18,900 lbs.)

BEAM	CONCRETE	STATION	LOSS		LOSS AS % OF 300 DAY LOSS			
			RELEASE (% Initial)	300 DAY	RELEASE	30 DAY	60 DAY	90 DAY
L1-5	LW	A	7.30	16.34	44.7	83.2	92.0	94.8
		B	7.36	15.58	47.2	85.3	93.3	96.3
		C	7.44	14.16	52.5	91.1	95.1	97.1
R1-5	LW	A	6.30	13.21	47.4	81.7	88.6	89.3
		B	5.91	12.55	47.1	81.2	87.2	88.8
		C	6.01	12.41	48.4	82.9	89.0	92.6
L3-5	NW	A	5.49	13.92	39.4	90.1	96.3	96.9
		B	6.22	13.04	47.7	91.2	95.0	98.5
		C	7.46	14.21	52.5	91.4	95.1	96.7
L4-5	LW	A	12.91	25.12	51.4	88.5	92.6	98.7
		B	12.54	24.02	52.2	89.3	91.9	93.6
		C	11.73	22.65	51.8	90.5	91.6	92.4
R4-5	LW	A	10.96	21.62	50.7	85.5	91.1	93.6
		B	11.00	20.73	48.7	83.4	88.2	91.3
		C	10.43	20.91	49.9	82.4	88.9	93.2

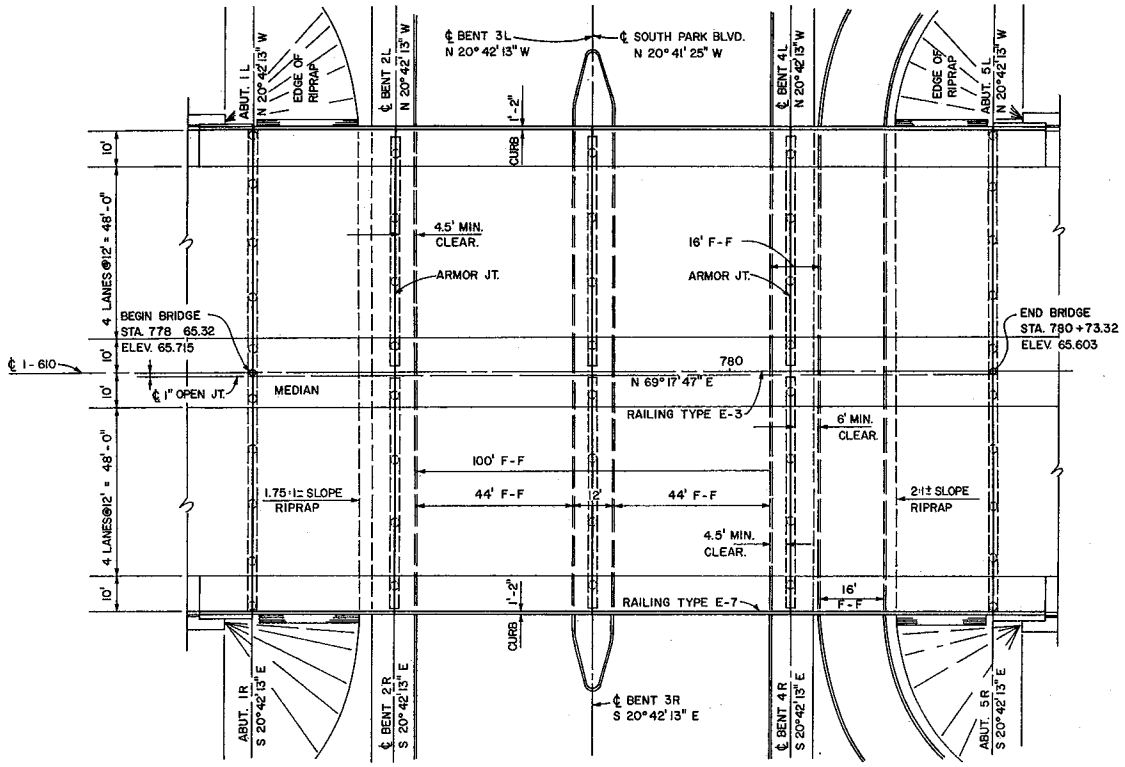

PLAN VIEW

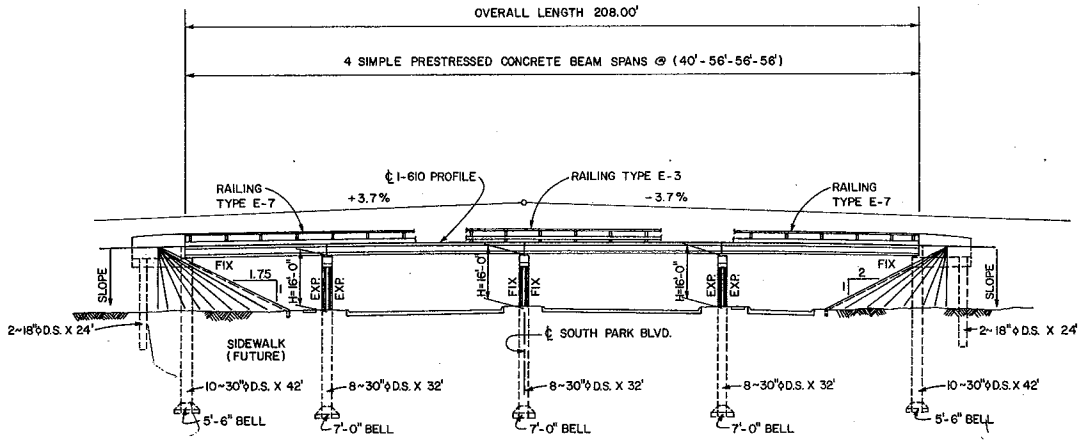

ELEVATION VIEW

FIGURE 5-1 GENERAL PLAN OF BRIDGE

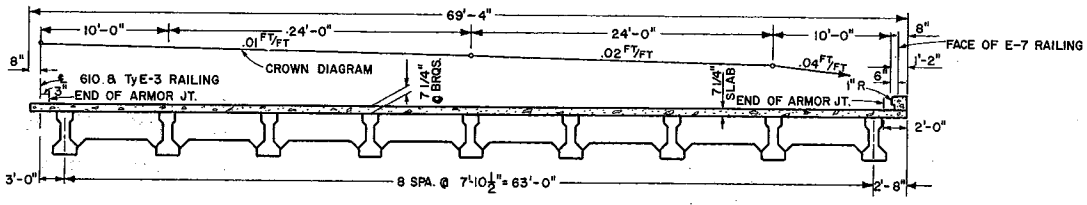

CROSS SECTION-WESTBOUND
SHOWING INTERIOR DIAFRAMS
LOOKING IN DIRECTION OF DECREASING STATIONS

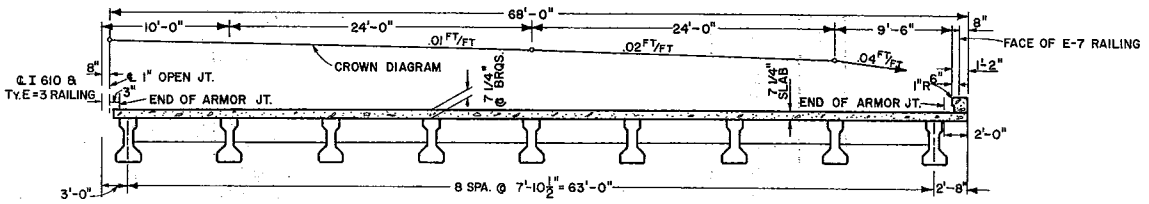

CROSS SECTION-EASTBOUND
SHOWING EXTERIOR DIAFRAMS
LOOKING IN DIRECTION OF INCREASING STATIONS

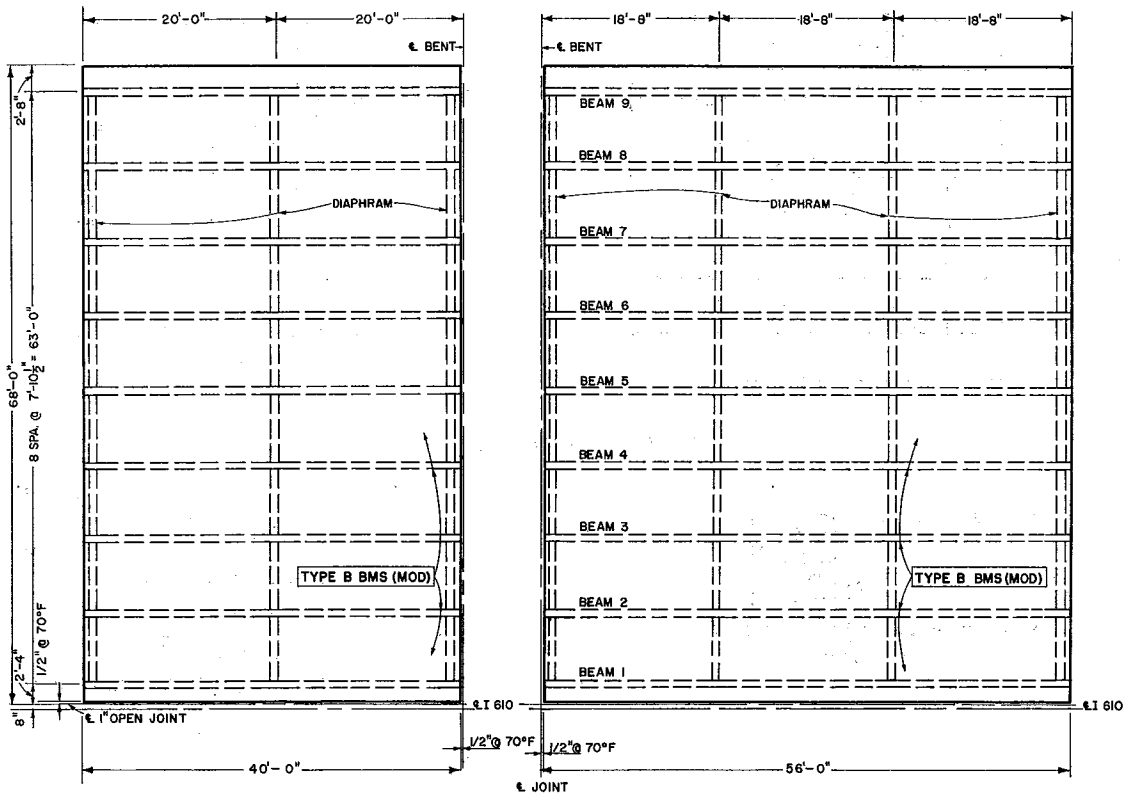

TYPICAL 40'-0" SPAN
PLAN

TYPICAL 56'-0" SPAN
PLAN

FIGURE 5-2 BRIDGE PLAN AND SECTION DETAILS

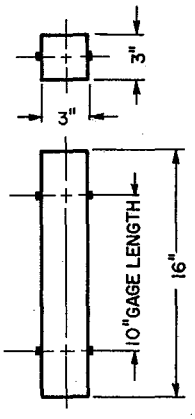

(a) SHRINKAGE PRISM

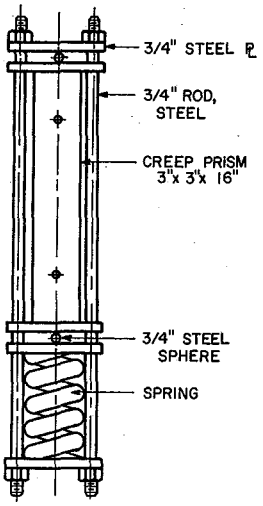

(b) SPRING LOADED CREEP PRISM

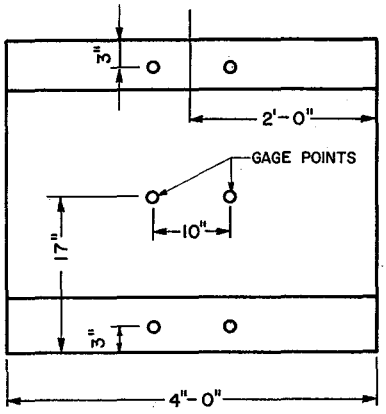

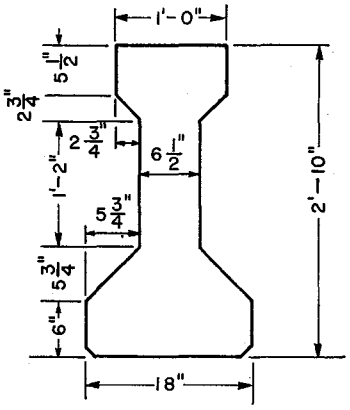

(c) 4 ft SHRINKAGE BEAM

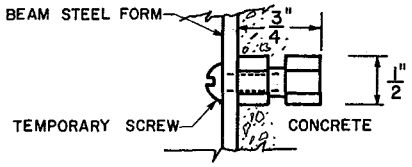

(d) GAGE INSERT

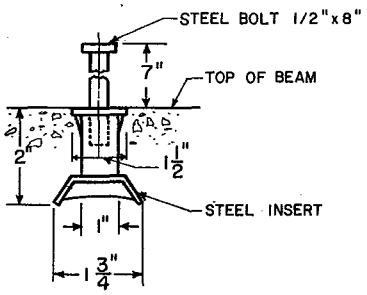

(e) ELEVATION INSERT

FIGURE 5-3 TEST SPECIMENS

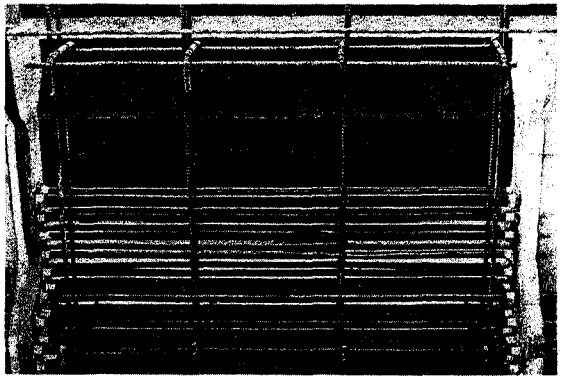

(a) PLASTIC SHEATH STRANDS

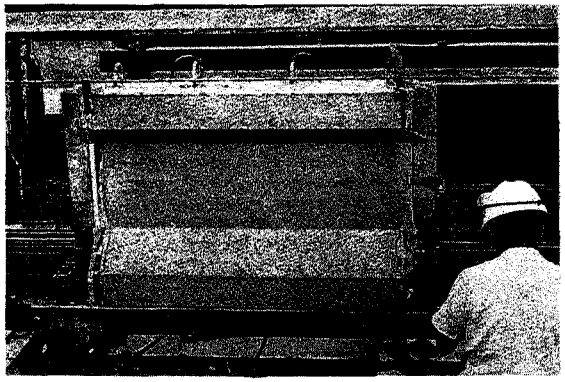

(b) IMMEDIATELY AFTER REMOVAL OF FORMS

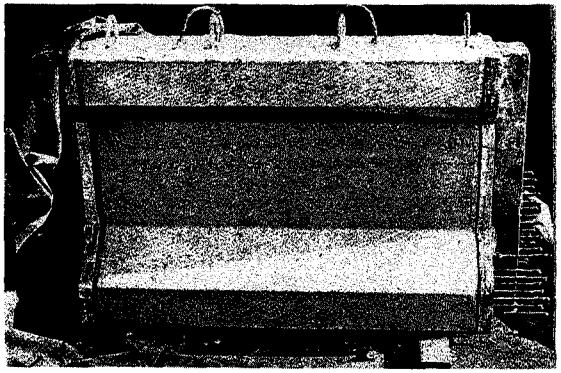

(c) AFTER REMOVAL FROM PRESTRESSING LINE

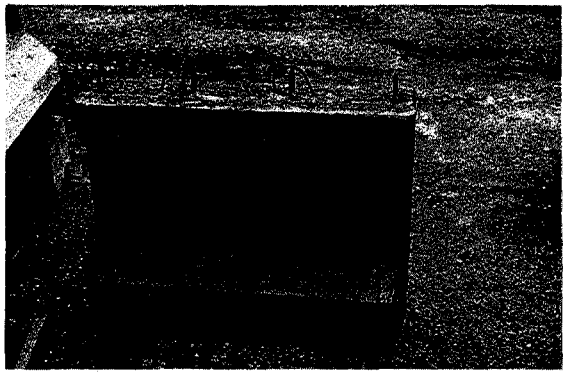

(d) IN YARD STORAGE

FIGURE 5-4 SHRINKAGE BEAMS

FIGURE 5-5 CREEP PRISMS IN YARD STORAGE

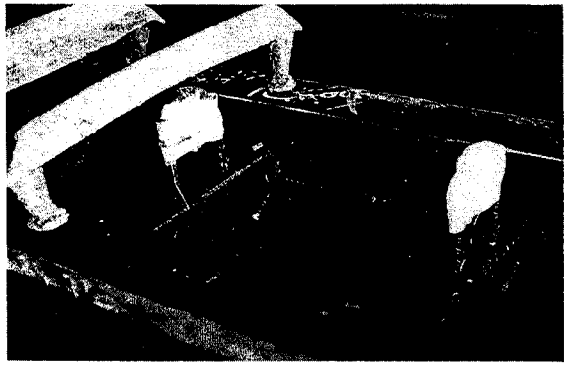

FIGURE 5-6 THERMOCOUPLE LEADS DONE-UP BEFORE CASTING

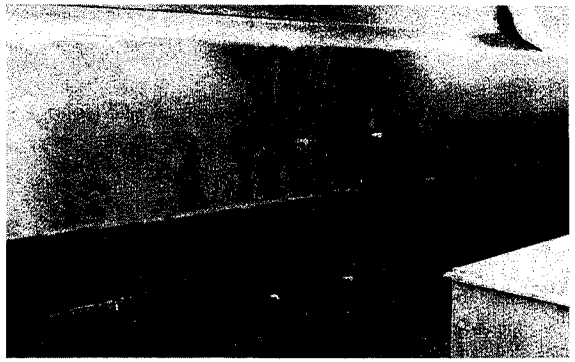

(a) ATTACHED TO BEAM FORMS BEFORE CASTING

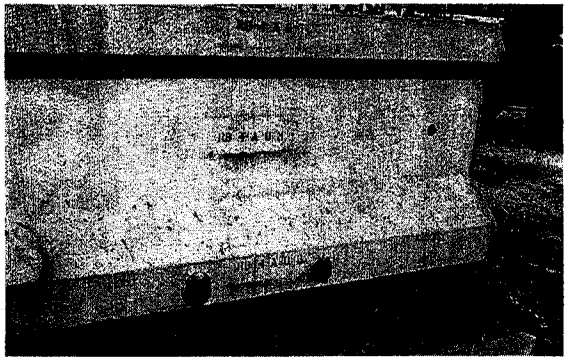

(b) AT BEAM STATION "A"

FIGURE 5-7 BEAM GAGE POINTS

(a) BEING CAST

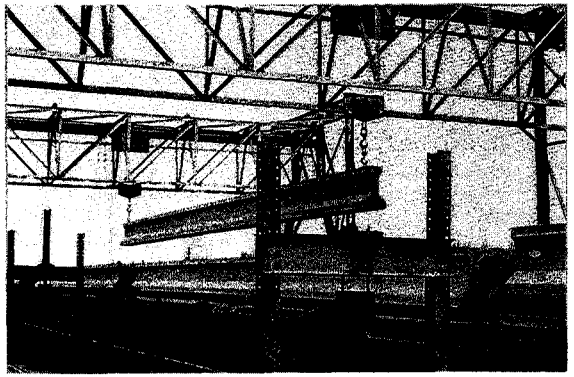

(b) BEING MOVED FROM LINE

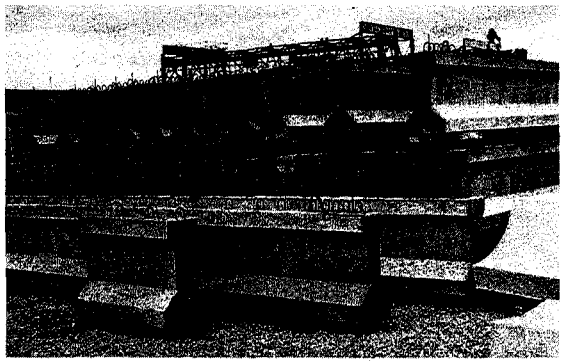

(c) IN YARD STORAGE

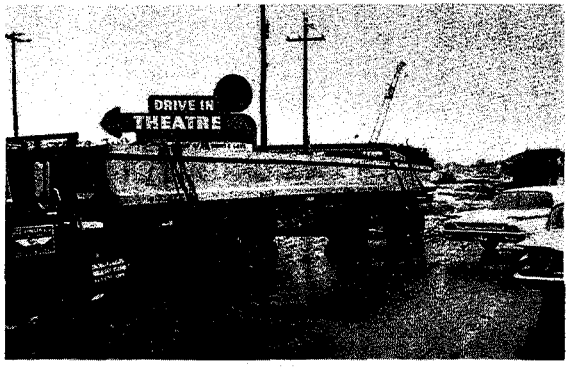

(d) IN TRANSIT TO BRIDGE SITE

FIGURE 5-8 BRIDGE BEAMS

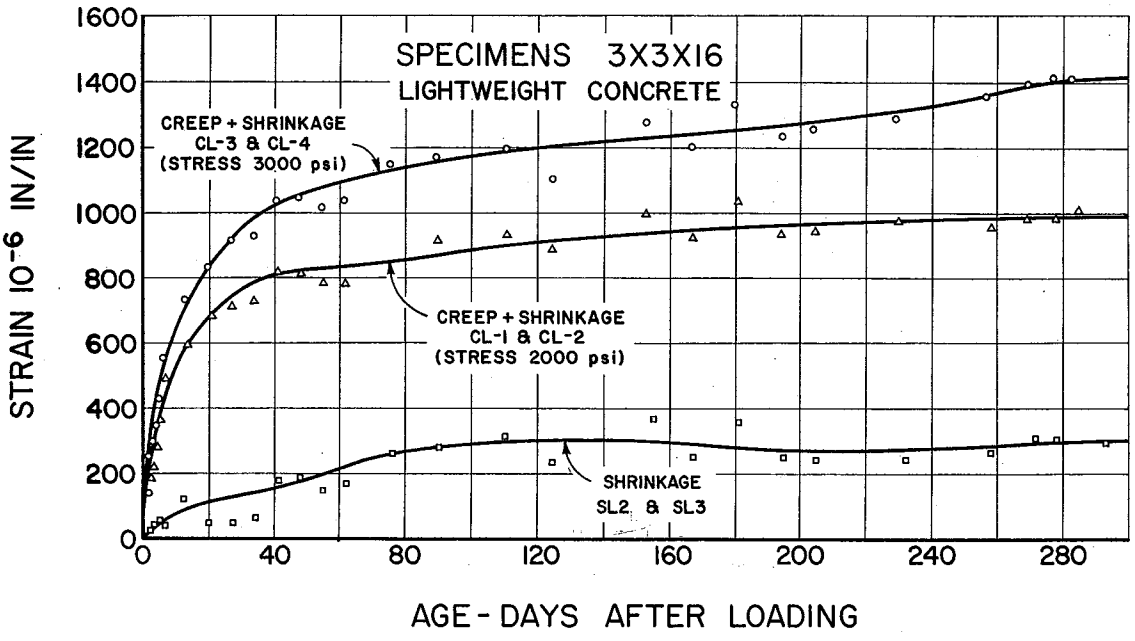

FIGURE 5-9 CREEP AND SHRINKAGE IN 3X3X16 SPECIMENS

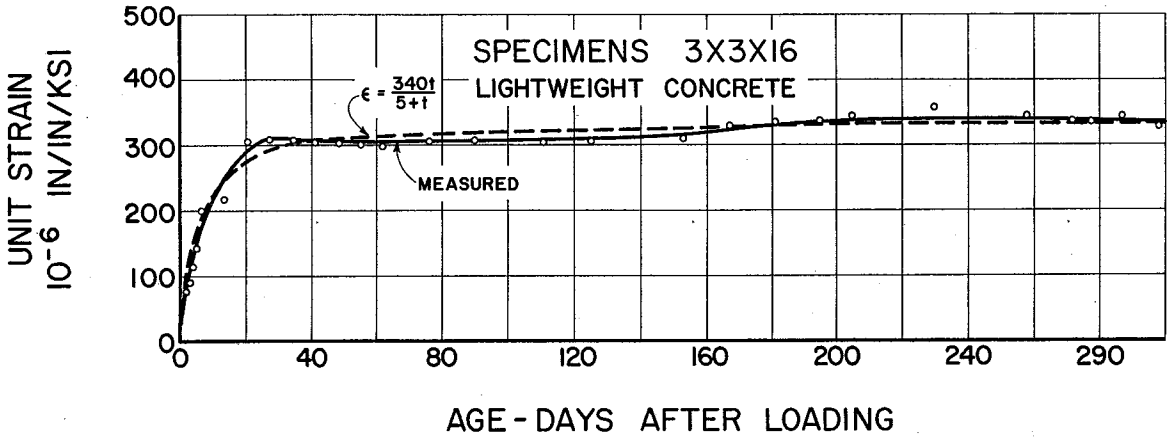

FIGURE 5-10 UNIT CREEP CURVE OF LIGHTWEIGHT CONCRETE

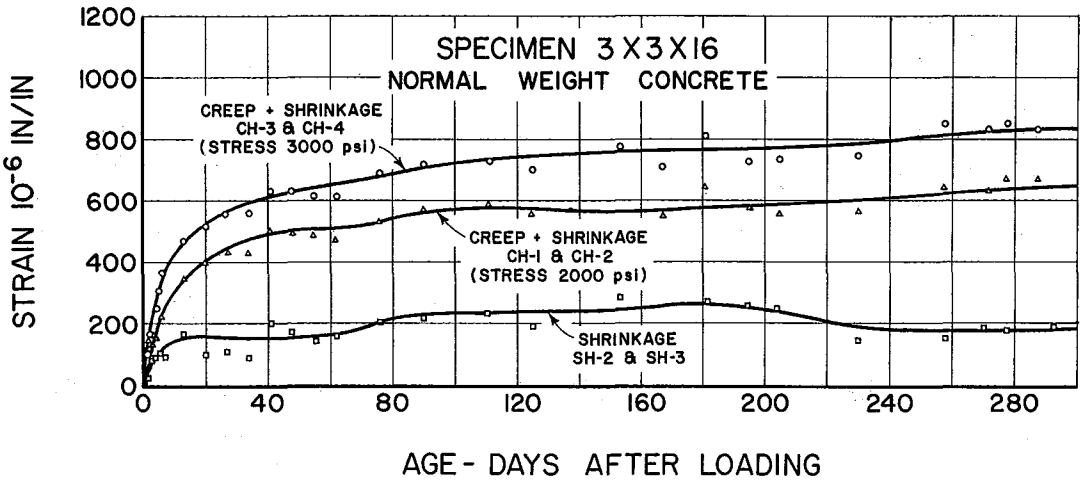

FIGURE 5-11 CREEP AND SHRINKAGE STRAINS IN 3X3X16 SPECIMENS

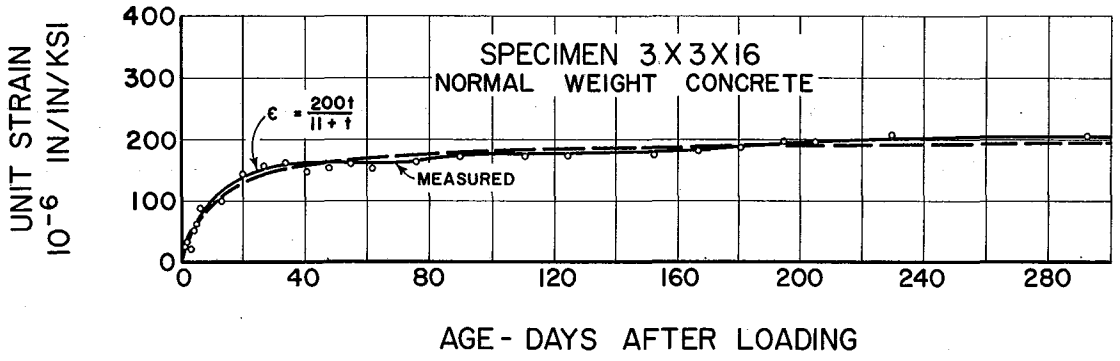

FIGURE 5-12 UNIT CREEP CURVE OF NORMAL WEIGHT CONCRETE

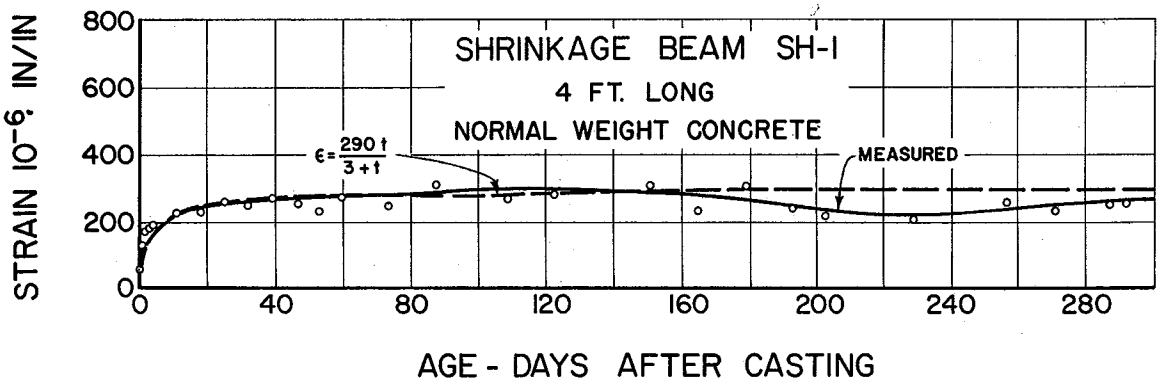

FIGURE 5-13 SHRINKAGE CURVE OF NORMAL WEIGHT CONCRETE

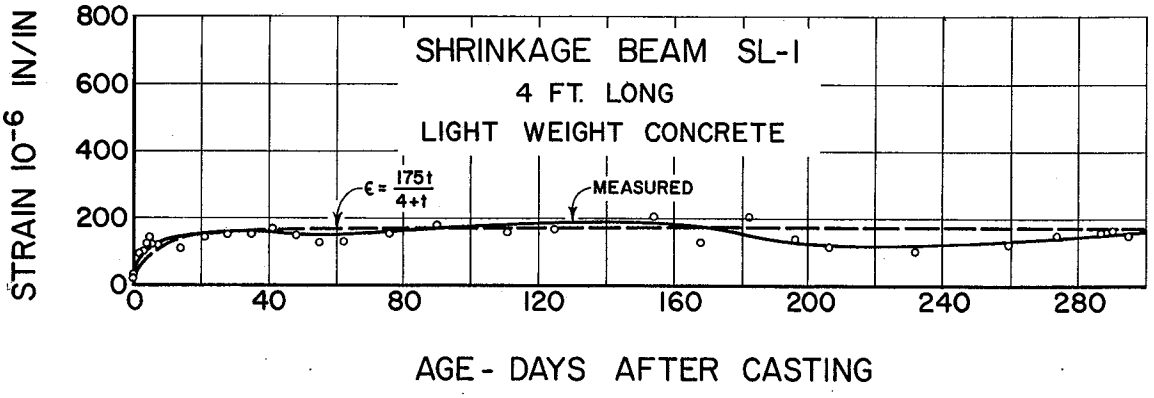

FIGURE 5-14 SHRINKAGE CURVE OF LIGHT-WEIGHT CONCRETE

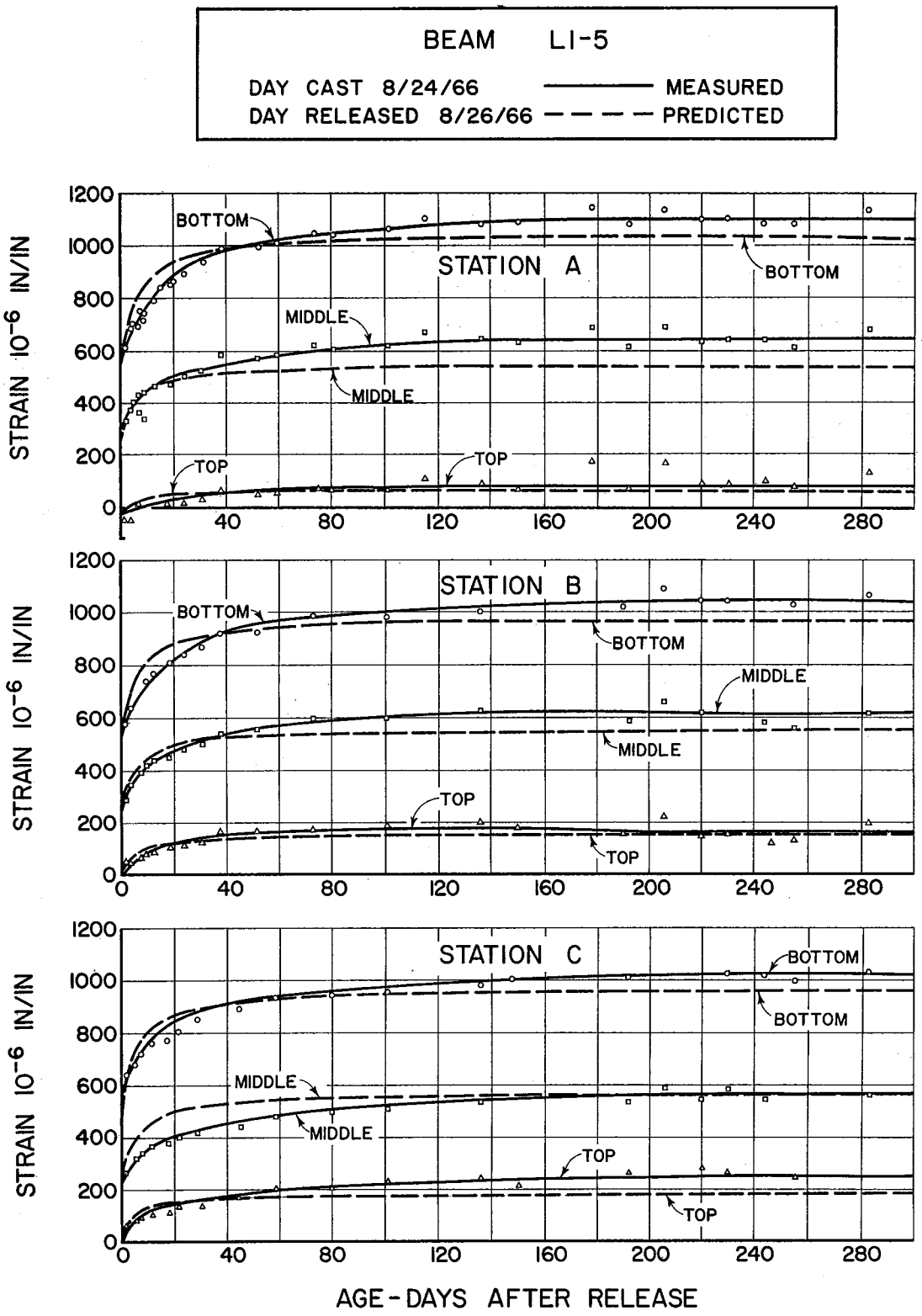

FIGURE 5-15 STRAINS IN BRIDGE BEAM LI-5

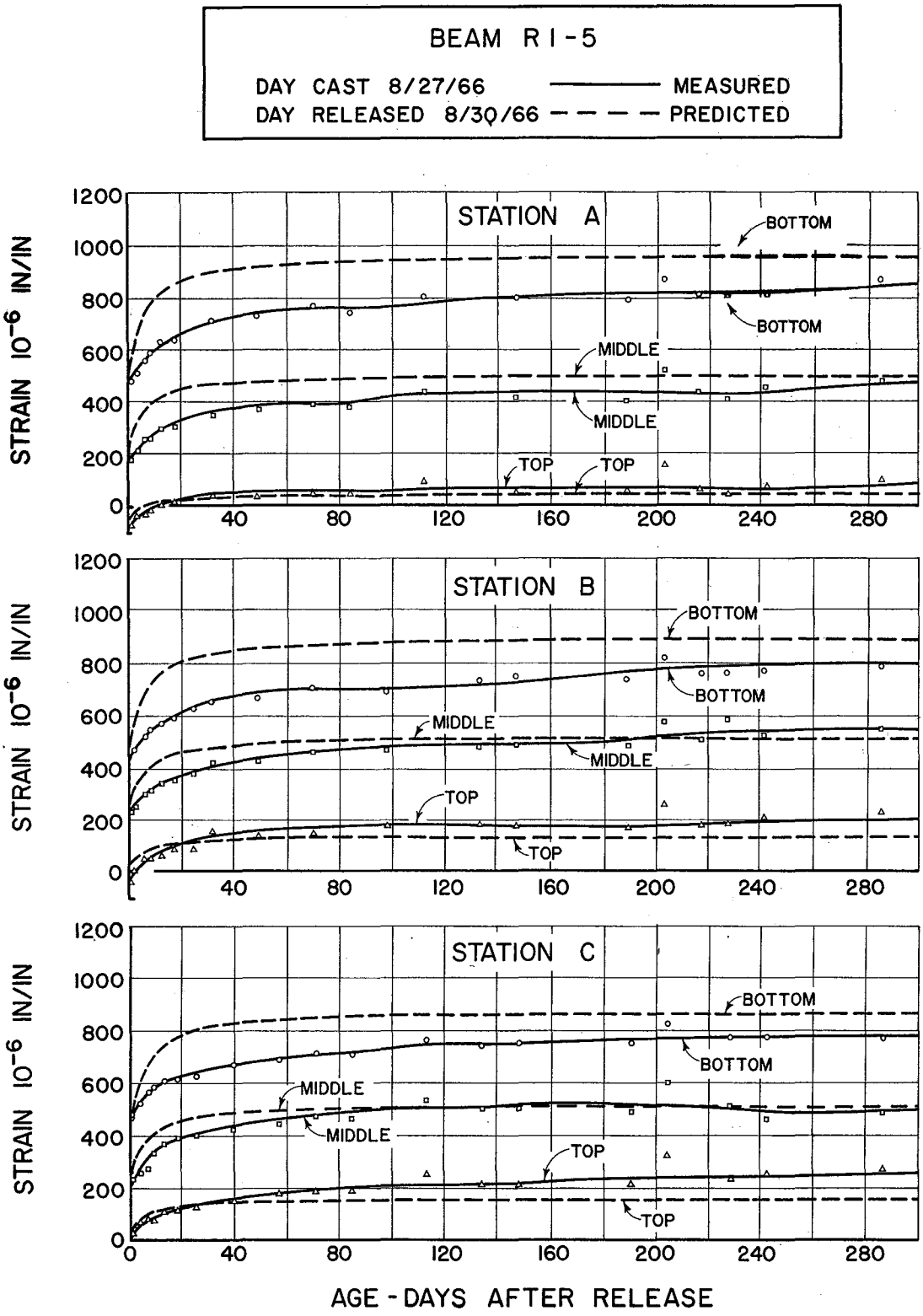

FIGURE 5-16 STRAIN IN BRIDGE BEAM R1-5

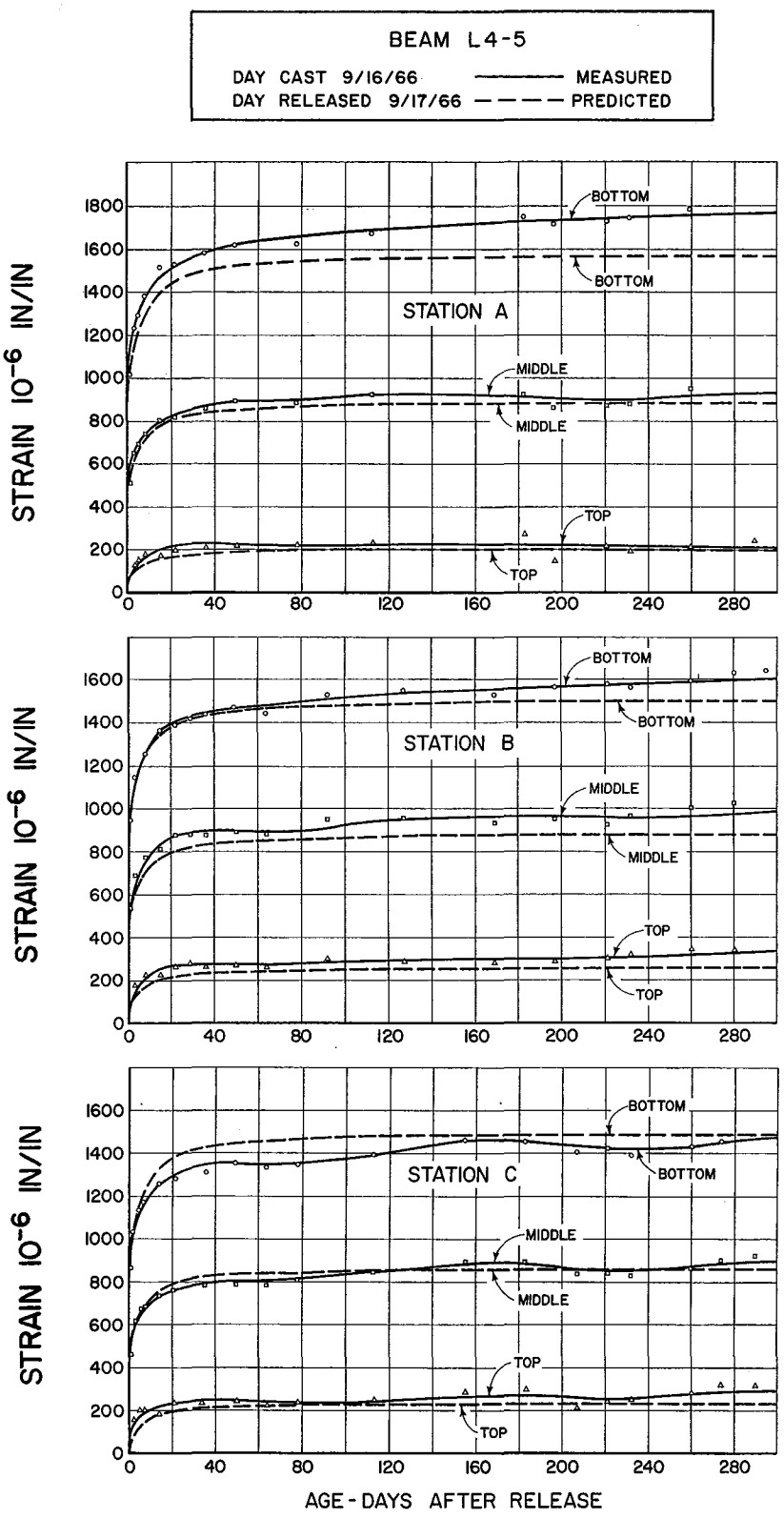

FIGURE 5-17 STRAINS IN BRIDGE BEAM L4-5

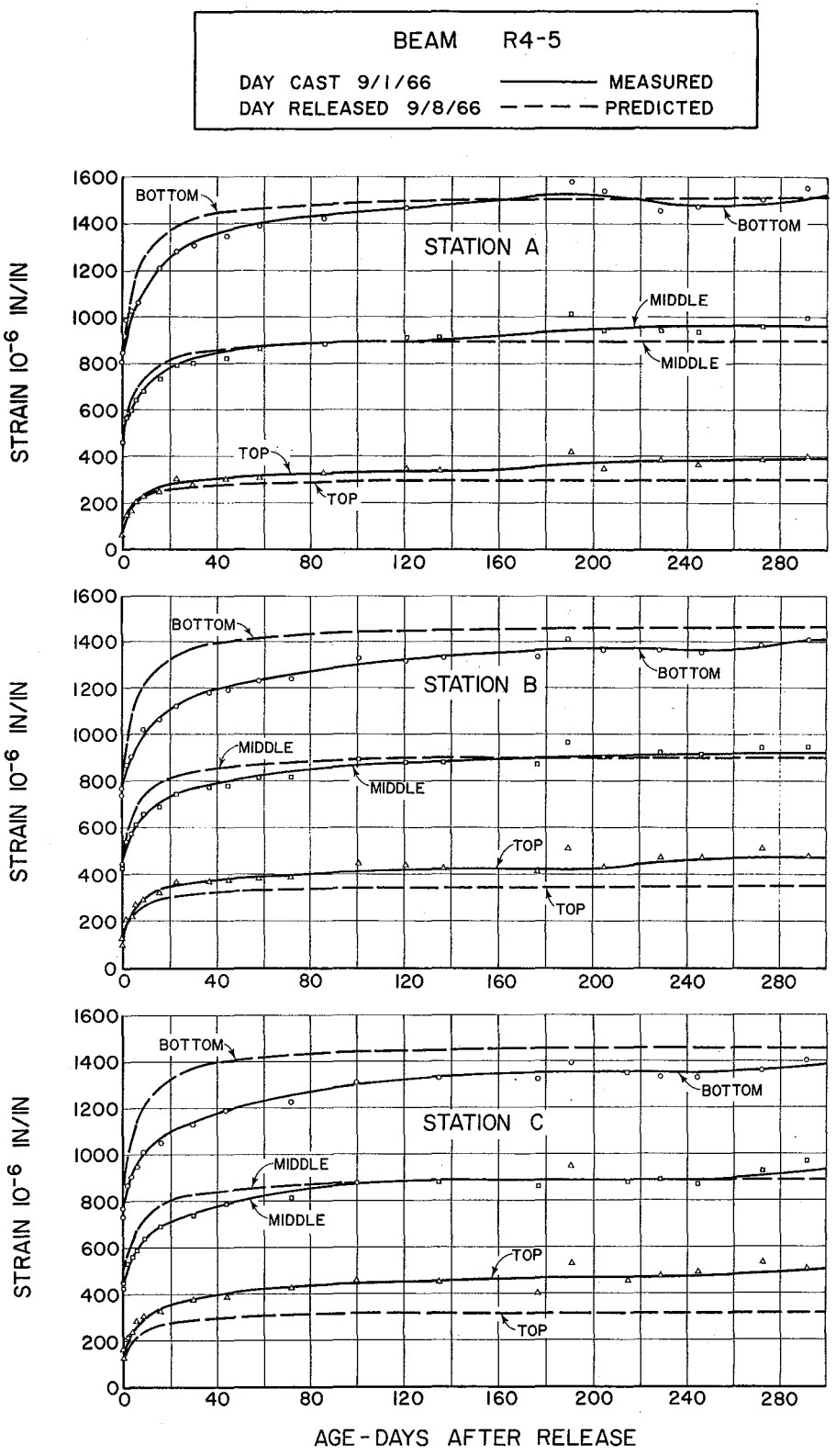

FIGURE 5-18 STRAINS IN BRIDGE BEAM R4-5

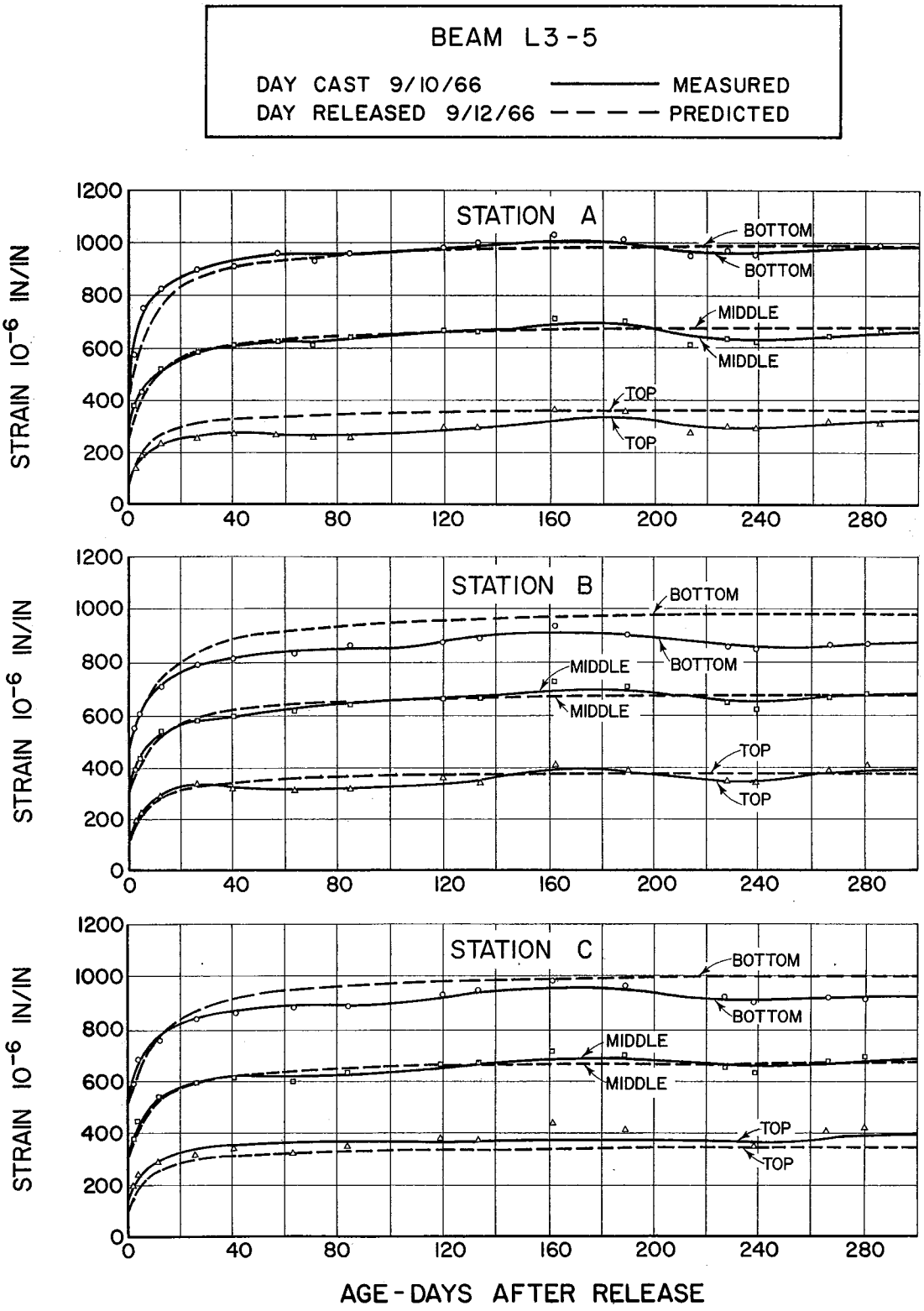

FIGURE 5-19 STRAIN IN BRIDGE BEAM L3-5

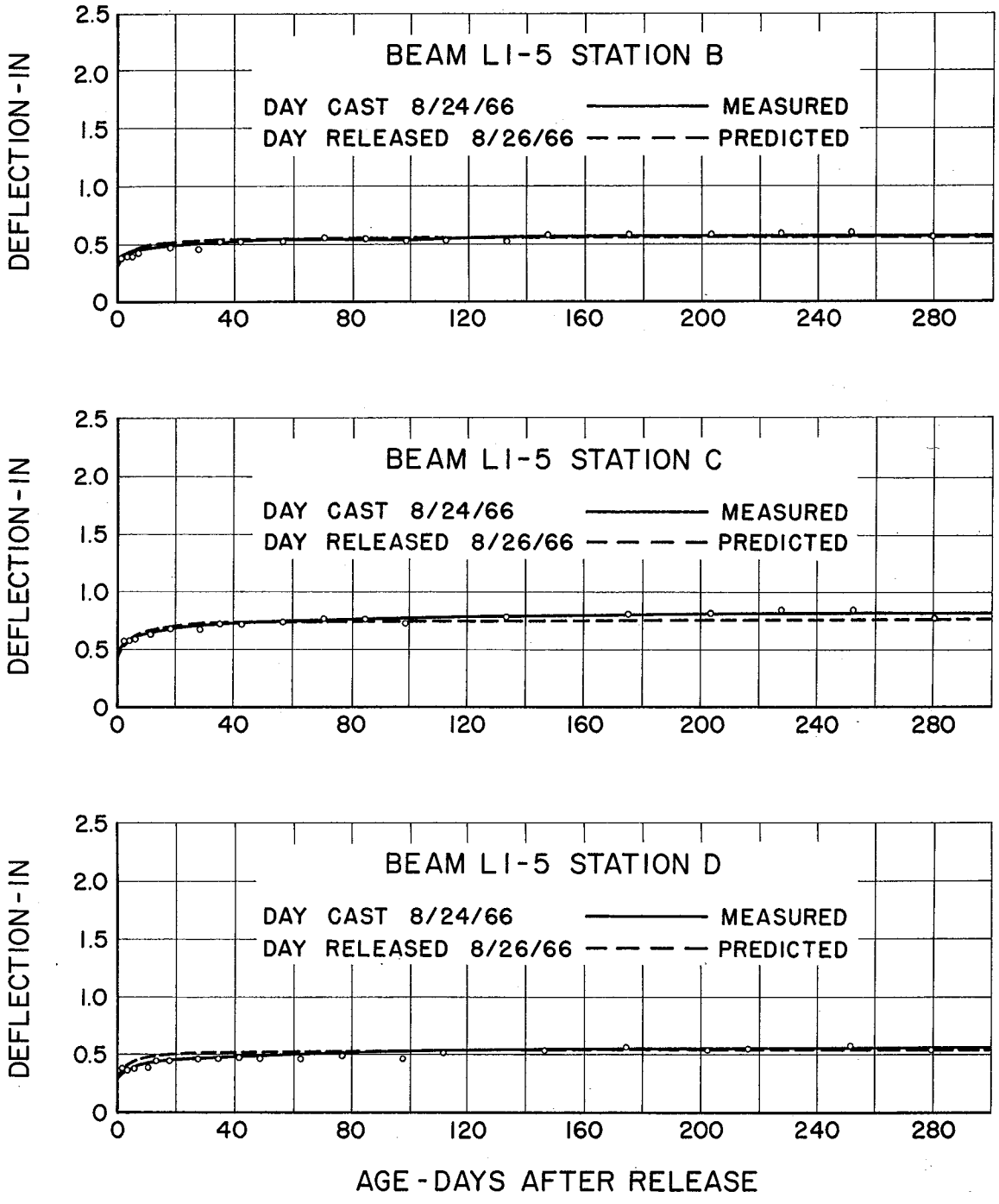

FIGURE 5-20 DEFLECTION OF BRIDGE BEAMS

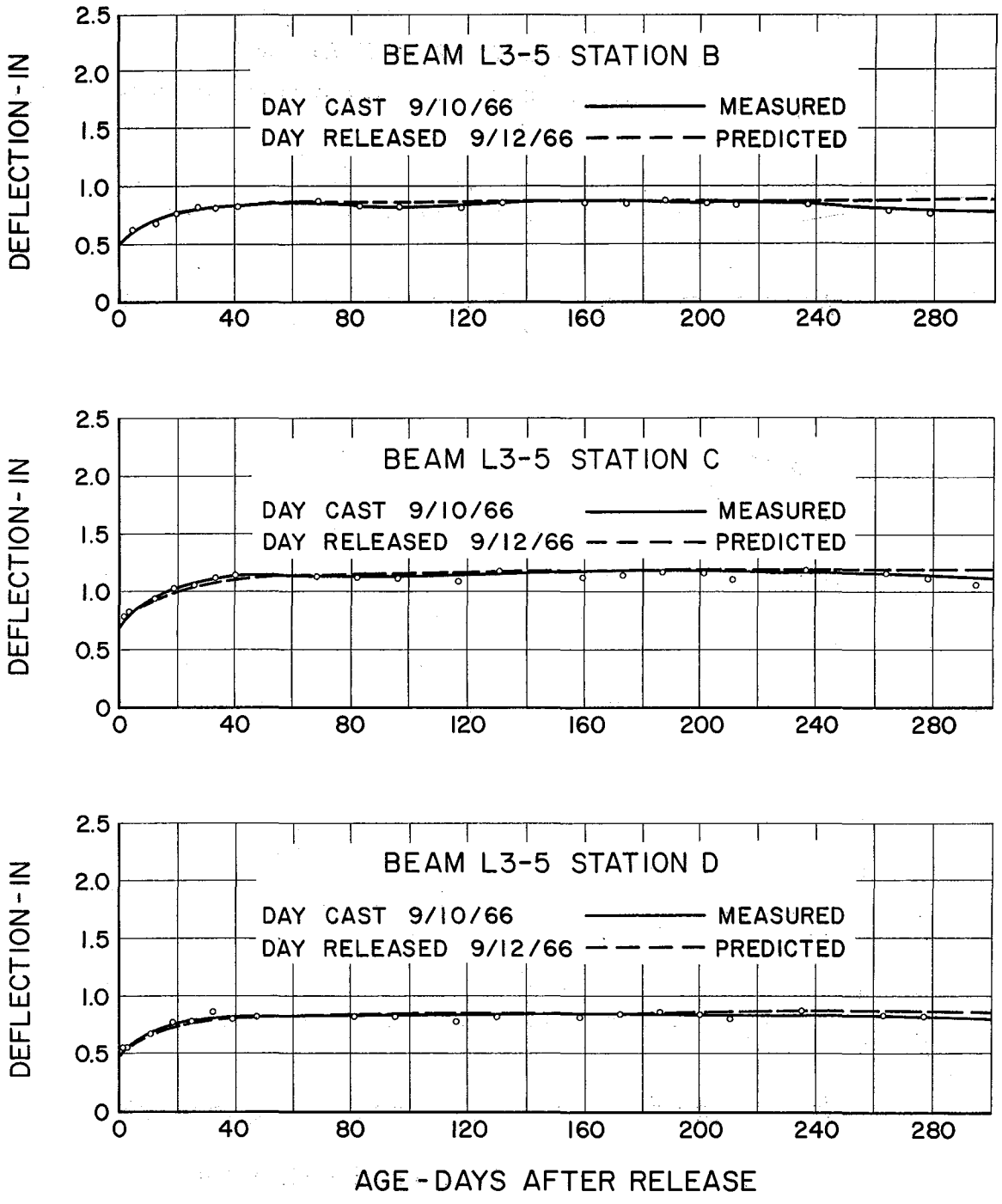

FIGURE 5-21 DEFLECTION OF BRIDGE BEAMS

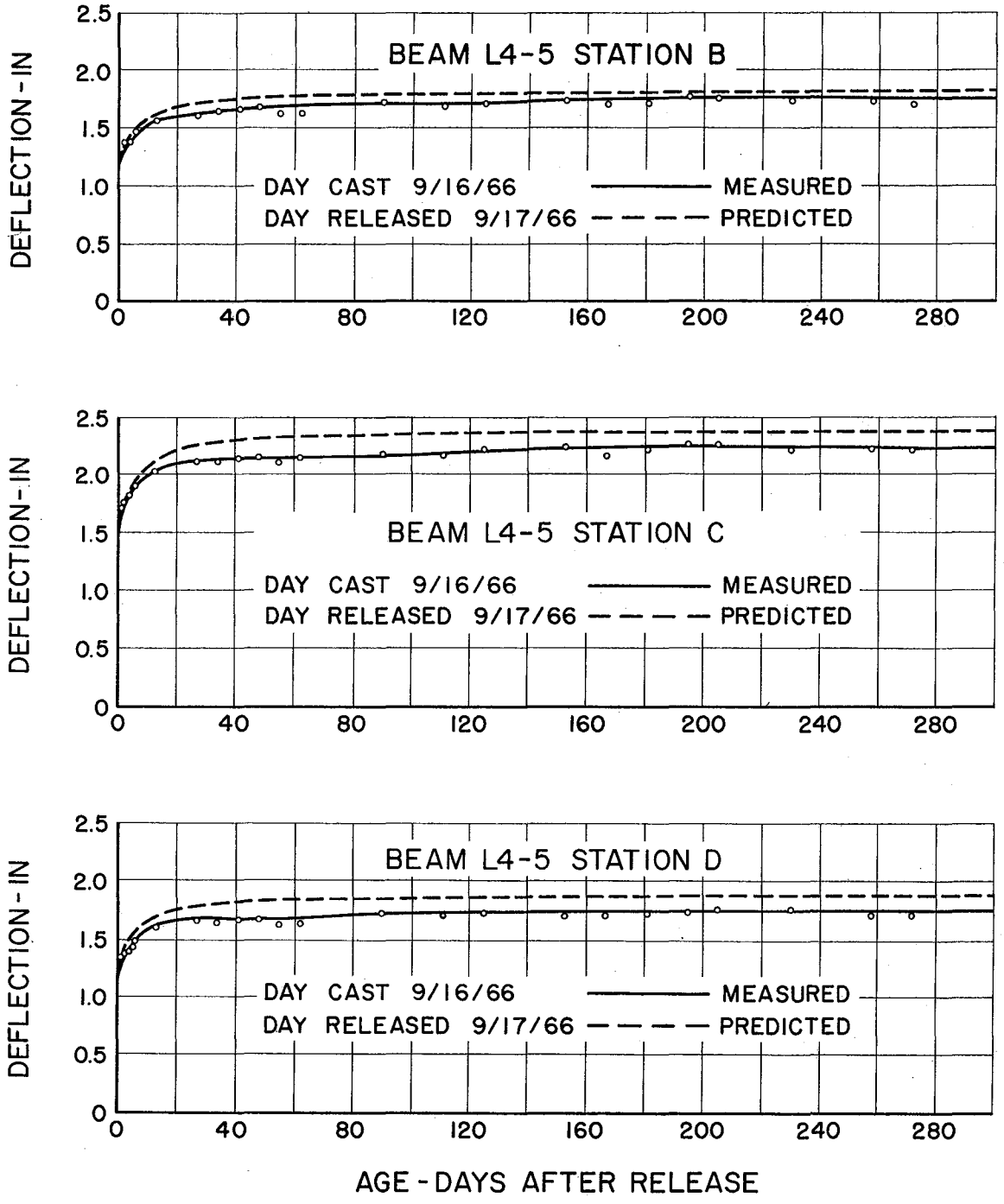

FIGURE 5-22 DEFLECTION OF BRIDGE BEAMS

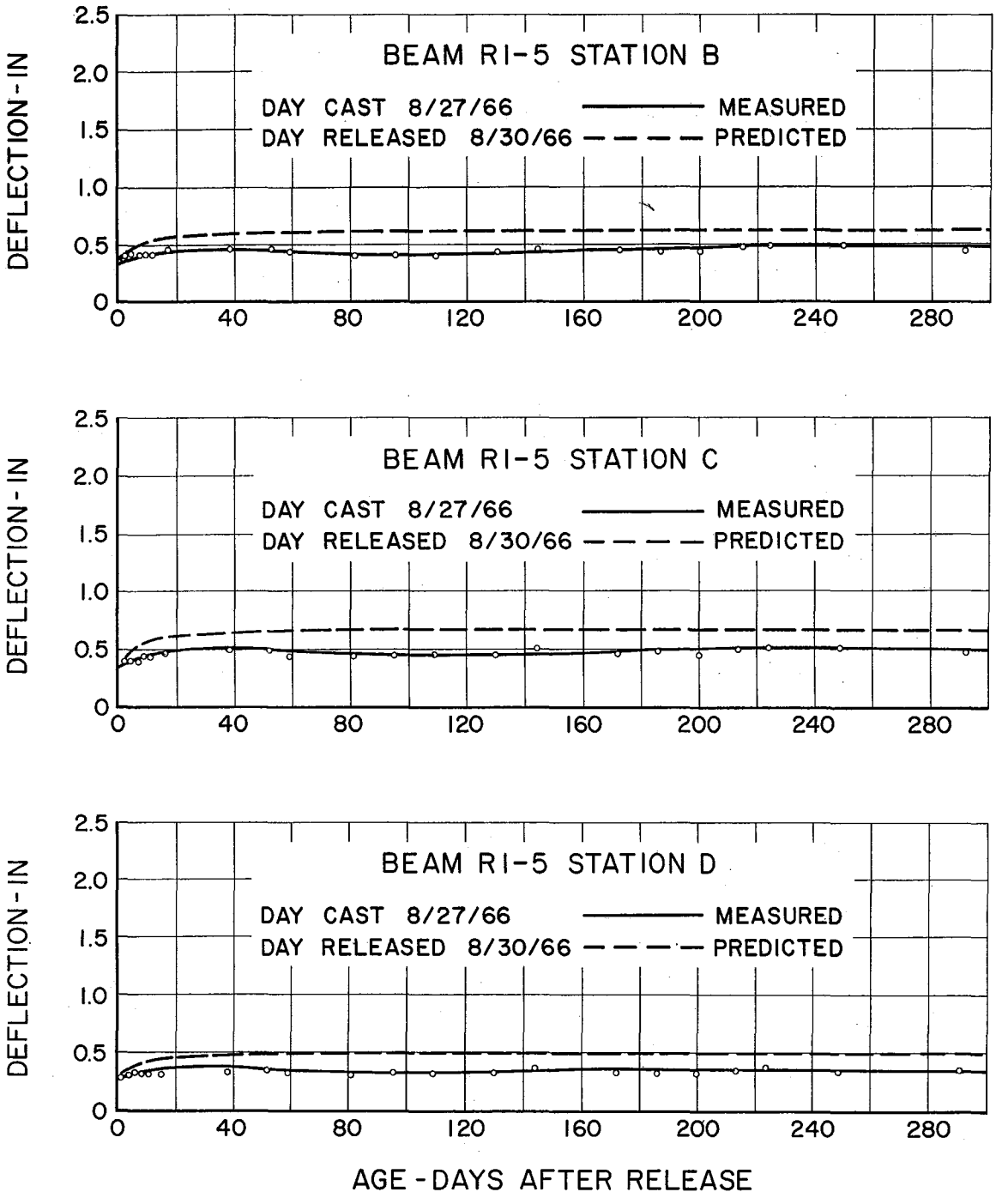

FIGURE 5-23 DEFLECTION OF BRIDGE BEAMS

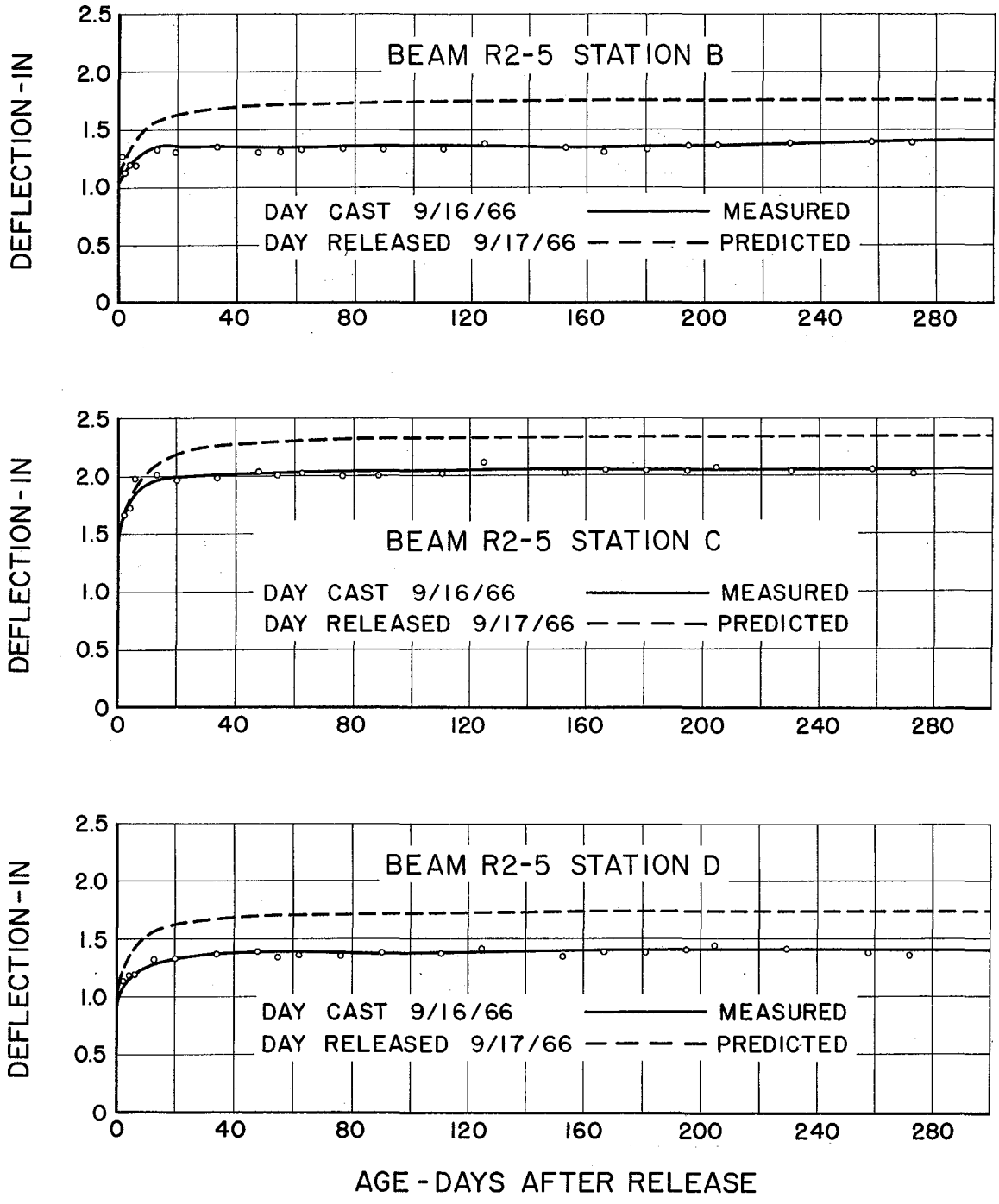

FIGURE 5-24 DEFLECTION OF BRIDGE BEAMS

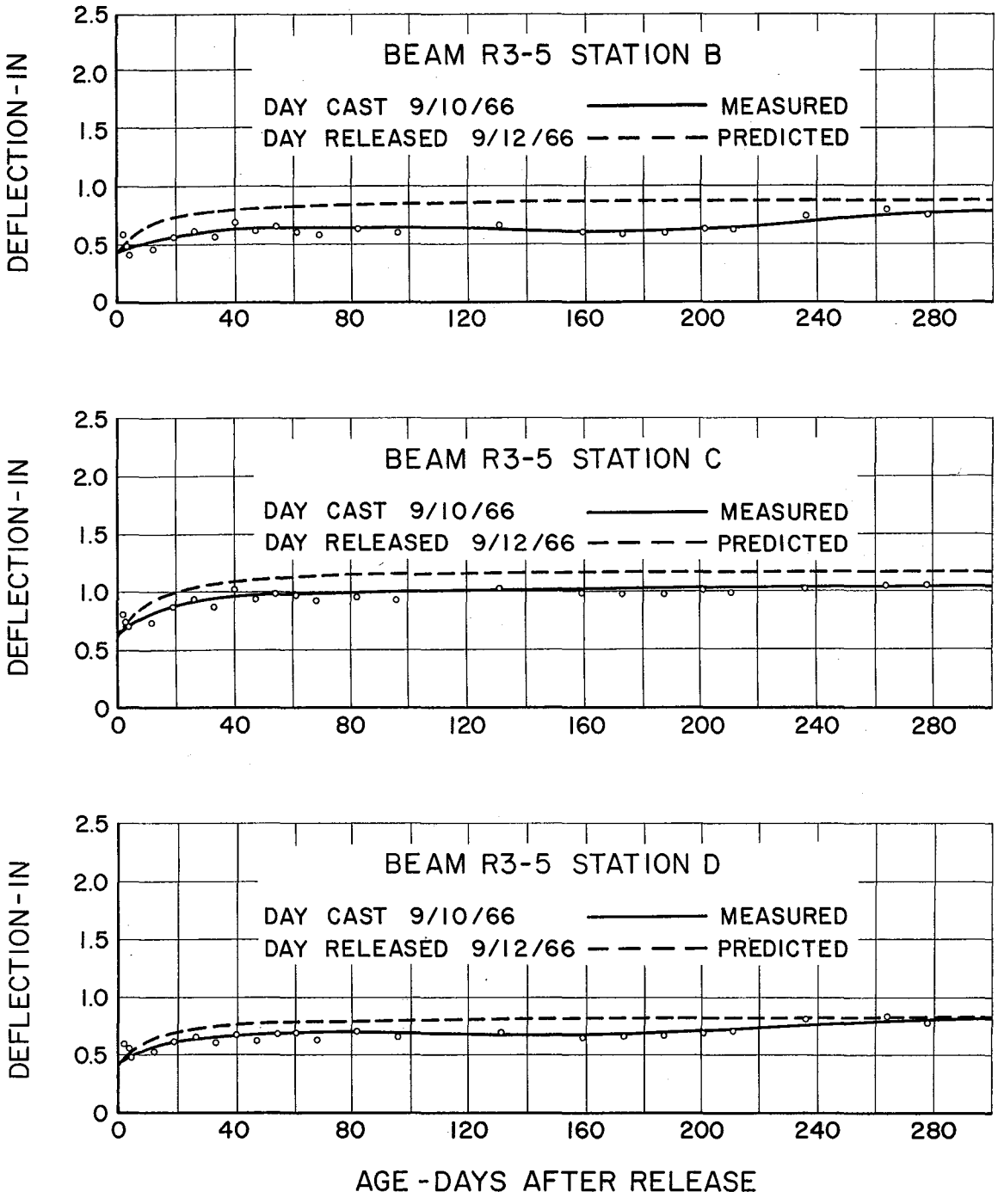

FIGURE 5-25 DEFLECTION OF BRIDGE BEAMS

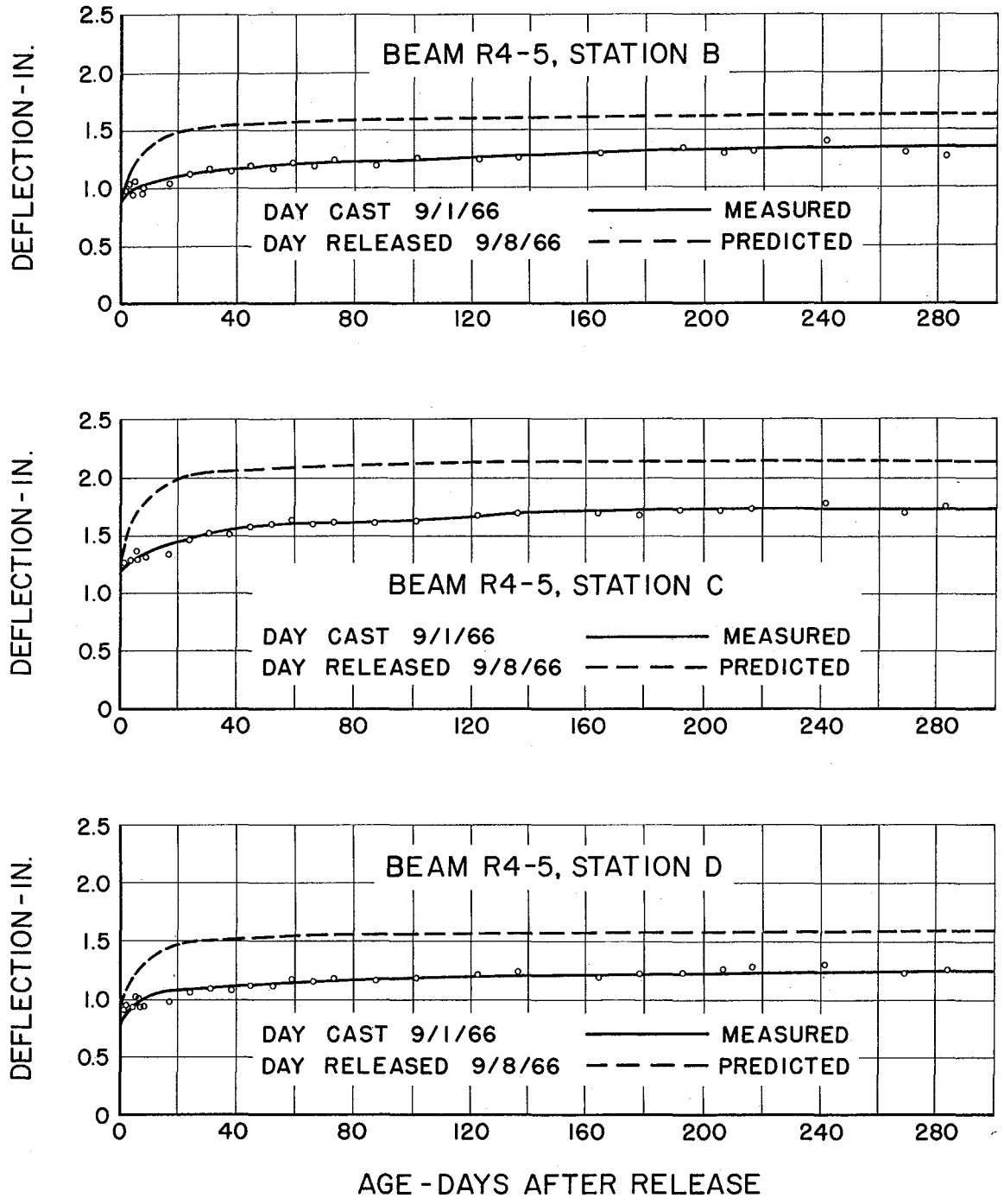

FIGURE 5-26 DEFLECTION OF BRIDGE BEAMS

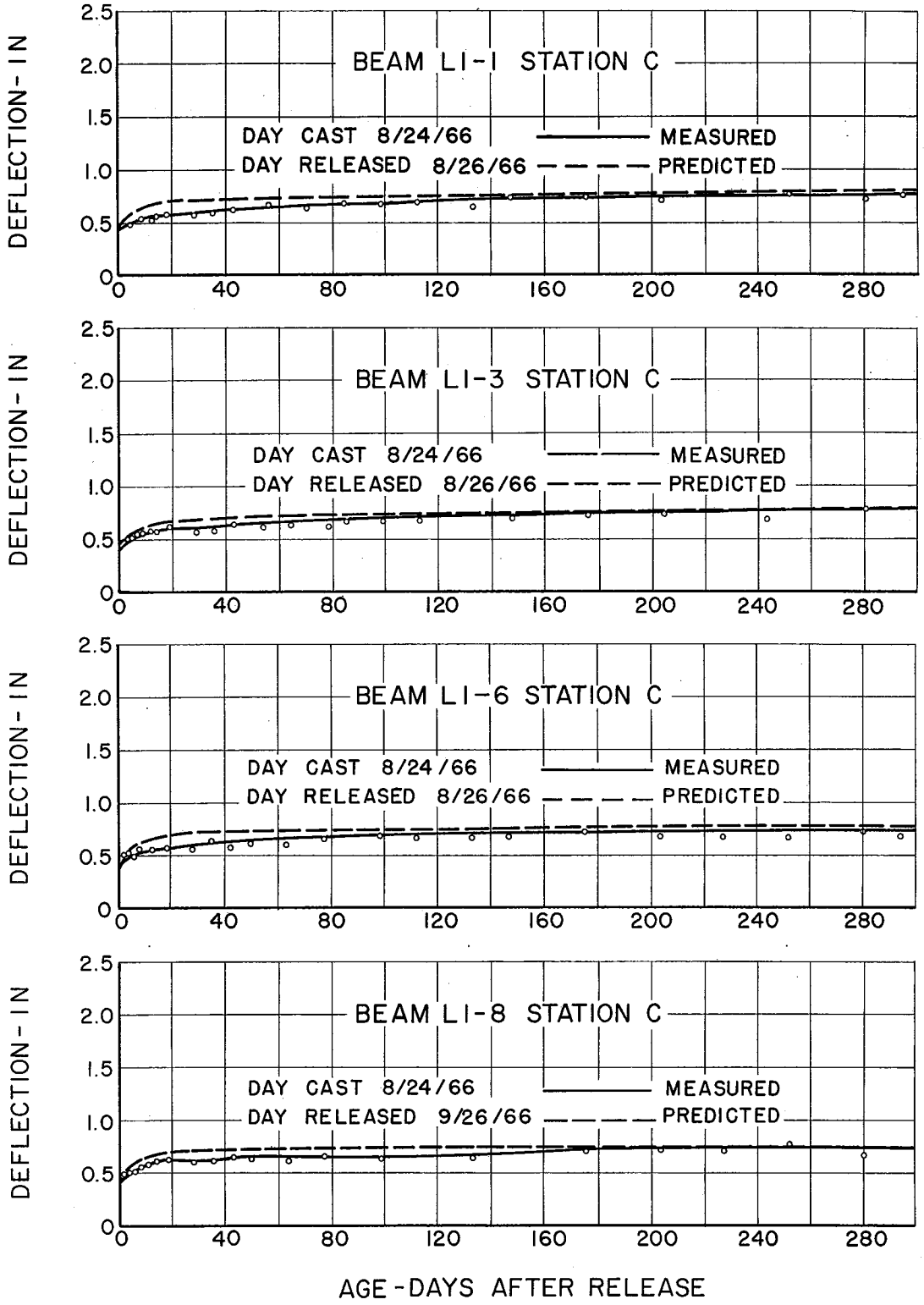

FIGURE 5-27 DEFLECTION OF BRIDGE BEAMS

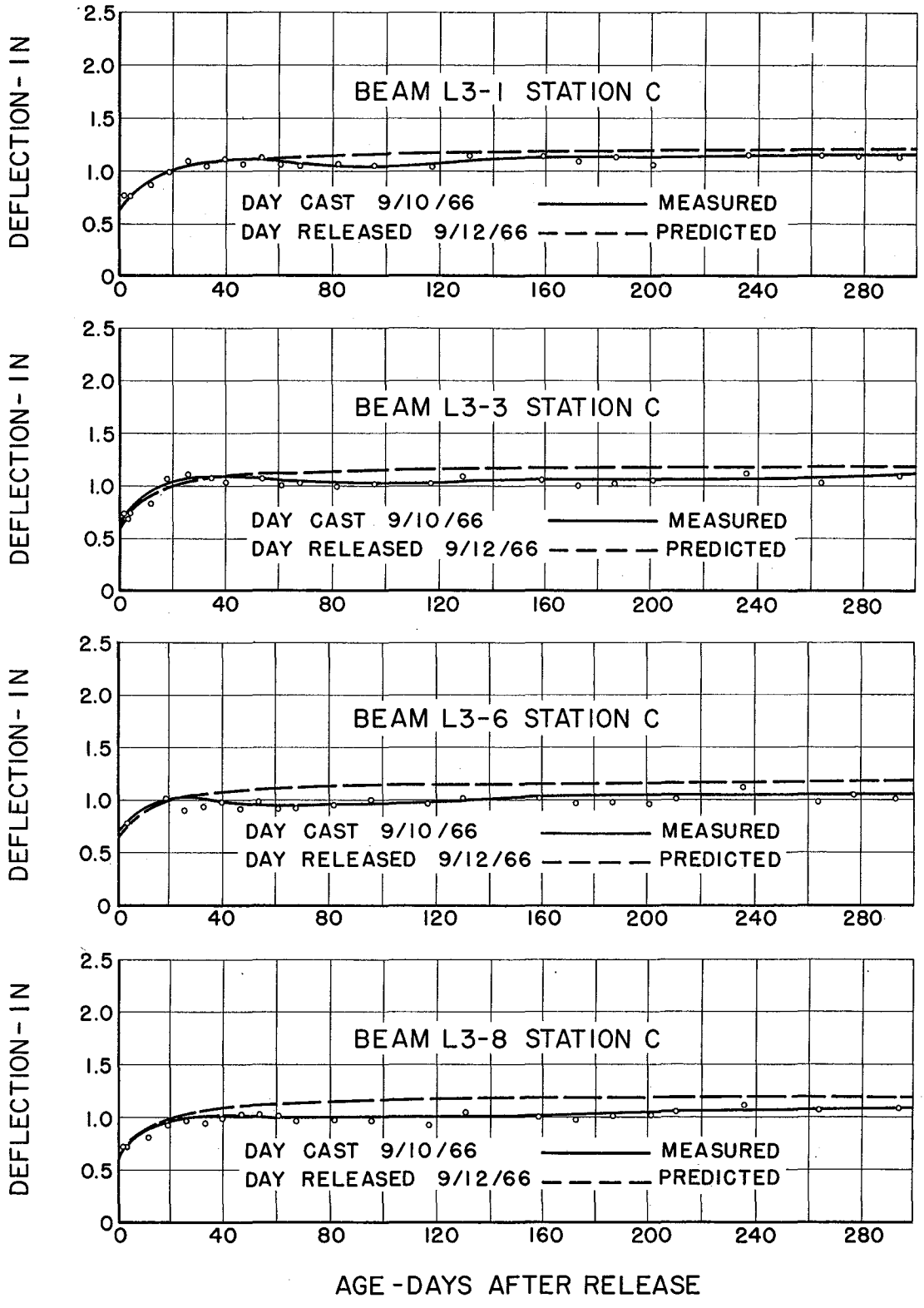

FIGURE 5-28 DEFLECTION OF BRIDGE BEAMS

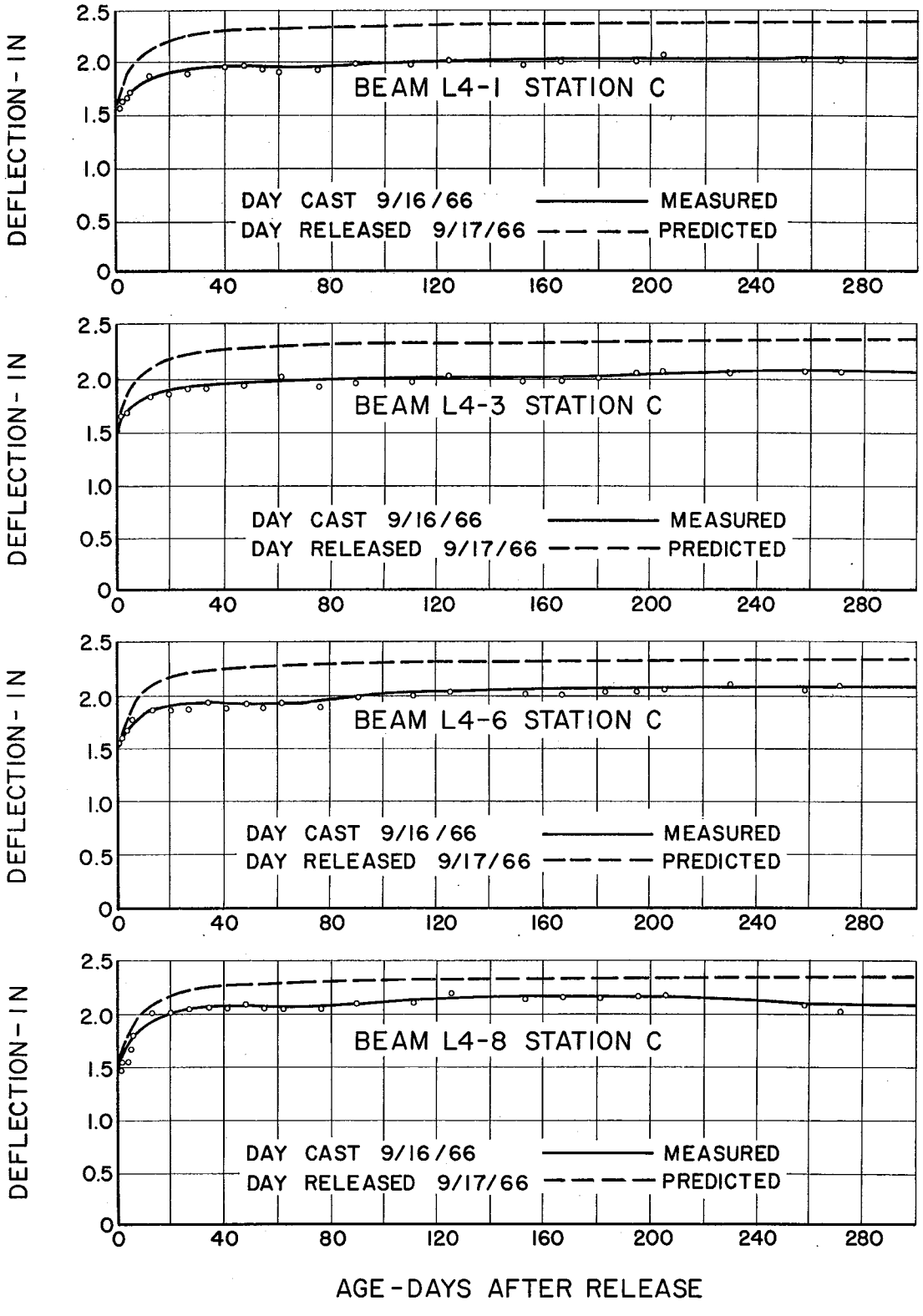

FIGURE 5-29 DEFLECTION OF BRIDGE BEAMS

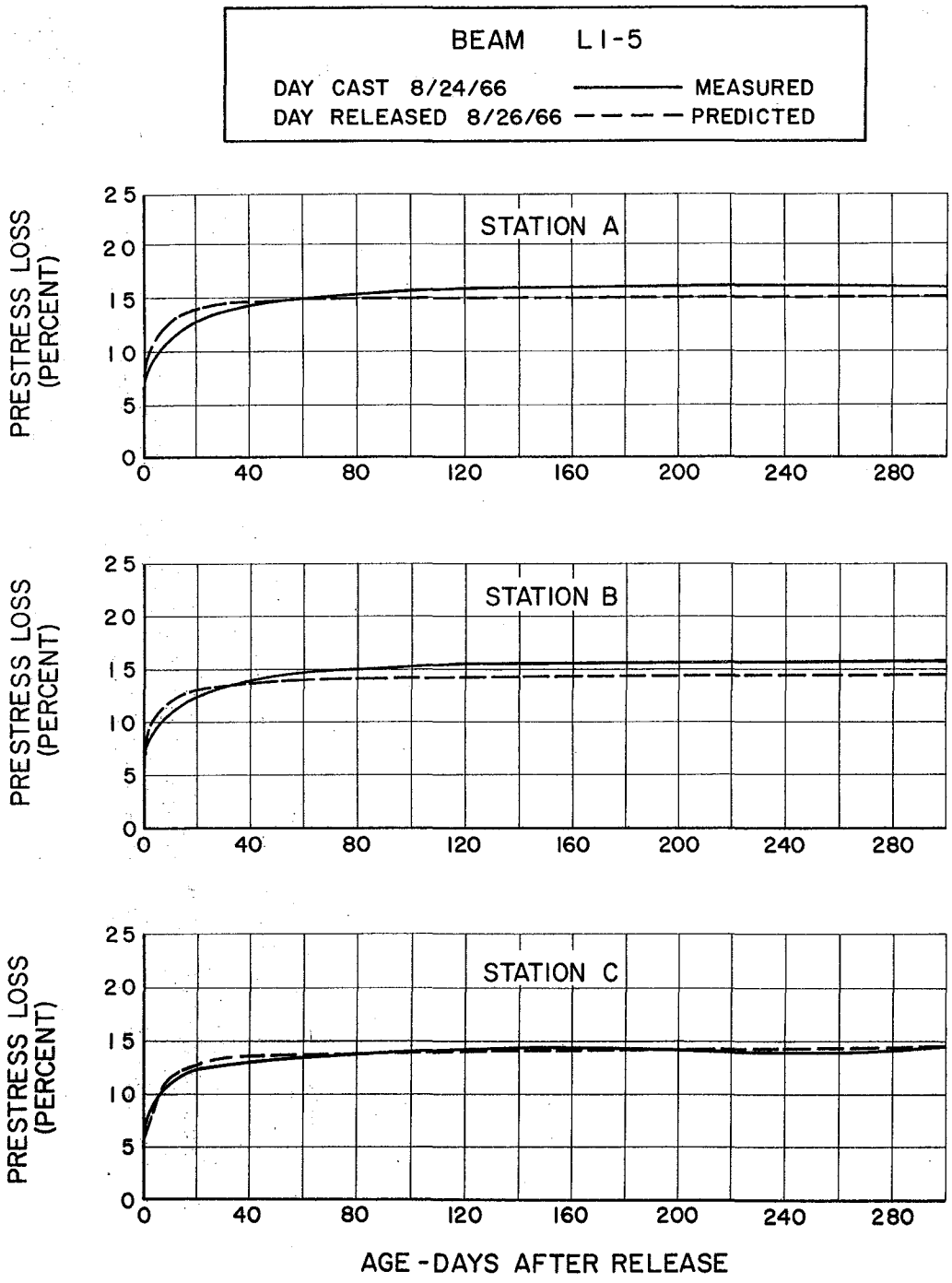

FIGURE 5-30 PRESTRESS LOSS IN BRIDGE BEAM L1-5

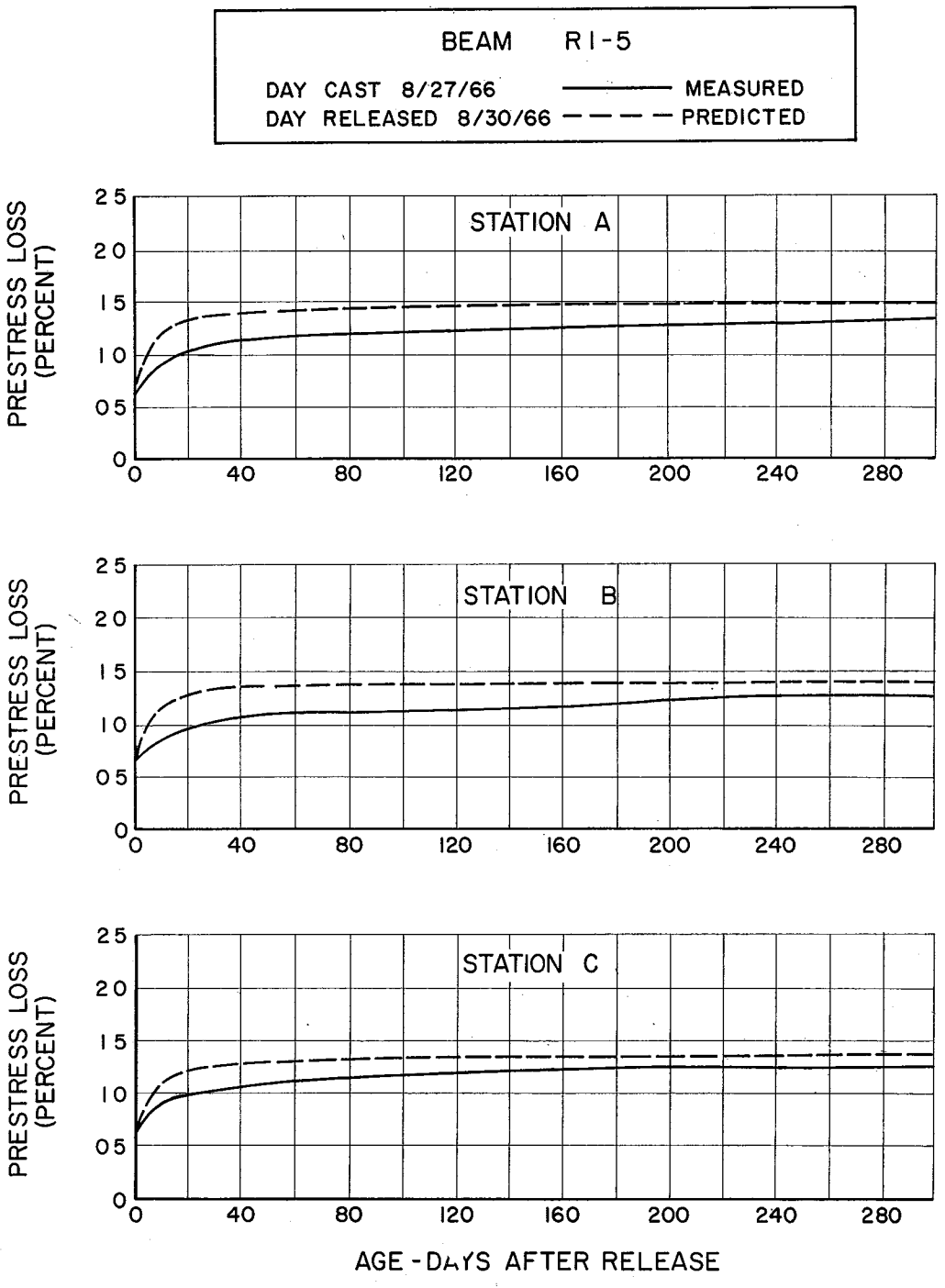

FIGURE 5-31 PRESTRESS LOSS IN BRIDGE BEAM R1-5

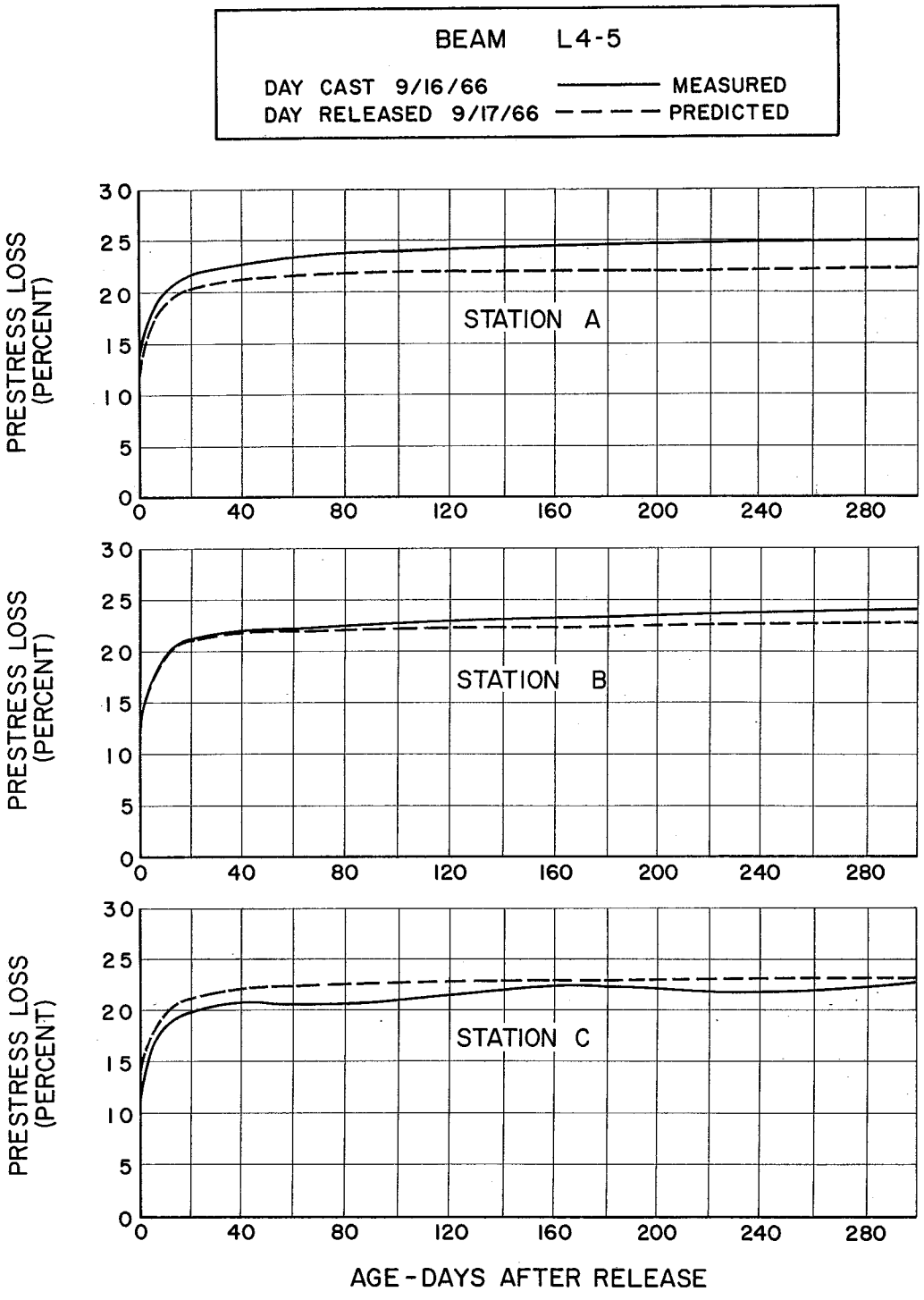

FIGURE 5-32 PRESTRESS LOSS IN BRIDGE BEAM L4-5

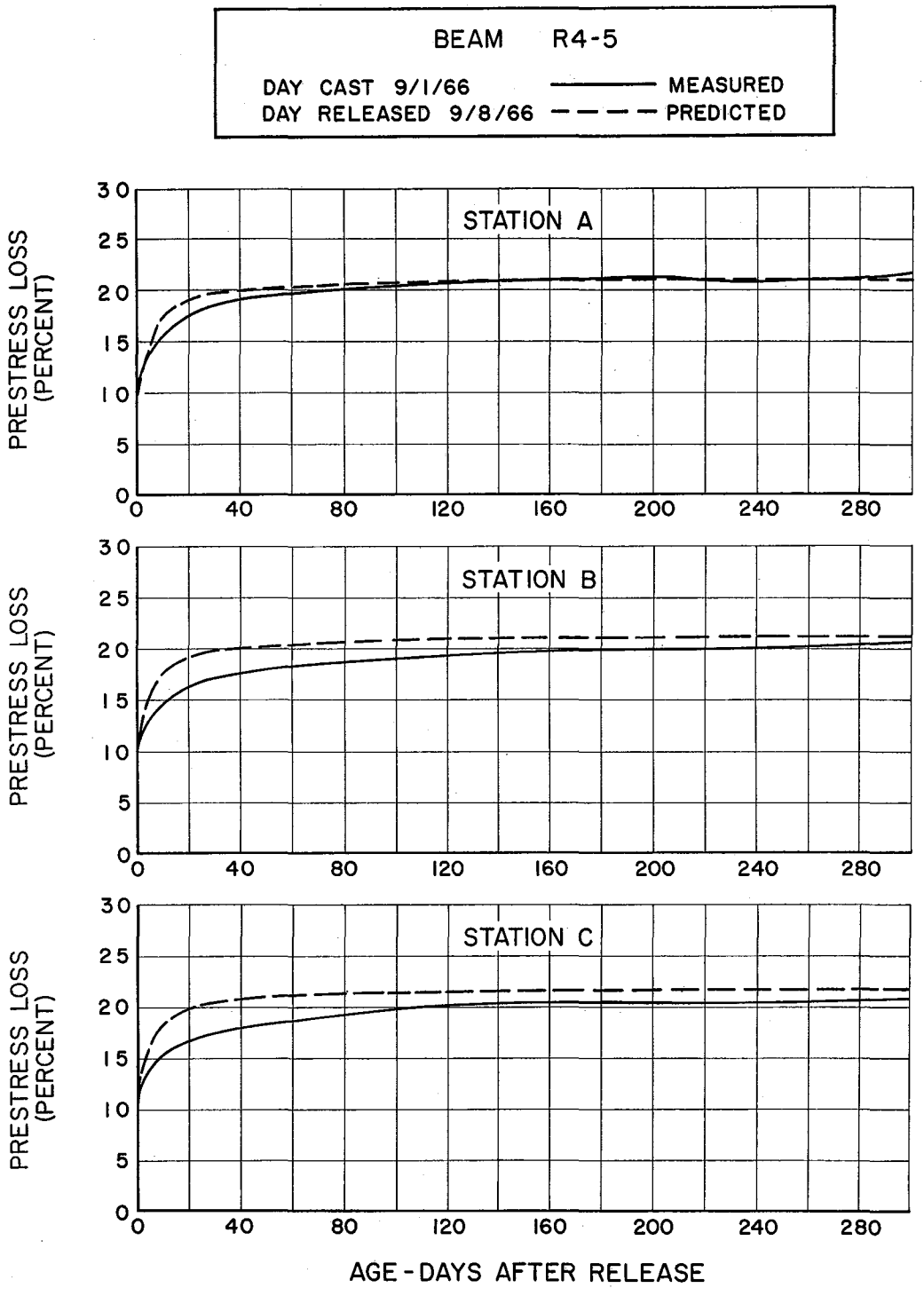

FIGURE 5-33 PRESTRESS LOSS IN BRIDGE BEAM R4-5

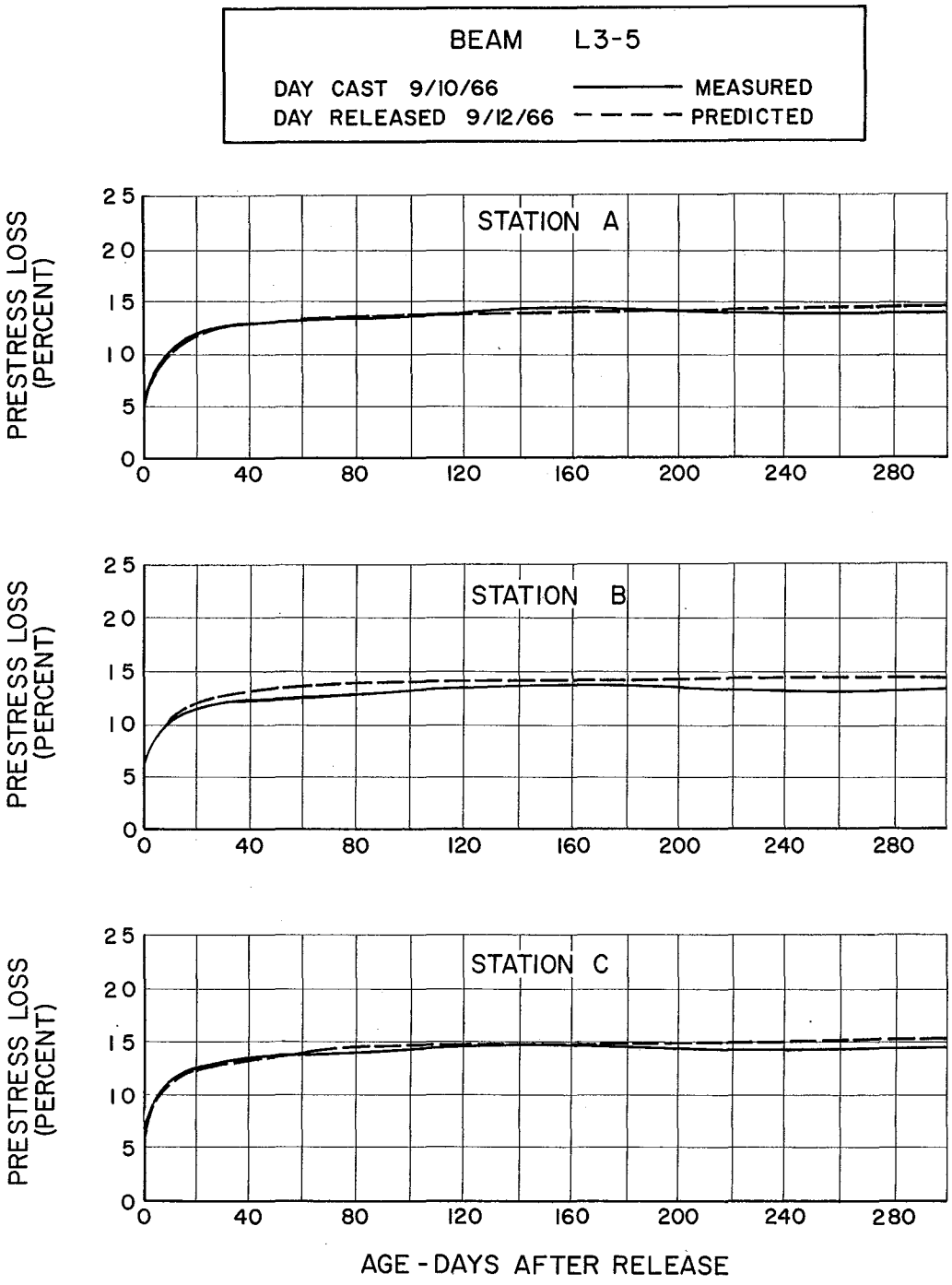

FIGURE 5-34 PRESTRESS LOSS IN BRIDGE BEAM L3-5

REFERENCES

1. Symposium on Creep of Concrete, ACI Publication SP-9, American Concrete Institute, Detroit, Michigan, 1964, 160 pp.

2. Shidler, J. J., "Lightweight Aggregate Concrete for Structural Use," ACI Journal, Proceedings, Vol. 54, No. 1, October 1957, pp. 299-328.

3. Best, C. H. and Palivka, M., "Creep of Lightweight Concrete," Magazine of Concrete Research (London), Vol. 11, No. 33, November 1959, pp. 129-134.

4. Jones, Trumen R., Hirsch, T. J. and Stephenson, Henson K., "The Physical Properties of Structural Quality Lightweight Aggregate Concrete," Texas Transportation Institute, Texas A&M University, College Station, Texas, August 1959.

5. Reichard, T. W., "Creep and Drying Shrinkage of Lightweight and Normal Weight Concrete," Nat'l. Bureau of Stds., Monograph 74, March 4, 1964, U. S. Gov. Printing Office, Washington, D. C.

6. Beecroft, Gordon, W., "Creep and Shrinkage of Two Lightweight Aggregate Concretes," Highway Research Board Bulletin 307, Nat'l. Academy of Sciences, Nat'l Research Council, Washington, D. C., 1962, pp. 26-41.

7. Yang, David Dar-wei, Creep in Prestressed Lightweight Aggregate Concrete, Ph.D. Dissertation, Texas A&M University, College Station, Texas, August 1966, 123 pp.

8. Furr, Howard L., "Creep Tests of Two-Way Prestressed Concrete," ACI Journal, Proceedings, Vol. 64, No. 6, June 1967, pp. 288-294.

9. Ross, A. D., "Creep of Concrete Under Variable Stress," Journal ACI, Vol. 29, No. 9, March 1958, pp. 739-758.

10. Corley, W. G., Sozen, M. A., and Siess, C. P., "Time Dependent Deflections of Prestressed Concrete Beams," Highway Research Board Bulletin 307, National Academy of Sciences, National Research Council, Washington, D. C., pp. 1-25.

11. Hatt, W. K., "The Effect of Moisture on Concrete," Proc. ASCE, May 1925, pp. 757-793.

12. Roll, Frederic, "Long Time Creep-Recovery of Highly Stressed Concrete Cylinders," Paper Number 4, Reference 1, pp. 95-114.

13. Neville, Adam M. and Meyers, Bernard L., "Creep of Concrete: Influencing Factors and Prediction," Paper Number 1, Reference 1, pp. 1-31.

14. Hanson, J. A., "A 10-Year Study of Creep Properties of Concrete," Concrete Laboratory Report, No. SP-38, U. S. Bureau of Reclaimation, Denver, Colorado, 1953.

15. Davis, Raymond E. and Davis, Harmer E., "Flow of Concrete Under Sustained Compressive Stress," Proc. ACI, Vol. 27, 1930-31, pp. 837-901.

16. Miller, Alfred L., "Warping of Reinforced Concrete Due to Shrinkage," Journal ACI, May 1958, No. 11, Vol. 29, pp. 939-950.

17. Birkeland, Halvard W., "Differential Shrinkage in Composite Beams," Journal ACI, May 1960, No. 11, Vol. 31, pp. 1123-1136.

18. Ferguson, Phil M., Discussion of "Warping of Reinforced Concrete in (Miller's paper in Reference 1 above)," in Journal ACI, December 1958, No. 6, Vol. 30, pp. 1393-1398.

19. Evans, R. H., and Parker, A. S., "Behavior of Prestressed Concrete Composite Beams," Journal ACI, No. 9, Vol. 26, May 1955, pp. 861-878.

20. Pickett, Gerald, "The Effects of Charge in Moisture-Content of the Creep of Concrete Under a Sustained Load," Journal ACI, No. 4, Vol. 13, February 1942, pp. 333-355.

21. Branson, Dan E. "Time-Dependent Effects in composite Concrete Beams," Journal ACI, Proc. Vol. 61, No. 2, February 1964, pp. 213-229.

22. Branson, D. E., and Ozell, A. M., "Camber of Prestressed Concrete Beams," ACI Journal, Proc. Vol. 57, No. 12, June 1961, pp. 1549-1574.

23. Mattock, Alan H., "Precast-Prestressed Concrete Bridges: 5. Creep and Shrinkage Studies," Journal, Portland Cement Association, Vol. 3, No. 2, May 1961, pp. 32-66.

24. Lorman, William R., "The Theory of Concrete Creep," Proc. of ASTM, Vol. 40, 1940, pp. 1082-1102.

25. Scordelis, A. C., Branson, Dan E., and Sozen, Mete A, (Subcommittee 5, ACI Committee 435), "Deflections of Prestressed Concrete Members," ACI Proc. V. 60, Dec. 1963, pp. 1697-1728.

APPENDIX A

The force in prestressing steel after its release from anchorage is computed below as a function of the anchor force. Elastic action is assumed in both steel and concrete.

The sketches below show the beam as it is assumed before and after release, the beam section, and the elastic strains in a unit length element taken from any position along the length of the beam.

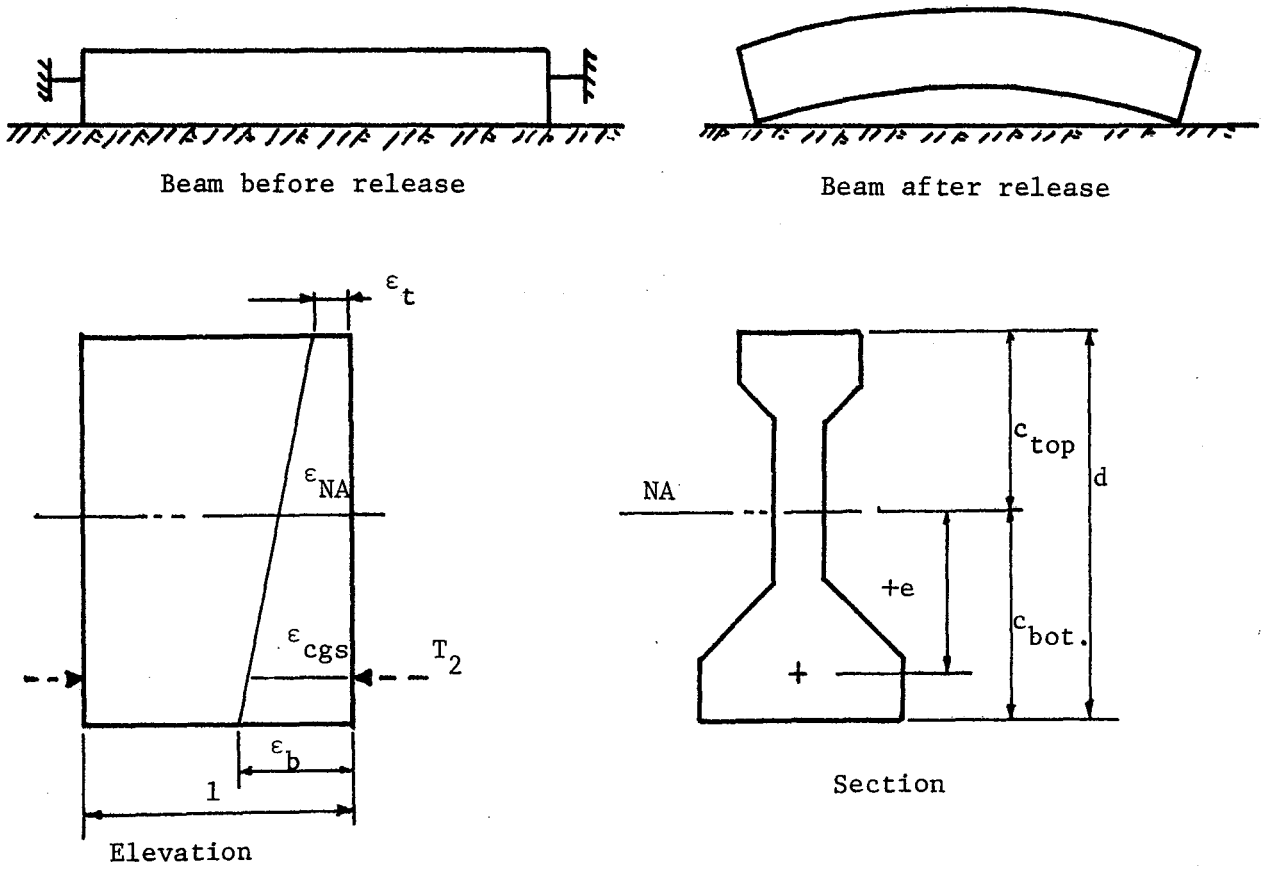

Fig. A-1. Beam Strains at Release

Notation

T_1	Anchor force in prestressing steel
T_2	Force in prestressing steel immediately after release of the anchorage. This force is equal to T_1 minus elastic loss due to release.
ΔT	Elastic loss of prestressing steel force upon release
M_{DL}	Dead load moment, due to self weight, at the section under consideration
ε	Elastic strain (see Fig. A-1). The subscript c denotes concrete; s, steel.
A	Gross section area
NA	Centroid of gross section area
A_{st}	Total area of prestressing steel
p	Steel ratio = A_{st}/A
E_s, E_c	Modulus of elasticity of prestressing steel and of concrete, respectively
n	E_s/E_c

Computations

$$T_2 = T_1 - \Delta T$$

$$\varepsilon c = \varepsilon s \text{ (at cgs)}$$

$$\varepsilon c_{cgs} = \varepsilon_{NA} + \varepsilon \text{ due to bending}$$

Concrete: $$\varepsilon_{cgs} = \frac{T_2}{AE_c} + \frac{T_2 e^2}{IE_c} - \frac{M_{DL} e}{IE_c}$$

Steel: $$\varepsilon_{cgs} = \frac{T_1 - T_2}{A_{st} E_s}$$

$$\frac{T_1 - T_2}{A_{st}E_s} = \frac{T_2}{AE_c} + \frac{T_2 e^2}{IE_c} - \frac{M_{DL} e}{IE_c}$$

$$T_2 \left[\frac{1}{A_{st}E_s} + \frac{1}{AE_c} + \frac{e^2}{IE_c}\right] = \frac{T_1}{A_{st}E_s} + \frac{M_{DL} e}{IE_c}$$

Substituting $p = \frac{A_{st}}{A}$ and $n = \frac{E_s}{E_c}$

$$T_2 = \frac{T_1 + M_{DL}\ e\ A_{st}\ \frac{n}{I}}{1 + pn + e^2\ p\ A\ \frac{n}{I}}$$

APPENDIX B

Loss of Spring Load Due to Strain in Tie Rods and in Concrete Creep and Shrinkage

See Figure 2.1 for details of the test frame.

F = initial load on concrete

L = length at steel tie rods = 27 in.

A = area at steel tie rods = 4 x .44 = 1.76 in.^{2}

Elastic elongation of rods = $\frac{FL}{AE} = \frac{27F}{1.76 \times 30 \times 10^6} = (.511 \times 10F^{-6})$ in.

C = spring constant for Chapter II specimens

= 10,000 lb/in for 10 - 1 & 2

= 20,000 lb/in for 15 - 1 & 2 and 20 - 1 & 2

F_o = load in loading machine before release to tie rods

$\Delta_{c+s} = (\varepsilon_{creep} + \varepsilon_{shrink}) L_{specimen} = \varepsilon_{c+s} \times 16$

$F = F_o/(1 + .511 \times 10^{-6}C)$

ΔF = change in F due to creep and Shrinkage

$= (\Delta_{c+s})\ C$

Chapter II Specimens: ΔF due to Creep + Shrink = $\Delta_{c+s}C$

Specimen	10-1&2	15-1&2	20-1&2
F_o(lb)	10,000	15,000	20,000
C	10,000	20,000	20,000
F (lb)	9,950	14,850	19,800
ΔF (lb)	151	382	540
ε_{c+s}(in/in)	= 945 x 10^{-6}	1200 x 10^{-6}	1685 x 10^{-6}
Δ_{c+s}(in)	= 15,130 x 10^{-6}	19,200 x 10^{-6}	27,000 x 10^{-6}
$\frac{\Delta F}{F}$%	1.52	2.57	2.73

APPENDIX C

COMPUTER PROGRAM FOR THE STEP-BY-STEP METHOD

C.1 General

The listing of the computer program with header cards identifying each step is given in this appendix. Fortran IV language is used in accordance with Texas A&M University Data Processing Center requirements for the IBM 7094 Computer.

The program can be used to compute and out-put either of the following:

1. Maximum camber and camber at any 3 other points along the length of the beam at any time after release of prestressing strands.
2. In addition to 1 above, the following stresses and strains at any two points along the length of the span and at midspan,
   a. initial stresses and strains (no losses)
   b. steel stresses at any time after release
   c. concrete stresses at any 3 points across the depth of the beam, and at the centroid of the steel pattern at any time after release
   d. creep strains at the points specified by c above
   e. creep plus shrinkage strains at the points specified by c above
   f. total strains at the points specified by c above
   g. prestress loss at any time after release

C.2 Notation for data cards

ID	header card, identifying the project
IDB	header card, identifying the beam such as number, station, etc.
ENER	moment of inertia of beam cross section with respect to its centroidal axis ($in.^3$)
CGC	centroid of beam cross section measured from the bottom of the beam (in.)
D	overall depth of beam (in.)
UW	unit weight of beam concrete (lb./Lin.ft.)
AC	cross sectional area of beam ($in.^2$)
XL	length of beam, center line to center line of supports (ft)
H	hold-down point measured from center line of beam (ft)
STNO	number of steel strands
AST	cross sectional area of one strand ($in.^2$)
ED	eccentricity of strand pattern measured from CGC at center line of support (in.)
EM	eccentricity of strand pattern measured from CGC at midspan (in.)
PS	anchor force per strand (lbs.)
EC	modulus of elasticity of beam concrete (10^6 psi)
ES	modulus of elasticity of steel strands (10^6 psi)
EA, EB, EX	distance from center line of supports of 3 points whose camber is desired (ft)
ASH	ultimate shrinkage strain (10^{-6} in/in)
BSH	age at which half the ultimate shrinkage strain has occurred (days)
ACR	ultimate unit creep strain (10^{-6} in/in)

BCR	age at which half the ultimate creep strain has occurred (days)
XN	length of time increment (days)
XNT	end of prediction period (days)
XLX	number of strain increments
XA, XB, XC	distance from center line of support for 3 points at which stresses and strains are desired (ft.)
GT, GB, GM	location of 3 points across the depth of the beam at which stresses and strains are desired; GT measured from top of the beam, GB and GM measured from the bottom of the beam (in.)
XINC	number of days elapsed at which shrinkage occurred in beam before release of prestressing strands (days)

C.3 Arrangement of data cards

Data cards are arranged as shown in Figure C.1. Any number of beams can be run at one time as long as they are separated by a blank card. The last card in the data deck should carry the number of beams to be run at the same time in columns 1-10.

C.4 Limitations

To avoid exceeding the capacity of IBM 7094, the following limitations should not be exceeded:

1. Maximum number of strain increments (XLX) equals 80.
2. Maximum number of time increments equals 199.

C.5 Remarks

1. Limitations set in C.4 above can be removed by changing the DIMENSION statements when larger capacity computers are used.

2. Computer time requirements vary between 5 and 30 seconds per beam depending on the level of accuracy and prediction period desired as set by XN, XLX, and XNT.

DATA CARDS

	1	11	21	31	41	51	61	71
1	ID - Header card identifying the project							
2	IDB - Header card identifying the beam							
3	ENER	CGC	D	UW	AC	XL	H	
4	STNO	AST	ED	EM	PS	EC	ES	
5	EA	EB	EX					
6	ASH	BSH	ACR	BCR	XN	XNT	XLX	
7	XA	XB	XC	GT	GB	GM	XINC	

Notes:
1. Cards number 1 and 2 may contain any information, alphabetic or numeric.
2. Each variable in cards number 3 through 7 may occupy any position within the 10 columns, and all values must be expressed in decimal form.
3. To run more than one beam at the same time, card number 8 should be a blank card, and then repeat cards number 2 through 7.
4. The last card in the data deck, card number 8, should carry the number of beams to be run at the same time in columns 1-10.

FIGURE C.1 ARRANGEMENT OF DATA CARDS

```
      $JOB  113821383T9001001000
      $IBBOX          15-H
      $EXECUTE        AGGIE


$IBFTC SINNO
C
C     PROGRAM FOR PREDICTING STRESSES, STRAINS, AND CAMBER IN PRESTRESS
C     CONCRETE BEAM
C
      DIMENSION ID(15),IDB(15),TST(200),TSS(200),TSM(200),TSB(200),
     *STLOSS(200),DIF(85,200)
      COMMON ASH,BSH,ACR,BCR
C
C     READ DATA
C
      READ(5,1000) (ID(I),I=1,12)
1     READ(5,1000) (IDB(I),I=1,12)
      READ(5,100) ENER,CGC,D,UW,AC,XL,H
      READ(5,100) STNO,AST,ED,EM,PS,EC,ES
      READ(5,100) FA,EB,EX
      READ(5,100) ASH,BSH,ACR,BCR,XN,XNT,XLX
      READ(5,100) XA,XB,XC,GT,GB,GM,XINC
C
C     WRITE HEADING
C
      WRITE(6,2000)(ID(I),I=1,12)
      WRITE(6,200) (IDB(I),I=1,12)
      WRITE(6,801) XL,STNO,D,AST,AC,ES
      WRITE(6,802) ENER,PS,CGC,ED,UW,EM,EC
      WRITE(6,803) ASH,BSH
      WRITE(6,804) ACR,BCR
C
C     COMPUTE BEAM PROPERTIES
C
      CT=D-CGC
      ZT=ENER/CT
      ZB=ENER/CGC
      DE=(EM-ED)/(XL*.5-H)
      M=1
      X=0.0
17    E=ED+DE*X
      IF(E-EM)11,11,12
12    E=EM
C
C     COMPUTE STRESSES AND STRAINS IMMEDIATELY AFTER RELEASE
C
11    DLM=(UW*XL*.5*X-UW*X**2*.5)*12.
      ZC=ENER/E
      AS=STNO*AST
      P=PS*STNO
      RP=AS/AC
      RN=ES/EC
      PSS=P*(1./(1.+RP*RN+E*E*AS*RN/ENER))/AS+(DLM*E*AS*RN/(ENER*(1.+RP*
     *RN+E*E*AS*RN/ENER)))/AS
      FCT=PSS*RP-PSS*AS*E/ZT+DLM/ZT
      FCB=PSS*RP+PSS*AS*E/ZB-DLM/ZB
      FCS=PSS*RP+PSS*AS*E/ZC-DLM/ZC
      ELT=FCT/EC
```

```
      ELB=FCB/EC
      SHRT=0.0
      CREEPT=0.0
      CREEPB=0.0
      L=1
      IN=XN+.01
      INT=XNT+.01+XN
      INC=XINC+.01
      DO 14 J=1,INT,IN
      I=J-1
C
C     COMPUTE INCREMENTAL CREEP AND SHRINKAGE STRAINS
C
      CRT=CR(FCT,I)-CR(FCT,I-IN)
      CRB=CR(FCB,I)-CR(FCB,I-IN)
      CRS=CR(FCS,I)-CR(FCS,I-IN)
      SHR=SHRK(I+INC)-SHRK(I+INC-IN)
      IF(I-INC)21,21,22
21    SHR=0.0
22    DSTS=SHR+CRS
      DP=DSTS*ES
      DF=DP*AS
      DFCT=DF/AC-DF*E/ZT
      DFCB=DF/AC+DF*E/ZB
      DFCS=DF/AC+DF*E/ZC
      FCT=FCT-DFCT
      FCB=FCB-DFCB
      FCS=FCS-DFCS
      DSTT=DFCT/EC
      DSTB=DFCB/EC
      DSTS=DFCS/EC
      CREEPT=CREEPT+CRT-DSTT
      CREEPB=CREEPB+CRB-DSTB
      SHRT=SHRT+SHR
      CST=CREEPT+SHRT
      CSB=CREEPB+SHRT
C
C     COMPUTE TOTAL STRAINS AND FINITE ELEMENT ROTATION
C
      TST(L)=CST+ELT
      TSB(L)=CSB+ELB
      DIF(L,M)=(TSB(L)-TST(L))/D*10.**(-6)
      L=L+1
14    CONTINUE
      X=X+XL/XLX
      MLX=(XLX+.01)/2.
      M=M+1
      IF(M-(MLX+2))17,18,18
18    M=M-2
      L=L-1
      WRITE(6,400)
C
C     COMPUTE MAXIMUM CAMBER
C
      DO 19 J=1,L
      A2=0.0
      ADD=0.0
      COUNT=XLX/2.
      DO 20 I=1,M
      ADD=ADD+(1.-(COUNT-.5)/(XLX/2.))*DIF(J,I)
```

```
      A2=A2+DIF(J,I)
      COUNT=COUNT-1.
20    CONTINUE
      A2A=(A2*2.)/(XLX*.5*XL**2*144.)
      ADA=(4./(XLX*.5*XL**2*144.))*ADD
      COE1=-ADA+A2A
      COE2=(-A2*.5+2.*ADD)/(XLX*.5)
      N=J*IN-IN
      YMAX=COE1*(XL/2.)**4*12.**4+COE2*(XL/2.)**2*144.
C
C     COMPUTE CAMBER AT 3 OTHER POINTS
C
      YA=YMAX-COE1*(XL/2.-EA)**4*12.**4-COE2*(XL/2.-EA)**2*144.
      YB=YMAX-COE1*(XL/2.-EB)**4*12.**4-COE2*(XL/2.-EB)**2*144.
      YC=YMAX-COE1*(XL/2.-EX)**4*12.**4-COE2*(XL/2.-EX)**2*144.
      WRITE(6,300)N,YA,YB,YC,YMAX
19    CONTINUE
      IF(XA)2,3,2
C
C     IF STRAINS AND STRESSES ARE DESIRED CALL SUBROUTINE STRAIN
C
2     CALL STRAIN(AC,XL,XA,XB,XC,GT,GB,GM,ENER,CGC,D,UW,EC,STNO,AST,ED,E
     *M,PS,ES,IN,INT,INC)
300   FORMAT(16X,I3,5X,F8.3,3X,F8.3,3X,F8.3,7X,F8.3)
400   FORMAT(16X,4H AGE,11X,22H PREDICTED CAMBER (IN),9X,8H MAXIMUM,/,15
     *X,7H (DAYS),3X,8H PT. (A),4X,8H PT. (B),4X,8H PT. (C),5X,7H CAMBER
     *//)
1000  FORMAT(12A6)
100   FORMAT(8F10.0)
2000  FORMAT(1H1,//,32X,12A6///)
200   FORMAT(32X,12A6///)
801   FORMAT(14X,54HBEAM PROPERTIES                          PRESTRESSING STE
     *EL,/,
     112X,12HSPAN       = ,F7.2,34H FT                  NO. STRANDS  = ,F7.
     20,/,
     312X,12HBM. DEPTH  = ,F7.2,34H IN                  AREA STRAND  = ,F7.
     44,4H IN2,/,
     512X,12HAREA       = ,F7.2,34H IN2                 ES           = ,F7.
     62,9H (E06)PSI)
802   FORMAT(12X,
     1    12HINERTIA    = ,F7.0,34H IN4                 INITIAL TEN. = ,F7.
     20,3H LB,/,
     312X,12HC.G.C.     = ,F7.2,34H IN                  ECC. AT END  = ,F7.
     42,3H IN,/,
     512X,12HUNIT WT.   = ,F7.2,34H LB/FT               ECC. AT CL   = ,F7.
     62,3H IN,/,
     712X,12HEC         = ,F7.2,34H (E06)PSI                        ,//)
803   FORMAT(12X,17HSHRINKAGE CURVE  ,F6.1,4H T/(,F5.1,5H +T ),//)
804   FORMAT(12X,17HUNIT CREEP CURVE ,F6.1,4H T/(,F5.1,5H +T ),//)
3     READ(5,100)CHEK
      IF(CHEK)99,1,99
99    STOP
      END



$IBFTC STRESS
      SUBROUTINE STRAIN(AC,XL,XA,XB,XC,GT,GB,GM,ENER,CGC,D,UW,EC,STNO,AS
     *T,ED,EM,PS,ES,IN,INT,INC)
```

```
      DIMENSION ID(15),IDB(15),TST(400),TSM(400),TSB(400),TSS(400),
     1STLOSS(400)
C
C     COMPUTE BEAM PROPERTIES AT GAGE POINTS
C
      CT=D-CGC-GT
      ZT=ENER/CT
      CB=CGC-GB
      ZB=ENER/CB
      CM=D-CGC-GM
      ZM=ENER/CM
      DE=(EM-ED)/(XL*.5-5.)
      K=1
9     IF(K-2)10,11,12
10    E=ED+DE*XA
      DLM=(UW*XL*.5*XA-UW*XA**2*.5)*12.
      ZC=ENER/E
      GO TO 13
11    E=ED+DE*XB
      DLM=(UW*XL*.5*XB-UW*XB**2*.5)*12.
      ZC=ENER/E
      GO TO 13
12    E=EM
      DLM=(UW*XL*.5*XC-UW*XC**2*.5)*12.
      ZC=ENER/E
13    AS=STNO*AST
      P=PS*STNO
      PIN=P/AS
C
C     COMPUTE INITIAL STESSES (NO LOSSES)
C
      FCT=-P*E/ZT+P/AC+DLM/ZT
      FCB=P*E/ZB+P/AC-DLM/ZB
      FCM=-P*E/ZM+P/AC+DLM/ZM
      FCS=P/AC-DLM/ZC
      WRITE(6,200) K,FCT,FCM,FCB,P
      RP=AS/AC
      RN=ES/EC
C
C     COMPUTE STRESSESAND STRAINS IMMEDIATELY AFTER RELEASE
C
      PSS=P*(1./(1.+RP*RN+E*E*AS*RN/ENER))/AS+(DLM*E*AS*RN/(ENER*(1.+RP
     *RN+E*E*AS*RN/ENER)))/AS
      FCT=PSS*RP-PSS*AS*E/ZT+DLM/ZT
      FCM=PSS*RP-PSS*AS*E/ZM+DLM/ZM
      FCB=PSS*RP+PSS*AS*E/ZB-DLM/ZB
      FCS=PSS*RP-DLM/ZC+PSS*AS*E/ZC
      ELT=FCT/EC
      ELM=FCM/EC
      ELB=FCB/EC
      ELS=FCS/EC
      WRITE(6,500) ELT,ELM,ELB,ELS
      SHRT=0.0
      CREEPT=0.0
      CREEPM=0.0
      CREEPB=0.0
      CREEPS=0.0
      WRITE(6,300)
      L=1
      DO 14 J=1,201,IN
```

```
      I=J-1
C
C     COMPUTE INCREMENTAL CREEP AND SHRINKAGE STRAINS
C
      CRT=CR(FCT,I)-CR(FCT,I-IN)
      CRM=CR(FCM,I)-CR(FCM,I-IN)
      CRB=CR(FCB,I)-CR(FCB,I-IN)
      CRS=CR(FCS,I)-CR(FCS,I-IN)
      IF(I)16,16,17
16    SHR=0.0
      GO TO 18
17    SHR=SHRK(I+INC)-SHRK(I-IN+INC)
18    DSTS=SHR+CRS
      DP=DSTS*ES
      PSS=PSS-DP
      DF=DP*AS
      DFCT=DF/AC-DF*E/ZT
      DFCM=DF/AC-DF*E/ZM
      DFCB=DF/AC+DF*E/ZB
      DFCS=DF/AC+DF*E/ZC
      FCT=FCT-DFCT
      FCM=FCM-DFCM
      FCB=FCB-DFCB
      FCS=FCS-DFCS
      DSTT=DFCT/EC
      DSTM=DFCM/EC
      DSTB=DFCB/EC
      DSTS=DFCS/EC
      PSS=PSS+DSTS*ES
      CREEPT=CREEPT+CRT-DSTT
      CREEPM=CREEPM+CRM-DSTM
      CREEPB=CREEPB+CRB-DSTB
      CREEPS=CREEPS+CRS-DSTS
      SHRT=SHRT+SHR
      CST=CREEPT+SHRT
      CSM=CREEPM+SHRT
      CSB=CREEPB+SHRT
      CSS=CREEPS+SHRT
      P=PSS
      WRITE(6,400)I,P,FCT,FCM,FCB,FCS,CREEPT,CREEPM,CREEPB,CREEPS,CST,CS
     1M,CSB,CSS
C
C     COMPUTE TOTAL STRAINS AND PRESTRESS LOSS
C
      TST(L)=CST+ELT
      TSM(L)=CSM+ELM
      TSB(L)=CSB+ELB
      TSS(L)=CSS+ELS
      STLOSS(L)=(PIN-PSS)*100./PIN
      L=L+1
14    CONTINUE
      WRITE(6,800) K
      WRITE(6,600)
      L=L-1
      I=0
      DO 15 J=1,L
      WRITE(6,700) I,TST(J),TSM(J),TSB(J),TSS(J),STLOSS(J)
      I=I+IN
15    CONTINUE
      K=K+1
```

```
      IF(K-3)9,9,99
200   FORMAT(1H1,11X,8HSECTION ,I2,/10X,16HINITIAL STRESSES,/,10X,7H TOP
     1 = ,F6.0,10H MIDDLE = ,F6.0,10H BOTTOM = ,F6.0,3X,16HSTEEL TENSION
     2 = ,F8.0//)
300   FORMAT(5X,4H AGE,3X,13H STEEL STRESS,5X,22H CONCRETE STRESS (PSI),
     116X,13H CREEP (E-06),13X,25H CREEP + SHRINKAGE (E-06)/4X,7H (DAYS)
     2,4X,6H (PSI),8X,4H TOP,1X,7H MIDDLE,7H BOTTOM,9H AT STEEL,5X,
     34H TOP,1X,7H MIDDLE,7H BOTTOM,9H AT STEEL,5X,4H TOP,1X,7H MIDDLE,
     47H BOTTOM,9H AT STEEL//)
400   FORMAT(6X,I3,5X,F8.0,7X,F5.0,2X,F5.0,2X,F5.0,3X,F5.0,6X,F5.0,2X,
     1F5.0,2X,F5.0,3X,F5.0,5X,F5.0,2X,F5.0,2X,F5.0,3X,F5.0)
500   FORMAT(/,10X,23H ELASTIC STRAINS (E-06),/10X,7H TOP = ,F6.0,
     13X,10H MIDDLE = ,F6.0,3X,10H BOTTOM = ,F6.0,3X,12H AT STEEL = ,
     2F6.0///)
600   FORMAT(5X,4H AGE,10X,30H TOTAL PREDICTED STRAIN (E-06),14X,
     112H STRESS LOSS,/,4X,7H (DAYS),5X,4H TOP,4X,7H MIDDLE,3X,7H BOTTOM
     2,2X,9H AT STEEL,11X,11H (PER CENT)//)
700   FORMAT(6X,I3,5X,F7.0,3X,F7.0,3X,F7.0,3X,F7.0,15X,F7.3)
800   FORMAT(1H1,10X,9H SECTION ,I2,//)
99    RETURN
      END



$IBFTC CREEP
      FUNCTION CR(FC,I)
      COMMON ASH,BSH,ACR,BCR
C
C     COMPUTE CREEP AT ANY TIME
C
      IF(I)1,1,5
1     CR=0.0
      GO TO 10
5     T=I
      CREEP=(ACR*T)/(BCR+T)
      CR=FC*CREEP/1000.
10    RETURN
      END



$IBFTC SHRINK
      FUNCTION SHRK(I)
      COMMON ASH,BSH,ACR,BCR
C
C     COMPUTE SHRINKAGE AT AND TIME
C
      IF(I)1,1,5
1     SHRK=0.0
      GO TO 10
5     T=I
      SHRK=(ASH*T)/(BSH+T)
10    RETURN
      END
```